THE EFFECT OF DISSOLVED OZONE ON THE CORROSION BEHAVIOR OF MONEL 400, MONEL K-500, CDA 706, AND CDA 715 IN SEAWATER

J.H. Stevens and D.J. Duquette
Rensselaer Polytechnic Institute
Troy, New York 12180

October 1998

Report No. 5 to the Office of Naval Research
Contract No. N00014-94-1-0093

Unclassified

SECURITY CLASSIFICATION OF THIS PAGE

REPORT DOCUMENTATION PAGE

1a. REPORT SECURITY CLASSIFICATION Unrestricted	1b. RESTRICTIVE MARKINGS None
2a. SECURITY CLASSIFICATION AUTHORITY	3. DISTRIBUTION/AVAILABILITY OF REPORT Unrestricted
2b. DECLASSIFICATION/DOWNGRADING SCHEDULE	
4. PERFORMING ORGANIZATION REPORT NUMBER(S) 5	5. MONITORING ORGANIZATION REPORT NUMBER(S)
6a. NAME OF PERFORMING ORGANIZATION Rensselaer Polytechnic Institute 6b. OFFICE SYMBOL (If applicable)	7a. NAME OF MONITORING ORGANIZATION
6c. ADDRESS (City, State and ZIP Code) Materials Science and Engineering Dept. Troy, NY 12180-3590	7b. ADDRESS (City, State and ZIP Code)
8a. NAME OF FUNDING/SPONSORING ORGANIZATION Office of Naval Research 8b. OFFICE SYMBOL (If applicable) Code 1131M	9. PROCUREMENT INSTRUMENT IDENTIFICATION NUMBER
8c. ADDRESS (City, State and ZIP Code) 800 N. Quincy Street Arlington, VA 22217-5000	10. SOURCE OF FUNDING NOS. PROGRAM ELEMENT NO. / PROJECT NO. N00014-94-10093 / TASK NO. / WORK UNIT NO.
11. TITLE (Include Security Classification) The Effect of Dissolved Ozone on the Corrosion Behavior of Monel 400, Monel K-500, CDA 706, and CDA 715 in Seawater	
12. PERSONAL AUTHOR(S) J. H. Stevens, D. J. Duquette	
13a. TYPE OF REPORT Technical 13b. TIME COVERED FROM 3/98 TO 10/98	14. DATE OF REPORT (Yr., Mo., Day) 1998, October, 29 15. PAGE COUNT 164
16. SUPPLEMENTARY NOTATION None	

17. COSATI CODES			18. SUBJECT TERMS (Continue on reverse if necessary and identify by block number)
FIELD	GROUP	SUB. GR.	

19. ABSTRACT (Continue on reverse if necessary and identify by block number)

Ozone is being considered as an alternative to chlorine based biocides for use in marine heat exchange systems. Ozone has several advantages over chlorine based biocides: including stronger oxidizing power, the ability to be produced on site, and degradation to oxygen. Before ozone is used in heat exchange systems it is important to understand its impact on the corrosion behavior of the metals used in these systems.

Two separate studies were carried out: the first at the Corrosion Lab, Rensselaer Polytechnic Institute in Troy, NY comparing ozonated and aerated seawater for thirty, sixty, and ninety days, and the second, at the LaQue Center for Corrosion Technology, Inc. in Wrightsville Beach, N.C. which compared ozonated and chlorinated seawater environments for sixty days. Electrochemical experiments were performed and compared with crevice coupon immersion tests to determine effects of dissolved ozone on the corrosion behavior of Monel 400, Monel K-500, 90Cu/10Ni (CDA 706), and 70Cu/30Ni (CDA 715).

Studies in-lab correctly predicted the morphology of crevice corrosion in ozonated seawater but, did not predict the extent of corrosion seen in the North Carolina tests.

20. DISTRIBUTION/AVAILABILITY OF ABSTRACT UNCLASSIFIED/UNLIMITED ☒ SAME AS RPT. ☐ DTIC USERS ☐	21. ABSTRACT SECURITY CLASSIFICATION Unrestricted
22a. NAME OF RESPONSIBLE INDIVIDUAL D. J. Duquette	22b. TELEPHONE NUMBER (Include Area Code) (518) 276-6448 22c. OFFICE SYMBOL

DD FORM 1473, 83 APR EDITION OF 1 JAN 73 IS OBSOLETE.

In-lab tests exhibited the pitting and crevice behavior of these alloys in ozonated seawater with attack occurring immediately outside the mouth of the crevice. But, in-lab tests did not show the extent of corrosion observed in North Carolina, which consumed up to half the thickness of the plate after sixty days of exposure to ozonated seawater. The difference in severity was due to a flocculating black corrosion product associated with nickel dissolu having ozone and the flow present in the tanks at LaQue Center for Corrosion Technology. This black flocculant was present in lab studies but flushed away in North Carolina studies. The flow created a reduced boundary layer over the surface of the sample accelerating transp to and away from the sample surface as well as stagnant layers due to the geometry of the crevice. Attack was generally concentrated at the mouth of the crevice, being much more severe on the Monel alloys than the Cu-Ni alloys. The difference between the alloys is due to the differing types of films formed on these alloys.

Also included in the appendices are the results of tests run concurrently on nickel based alloys and stainless steels. Investigated were IN625 Hastelloy C-22, C-2000, and C-276. The nickel base alloys perform well in aerated and chlorinated seawater, although they do exhibit crevice corrosion immediately outisde the crevice after exposure to ozonated seawater.

The stainless steel alloys 316SS, AL6XN, and Ferralium 255 also showed little or no signs of corrosion after exposure to aerated or chlorinated seawater. In ozonated seawater a more classical crevice corrosion situation was observed. Localized corrosion was concentrated beneath the non-metallic washer due to formation of HF acid as the washer broke down in the presence of ozone. Of the alloys investigated here 316SS displayed the most extensive corrosion. Ferralium 255 showed less corrosion, although the corrosion that did occur was preferentially at the ferrite phase. AL6XN displayed the best corrosion resistance of all the alloys studied in ozonated seawater, exhibiting minimal crevice or general attack.

Table of Contents

List of Tables

List of Figures

Abstract

Ozone is being considered as an alternative to chlorine based biocides for use in marine heat exchange systems. Ozone has several advantages over chlorine based biocides: including stronger oxidizing power, the ability to be produced on site, and degradation to oxygen. Before ozone is used in heat exchange systems it is important to understand its impact on the corrosion behavior of the metals used in these systems.

Two separate studies were carried out: the first at the Corrosion Lab, Rensselaer Polytechnic Institute in Troy, NY comparing ozonated and aerated seawater for thirty, sixty, and ninety days, and the second, at the LaQue Center for Corrosion Technology, Inc. in Wrightsville Beach, N.C. which compared ozonated and chlorinated seawater environments for sixty days. Electrochemical experiments were performed and compared with crevice coupon immersion tests to determine effects of dissolved ozone on the corrosion behavior of Monel 400, Monel K-500, 90Cu/10Ni (CDA 706), and 70Cu/30Ni (CDA 715).

Studies in-lab correctly predicted the morphology of crevice corrosion in ozonated seawater but, did not predict the extent of corrosion seen in the North Carolina tests. In-lab tests exhibited the pitting and crevice behavior of these alloys in ozonated seawater, with attack occurring immediately outside the mouth of the crevice. But, in-lab tests did not show the extent of corrosion observed in North Carolina, which consumed up to half the thickness of the plate after sixty days of exposure to ozonated seawater. The difference in severity was due to a flocculating black corrosion product associated with nickel dissolution having ozone and the flow present in the tanks at LaQue Center for Corrosion Technology. This black flocculant was present in lab studies but flushed away in North Carolina studies. The flow created a reduced boundary layer over the surface of the sample accelerating transport to and away from the sample surface as well as stagnant layers due to the geometry of the crevice. Attack was generally concentrated at the mouth of the crevice,

being much more severe on the Monel alloys than the Cu-Ni alloys. The difference between the alloys is due to the differing types of films formed on these alloys.

Also included in the appendices are the results of tests run concurrently on nickel based alloys and stainless steels. Investigated were IN625 Hastelloy C-22, C-2000, and C-276. The nickel base alloys perform well in aerated and chlorinated seawater, although they do exhibit crevice corrosion immediately outside the crevice after exposure to ozonated seawater.

The stainless steel alloys 316SS, AL6XN, and Ferralium 255 also showed little or no signs of corroson after exposure to aerated or chlorinated seawater. In ozonated seawater a more classical crevice corrosion situation was observed. Localized corrosion was concentrated beneath the non-metallic washer due to formation of HF acid as the washer broke down in the presence of ozone. Of the alloys investigated here 316SS displayed the most extenisve corrosion. Ferralium 255 showed less corrosion, although the corrosion that did occur was preferentially at the ferrite phase. AL6XN displayed the best corrosion resistance of all the alloys studied in ozonated seawater, exhibiting minimal crevice or general attack.

Introduction

For over a century ozone has been used in municipal water systems to remove taste, odor, color, and disinfect the water making it safe for consumption. Interest has grown recently in using ozone as a biocide replacing chlorine based biocides in seawater. Concern is also beginning to rise because of the adverse affects of byproducts of chlorine based biocides. As an alternative ozone offers several advantages, including: a higher oxidizing potential, the ability to be produced on site, and a relatively short half-life, breaking down to oxygen. For these reasons ozone is being considered in marine applications to control biofouling in heat exchange systems. Biofouling reduces the efficiency of the heat exchange system by narrowing the diameter of the tubing, and also poses corrosion problems in the form of corrosive biological byproducts and under deposit corrosion.

These studies investigate the corrosion effects of ozone on Monel 400, Monel K-500, 90Cu/10Ni (CDA 706), and 70Cu/30Ni (CDA 715). These Ni-Cu and Cu-Ni alloys are typically used in marine service because of their resistance to corrosion in flowing seawater systems and resistance to biofouling in the case of the Cu-Ni alloys. Additionally, one these studies compares the effectiveness of ozone as a biocide with the biocide hypochlorite which it would replace.

The first group of experiments was conducted in the Corrosion Lab at Rensselaer Polytechnic Institute in Troy, NY. A comparison of the corrosion behavior of these alloys was made between ozonated and aerated seawater. Weight loss and crevice (metal-nonmetal) corrosion samples were used to observe the corrosion behavior. Electrochemical tests were also performed to gain a better understanding of the corrosion behavior seen on the coupon samples.

The second group of experiments was conducted at the LaQue Center for Corrosion Technology, Inc. in Wrightsville Beach, N.C.. A comparison was made between

ozonated and chlorinated seawater. The North Carolina site allowed a continuous supply of fresh seawater and the ability to test in warm unpolluted seawater. Comparisons were made using the same alloys, and samples were constructed to yield a metal-metal crevice of like metal as well as a metal- PTFE crevice.

These two studies were sponsored by the Office of Naval Research and were used to better understand and describe the corrosion of these alloys in ozonated seawater.

Historical Review and Background

Seawater

The major constituents of seawater are nearly uniform in their proportions throughout the world in connected seas. Knowing the total salt content and temperature of the seawater many properties can be determined later.[1] Table 1 lists the major constituents of seawater, with chlorinity defined as the total amount of chlorine, bromine, and iodine, in grams, contained in 1000g of seawater assuming that bromine and iodine have been replaced with chlorine.

Ion	parts per million
Chloride (Cl^-)	18980.0
Sulfate (SO_4^{--})	2649.0
Bicarbonate (HCO_3^-)	139.7
Bromine (Br^-)	64.6
Fluorine (F^-)	1.3
Boric Acid (H_3BO_3)	26.0
Sodium (Na^+)	10556.1
Magnesium (Mg^+)	1272.0
Calcium (Ca^{++})	400.1
Potassium (K^+)	380.0
Strontium (Sr^{++})	13.3

Table 1. The major constituents of seawater from Woods Hole, MA. Chlorinity=19.00g/kg.[2]

Seawater is quiet complex and factors affecting the corrosivity of seawater are not easily separated from one another. Dissolved oxygen is a major factor affecting the corrosivity of seawater. Typically, the higher the amount of dissolved oxygen the greater the corrosion rate. Biological activity can also affect corrosion rate. For example a biological slime develops which hinders transport to and from the metal surface thus limiting the corrosion rate. Other organisms may attach firmly and promote localized corrosion by forming crevices or initiating pitting.[3]

Ozone

Ozone has seen use disinfecting waters for over a century, primarily in Europe. Ozone has been used in the treatment of drinking waters for several purposes from disinfection to removal of color.[4] Traditionally ozone has been used in freshwater systems but is now beginning to see use in seawater applications as well. Recently, ozone has seen increased use as an alternative biocide to chlorine containing biocides due to environmental concern over the hazardous chlorination byproducts.

In water treatments ozone is one of the strongest oxidizers used. Table 2 lists the reduction potentials in standard state as well as in nominal conditions for oxidants present in the systems used in these experiments.

Reduction couple	e^o (V vs. SHE)	Nominal conditions in seawater	e (V vs. SHE) at nominal conditions
O_3/O_2	2.08	Ozonated, $p(O_3)$=0.024 atm	1.55
$HOCl/Cl^-$	1.48	Chlorinated, [HOCl]=33mg/l	1.16
$HOBr/Br^-$	1.33	Brominated, [HOBr}=25mg/l	1.08
O_2/OH^-	1.23	Oxygenated, $p(O_2)$=0.95 atm	0.75
O_2/OH^-	1.23	Aerated, $p(O_2)$-0.2 atm	0.73

Table 2. Reduction potential for oxidants present in seawater[5]

Wyllie, Brown, and Duquette have given a synopsis of the reactions involving ozone and seawater.[5] A summary of the reactions in seawater involving bromide and ozone are shown in figure 1. These are important reactions considering that the oxidation of bromide by ozone forms hypobromous acid (HOBr) which also acts as an oxidant.

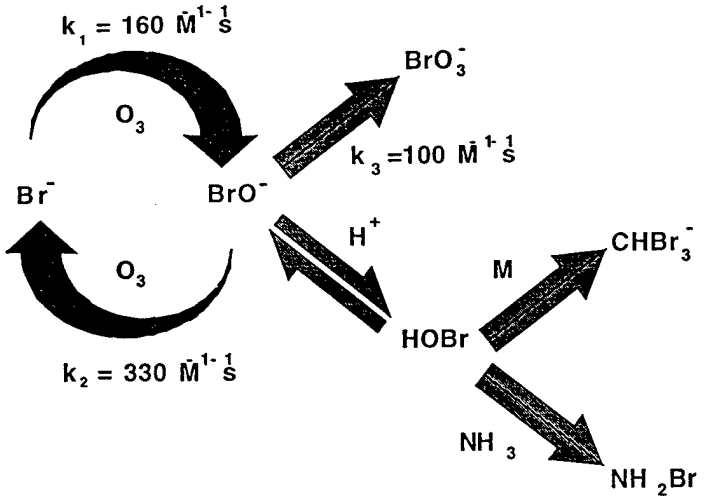

Figure 1. Summary of reactions involving ozone and bromide in seawater.

The bromide ion (Br^-) is oxidized by ozone to hypobromite (BrO^-) which can then react again with ozone returning to bromide or can associate with H^+ forming HOBr. The final alternative is further oxidation to form the bromate ion (BrO_3^-). The bromate ion is an undesirable end product in these reactions because it no longer plays a role as a biocide in the solution. Wyllie, Brown, and Duquette have found in their tests in ozonated artificial seawater that bromate is the predominant bromide species present in solution after approximately a week of ozonation.[5]

The chloride ion is oxidized in a similar manner however, the rate constant (k) is much slower and, although chloride is present in much larger amounts than bromide, relatively little of it reacts to form hypochlorite ($HOCl^-$), an effective biocide. The small amount of hypochlorite that will form will quickly react to oxidize bromide to hypobromite.

The stability and decomposition rate of ozone in water is governed by a wide variety of factors including pH, temperature, exposure to ultraviolet light, concentration of ozone and radical scavengers which can be either organic or inorganic. An important group of elements that can be oxidized by ozone, and are present in seawater, are the halides Cl- and Br-. The halides present a demand for ozone in the seawater itself. The components in

the solution that react with ozone before ozone has the ability to fulfill its designed role can be thought of as the ozone demand. For example the species in seawater Br^- creates a demand by reacting with ozone to ultimately form bromate, these reactions use ozone before the ozone will have an opportunity to act as a biocide which is its purpose in the solution.

Electrochemical

For corrosion to occur both an anode and cathode must be present and the reactions, when coupled, must be thermodynamically favorable. Examples of an anodic reaction is the dissolution of metal as shown in equation 1 where e^o is the standard half cell potential at standard state. Equation 2 shows an example of a cathodic reaction and its corresponding half-cell potential. The standard half cell potential are referenced to the standard hydrogen electrode (SHE) which is arbitrarily defined as 0.000V.

$$Cu = Cu^{++} + 2e^- \qquad e^o=0.342 \text{ V vs. SHE} \qquad (1)$$

$$O_2 + 4H^+ + 4e^- = 2H_2O \text{ (pH 0)} \qquad e^o=1.229 \text{ V vs. SHE} \qquad (2)$$

Half cell potentials can be added algebraically to obtain E, the potential of equilibrium between the anode and cathode. This value of E is related the change in free energy as shown in equation 3, where n is the number of equivalents exchanged and F is Faradays constant, equal to 96500 C/equivalent. The free energy (ΔG) must be negative for the reaction to be thermodynamically favorable.

$$\Delta G = -nFE \qquad (3)$$

Variations from standard state are typical, to calculate the half cell potential in such a case the Nernst equation is used, equation 4. Where, according to the chemical equation, m[Reactants]=n[Products], R is the gas constant, and T is the absolute temperature.

$$e = e^{o} - \frac{RT}{nF} \ln \frac{[\text{products}]^{n}}{[\text{reactants}]^{m}} \tag{4}$$

Because electrons are exchanged in this process the flow of electrons, or current can be equated to the corrosion rate as shown in equation 5, where r is corrosion rate, I is the current, a is atomic weight, and A is surface area exposed.

$$r = \frac{Ia}{AnF} \tag{5}$$

At the equilibrium potential the anodic current is equal to the cathodic current because the rates of these reactions must be equal. The current density (I/A) at which this occurs is the corrosion current density (i_{corr}). It is the combination of the anodic and cathodic currents, typically assuming that the area of the cathode is equal to the area of the anode.

Some of the tests used in this study involved polarizing the electrode away from its steady state equilibrium potential and current density; physically altering the potential of the system in either the cathodic or anodic direction. If the reaction is controlled by the rate of exchange of electrons the reaction is under activation control, resulting in a linear relationship between the potential and the log of the current density related through the Tafel constant β. The Tafel constant applies to both the cathodic and anodic direction although the anodic tafel constant may not equal the cathodic tafel constant. If high reaction rates consume the reduction reactants faster than they can arrive at the surface the cathodic reaction is under concentration control and the cathodic reaction will no longer increase in current for further changes in potential.[6] See figure 2 for a better understanding.

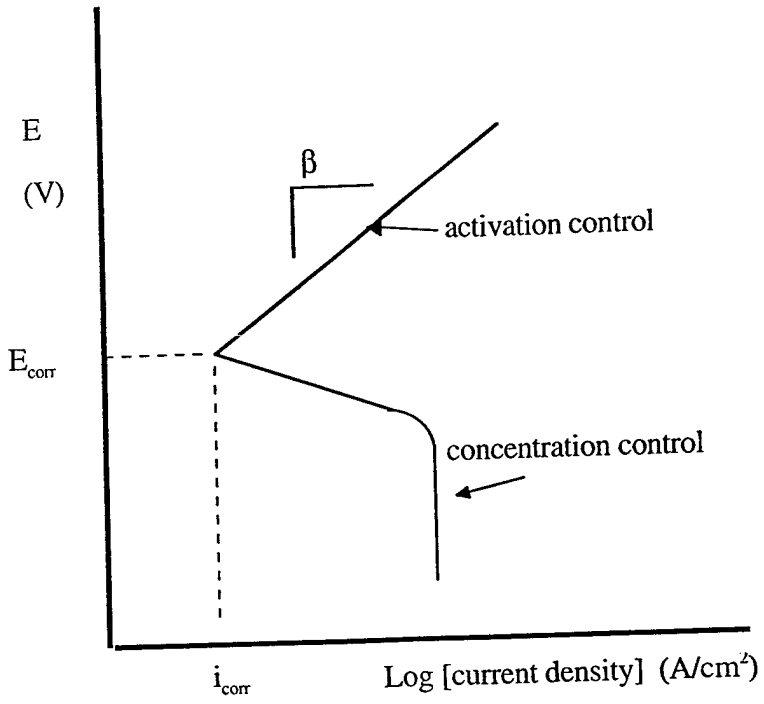

Figure 2. Example polarization curve showing activation control, concentration control, and tafel constant .

The polarization curves produced, typically potentiodynamic curves, (where the potential is changed in small steps and the current is recorded) can provide important information concerning the corrosion behavior of these alloys in these environments. In addition to the data above the curves can also indicate passivity and susceptibility to localized corrosion.

Uhlig gives two definitions of passivity: 1) " A metal is passive if it substantially resists corrosion in a given environment resulting from marked anodic polarization." and 2) "a metal is passive if it substantially resists corrosion in a given environment despite a marked thermodynamic tendency to react."[7] Passivity typically involves a thin oxide film, a good example being stainless steels where a chromium oxide film forms which is typically 10-100Å thick. Passivity is displayed in polarization curves as a region of very steep or no slope of the E versus i curve as shown in figure 3.

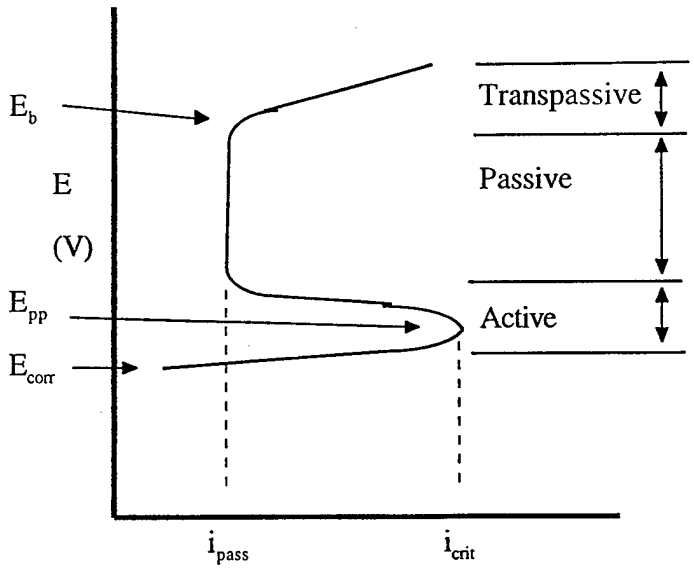

Figure 3. Schematic polarization curve of a metal showing passive behavior.

Figure 3 also shows other important features. There is a point at which the potential has been driven so far anodic to E_{corr} that the passive film breaks down. This breakdown occurs at the breakdown potential (E_b) and takes the metal into the transpassive region. Between the E_{corr} value and the passivation potential (E_{pp}) the metal is under activation control and displays active behavior. Above E_{pp} , and when the critical current density ($i_{crit.}$) is exceeded the passive film is stable with a current density (corrosion rate) of $i_{pass.}$.

To obtain an instantaneous corrosion rate the polarization resistance technique can be used. Also called linear polarization resistance, this process polarizes the sample only a few millivolts around the open circuit potential (E_{corr}). Generally in this region the polarization curves are linear and the overvoltage can be used to calculate the corrosion current density (i_{corr}). Equation 6 can be applied for both anodic and cathodic deviations from E_{corr} with η representing the overvoltage or polarization away from E_{corr} in either the

cathodic or anodic direction and i representing the anodic or cathodic current density at that overvoltage.

$$\eta = \beta \log \frac{i}{i_{corr}} \tag{6}$$

The resistance is related to the change in overvoltage versus over current density which is the slope of the resulting curve. This allows the determination of i_{corr} with the assumption of the anodic and cathodic tafel constants as shown in equation 7.

$$R_p = \frac{\beta_a \beta_c}{2.3 i_{corr}(\beta_a + \beta_c)} \tag{7}$$

Having found i_{corr} the corrosion rate can be calculated according to equation 5 as mentioned earlier.

Crevice Corrosion

Crevice corrosion is a form of localized corrosion attack occurring in locations that set up conditions for stagnant solution. Generally alloys suffering this type of attack have a passive film which must breakdown locally for a crevice to initiate.[6] The solutions that favor crevice corrosion contain an oxidizer (typically oxygen) and chloride, thus seawater can be particularly troublesome.

Within the crevice a typical corrosion process occurs with the reduction of oxygen and oxidation of the metal. As this continues all the oxygen in the crevice will be consumed. Corrosion will continue beyond this point because the reduction of oxygen can continue to occur immediately outside the crevice. Within the crevice anodic dissolution continues, which draws in chloride ions to balance the charge within the crevice. The crevice will also become more acid as metal ions combine to form hydroxides leaving an increased concentration of H^+ ions. The pit now becomes more acid, with the low pH and high chloride concentration breaking down the passive film protecting the creviced area.

This leads to large corrosion rates of the areas under the crevice. An example reaction is shown in equation 8.

$$M^+Cl^- + H_2O = MOH_{(s)} + H^+Cl^- \quad (8)$$

A separate type of crevice corrosion can occur with the presence of Cu. Because copper can form two cationic states it has the ability to be reduced. Copper ions will build up in the crevice and the reduction reaction will become the reduction of Cu^{++} to Cu^+ or Cu^+ to Cu^0 inside the crevice while the anodic reaction will occur immediately outside the crevice with Cu^o going to Cu^+ or Cu^{++}. Consequently crevice corrosion occurs immediately outside the crevice.

Recently Brown[8] explained a similar crevice corrosion morphology that occurs in highly corrosion resistant Ni-base alloys. Corrosion of these alloys was observed immediately outside the crevice in ozonated seawater and has been termed boundary layer corrosion (BLC). BLC is a result of transpassive dissolution of nickel and oxidation of the nickel ions resulting in the acidification of the stagnant layer immediately outside the crevice, and a corresponding loss of passivity. BLC was correlated with the pitting resistance equivalent number (PREN) which is a calculation of the particular fractions of the weight percent of alloying additions such as Cr, Mo, and W. Alloys with a PREN greater than 50 were susceptible to BLC.

Ni-Cu Alloys

Alloys of nickel and copper are typically used in flowing seawater applications. The flowing seawater helps to maintain passivity and prevent biofouling. The corrosion rates are typically so low that there is not enough dissolved copper ions to prevent biofouling.[9] These alloys form a passive film in systems containing oxygen that is generally stable with copper concentrations up to approximately 62-72wt.%.[7] Because these alloys rely on passivity for corrosion resistance in seawater, flowing conditions are necessary to prevent

the attachment of organisms which will cause pitting. In stagnant or quiescent conditions marine organisms will attach and set up an oxygen concentration cell causing severe pitting beneath the attachment point. Pitting or other forms of localized corrosion can occur without the aid of biofouling organisms however the attack will not be as severe. [9]

A study by Brown[10] found that ozone adversely affects the corrosion properties of Monel 400. As the ozone concentration is increased up to 2.3 mg/l a noble shift in the corrosion potential occurs as well as an increase in corrosion rate. Brown also found susceptibility to crevice corrosion indicated by the breakdown and repassivation potentials shifting below the corrosion potential in potentiodynamic investigations.

Cupronickels

Copper-nickel alloys (cupronickels) are readily used in seawater applications because of corrosion resistance that is built up due to the formation of a protective film, resistance to stress corrosion cracking, excellent performance under impingement attack and the presence of copper ions which prevent biofouling. Being a noble metal copper does not typically experience corrosion due to the reduction of hydrogen and thus is resistant to acids providing that the acid is free of oxygen or does not contain a oxidizing agent.[11] Anodic dissolution of copper typically forms the divalent ion (Cu^{++}). In chloride solutions complexes can for (such as $CuCl2^-$) which will shift the Cu^+/ Cu^{++} equilibrium causing the cuprous ion (Cu^+) to be the primary dissolution product.[12] The protective film formed on copper is typically Cu_2O a p-type semiconductor oxide which controls the corrosion process by limiting the migration of Cu ions and electrons through the film. Alloying additions such as nickel and iron, further slow the corrosion process by stabilizing the film and reducing the ionic conductivity.[7]

In clean, quiescent, seawater general corrosion usually occurs with corrosion rates typically less than 1mpy (mils per year).[12] Because these alloys are not dependent upon a

passive film for protection they are generally not susceptible to pitting in seawater. Local attack can be due to hard water, dirt or other particles in the water, or sulfides present in the water which deteriorate the protective film.[7]

Continuous chlorination has been found to increase the corrosion rate of CDA 706 and increase susceptibility to impingement attack.[11] Yang, Johnson, and Shim observed the corrosion effects on CDA 715 and CDA 706, in synthetic Lake Michigan water, found that the corrosion rates of these alloys generally increases in the presence of 1mg/l of ozone. However, with time, the corrosion rates will decrease due to the formation of a mineral scale layer. In the presence of an equal concentration of sodium hypochlorite the corrosion rates of these alloys also increased but not to the same extent as in the presence of ozone.[13] Lu, in her study of CDA 715 in ozonated 0.5 N NaCl solutions, found that a noble shift in corrosion potential occurs which is virtually independent of ozone concentration. Lu also found that dissolved ozone decreased corrosion susceptibility due to a thinner film containing a higher concentration of oxygen to chloride as measured by current density measurements.[14]

Experimental

Studies were carried out in two groups; a group of tests in the lab at Rensselaer Polytechnic Institute (RPI), and tests conducted at the LaQue Center for Corrosion Technology in Wrightsville Beach, NC.

In Lab

Seawater

Studies conducted in the lab at RPI were performed in filtered seawater obtained from Woods Hole Oceanographic Institute in Woods Hole, MA. Seawater was pumped from the MBL dock on 7 February 1997; results from an assay conducted 29 January 1997 are shown in table 3.

pH	8.08
Salinity	30.36%
Conductivity	46.56 mS
Temperature	6.1°C
Oxygen	10.95 mg/l
Ammonia	<0.075 mg/l
Nitrate	0.79 mg/l
Phosphate	3.99 mg/l
Copper	0.12 mg/l
Sulfide	0.006 mg/l

Table 3. Properties of seawater obtained from Woods Hole, MA.

Approximately 1000L of filtered Seawater were obtained, transported, and stored in 132L plastic containers double lined with polyethylene bags. Containers were sealed with a polyethylene bag, the lid was secured using duct tape.

Six 60L tanks were prepared of in lab studies. Three of these were ozonated at a rate of 0.3 m^3/hr (1SCFH) by bubbling an ozone/oxygen mixture into the seawater through fritted glass bubblers. The remaining three tanks were used as controls and aerated at 0.3 m^3/hr (1SCFH).

Tanks were ozonated/aerated for approximately ten days before samples were immersed to insure solution stability. The three ozonated tanks were monitored for pH; and concentrations of apparent residual ozone, bromide, bromate, and hypohalite. Apparent residual ozone concentration was measured using the Indigo Trisulfonate Method.[15,16] Concentrations of bromide, bromate, and hypohalites were measured with the titration procedures described by Wyllie, Brown, ad Duquette.[5] Solutions were monitored after 1 day, 1 week, and immediately before sample immersion, thereafter solution testing was done concurrently with sample testing. Aerated tanks were measured for pH and bromide concentration prior to sample immersion. Approximately 6L of solution was changed out each week to prevent concentration of by-products and account for evaporation. Distilled water or fresh seawater was used depending upon the results of the most recent titration test.

Gas Delivery

Ozone was generated from an oxygen concentrated feed gas supplied by an AirSep® AS-12 oxygen concentrator. The oxygen concentrator was set at 6.9E4 Pa (10psi) and 55% output capacity delivering a 90-95% oxygen gas stream (remainder nitrogen) to the ozone generator. An American Ozone™ GS2-14 ozone generator was used to produce ozone using corona discharge. The ozone generator was set to 2.0E4 Pa (3psi) and 85% power setting to produce 3.35% ozone in 90-95% oxygen or 47g O_3/m^3.

Ozone flow to the tanks was controlled through 316SS tubing and glass lined flow meters. Individual tanks were set to $0.03m^3$/hr (1SCFH) to supply ozone at 1.3g O_3/hr and oxygen at 39g O_2/hr. Form the flow meters the gas was delivered to the tanks via norprene™* and then PTFE tubing once inside the tank.

---

* Norprene, trademark of Norton, Co.

Gas delivery to the aerated tanks was handled in a similar manner, From the house compressed air system to flow meters which controlled the flow at $0.03m^3/hr$ (1SCFH). Again, norprene® and PTFE were used to deliver the air to the tanks.

Tanks were covered with unbleached polyvinylchloride sheets with holes cut for the incoming gas, a ventilation system to control outgassing, and a small port for sampling, pH measurements and water change out. Off-gassing ozone was vented through vinyl tubing with the aid of two small fans and diluted into the environment.

Samples Preparation

Four types of samples were used: weight loss samples 1.9x5.0x0.32cm (0.75"x2"x0.125") with a 0.95cm (3/8") hole in the center, crevice samples (identical in dimension to the weight loss samples), and electrochemical samples which were either wire or a flag specimen if wire samples were unavailable. Wire samples used were obtained from weld wire and thus the diameter varied between alloys.

Weight loss, crevice, and flag samples were obtained through Metal Samples and include several alloys designed for marine service. Alloys included are Monel 400 (UNS N04400), Monel K-500 (UNS N05500), CDA 706 (UNS C70600), and CDA 715 (UNS 71500). The composition of the alloys used, as determined from mill analysis, is shown in table 4.

	C	Cu	Fe	Mn	Ni	P	S	Si	Other
Monel 400	0.131	32.3	1.630	0.830	64.55	0.002	0.005	0.180	Al-0.160, Sn-0.002, Pb-0.002
Monel K-500	0.150	30.03	0.640	0.74	64.96	-	0.002	0.150	Al-2.880, Ti-0.450
CDA 706	0.001	88.17	1.450	0.440	9.79	0.002	0.004	-	Pb-0.010, Zn-0.080
CDA 715	0.001	68.62	0.580	0.580	30.01	0.002	0.004	-	Pb-0.010, Zn-0.090

Table 4. Compositions of Alloys investigate in lab studies.

Flat samples were prepared by lapping in fuel oil using 50μm Al_2O_3 as an abrasive, rinsing with a detergent and continuing to 400 and 600 grit Al_2O_3 abrasive paper rinsing with water between each step. Samples were further ultrasonically cleaned in ethanol and rinsed with distilled water. Wire samples were polished by hand to 600 grit with the aid of a power drill and SiC abrasive paper, then cleaned with ethanol and distilled water.

Crevices were created with PTFE crenelated washers. The washers were ultrasonically cleaned in ethanol and rinsed in distilled water and used as received.

Sample Assembly and Exposure

Weight loss coupon samples were threaded with a glass rod through the center hole and suspended in the tank. Three weight loss specimens of each alloy were placed in the tank with one being withdrawn after each 30 day interval up to 90 days.

Crevice coupons of each alloy were also in triplicate to be withdrawn at 30 day intervals up to 90 days. Crevice assembly was performed while submerged to accelerate

wetting and insure wetting within the crevice. Assembly was made by sandwiching the crevice coupon between two PTFE crenelated washers. The nut, bolt, and washers used to hold the assembly together were made of titanium; the bolt being wrapped in PTFE tape to insulate the bolt and prevent galvanic interference, a schematic of the assembly is shown in figure 4. Samples were tightened to one turn past finger tight and electric isolation of the sample from the bolt, nut, and washer was checked with a voltmeter. Crevice samples were suspended from glass rods by PTFE and ePTFE rings and string.

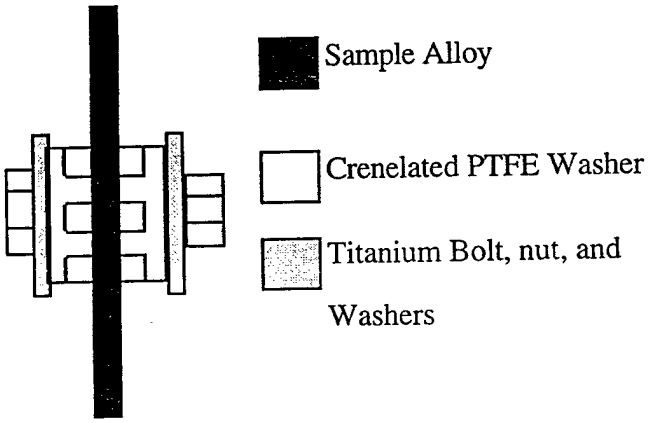

Figure 4. Schematic showing assembly of crevice samples.

Electrochemical samples in the form of wire were wrapped around a glass rod and suspended in the natural seawater environment. Where wire was unavailable flag samples drilled with a small hole where secured to a glass rod for suspension into the natural seawater solution. electrochemical tests were performed concurrently with removal of weight loss and crevice samples. One sample was left in the tank the entire ninety days, the others were tested at 30 day intervals in the tank and then removed for further testing in an electrochemical cell.

Figure 5 shows sample arrangement in tank. It can be observed that the electrochemical specimens (wires) are suspended from glass rods across the top portion of the supporting rack where as the weight loss and crevice samples are suspended on glass rods supported on the middle portion of the rack. The aeration bubbler is also shown in this figure. In the ozonated tanks this bubbler would be manufactured of fritted glass and be placed on the forward wall of the tank.

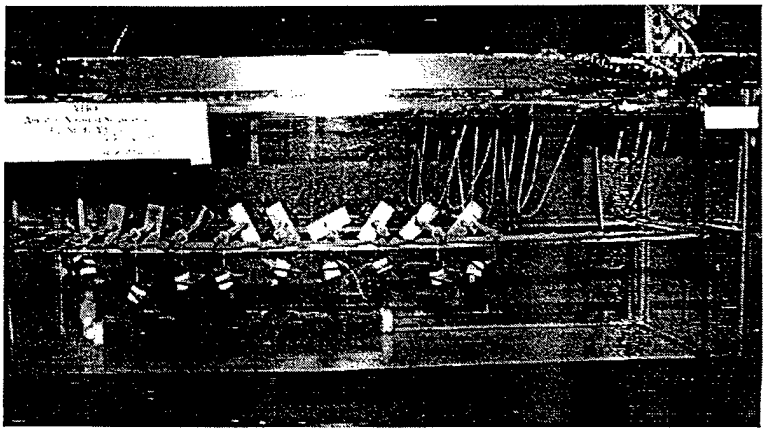

Figure 5. Tank set-up on in lab experiments

Upon removal weight loss and crevice samples were rinsed with distilled water and stored suspended in a dessiccator. Crevice samples were disassembled placing the metal plate in the dissiccator while cataloging the bolt, nut, and washers for later use if needed. Photographic records of each sample were also taken at this point.

Electrochemical Experiments

Electrochemical experiments were performed to aid in the understanding of the corrosion process. Linear polarization resistance and potentiodynamic scans were performed after open circuit potential measurements. Electrochemical studies were performed while submerged in the tank as well as in a separate electrochemical cell containing solution withdrawn from the tank. All electrochemical tests used a standard calomel reference electrode (SCE) using a EG&G PAR model 173 with a model 276

interface for control with a personal computer. The standard calomel electrode(SCE) is 0.241V vs. The standard hydrogen electrode (SHE)

In the tank open circuit potential measurements were made for four thousand seconds to obtain a steady potential value. Immediately after the open circuit measurement a linear polarization resistance scan was performed to observe the instantaneous corrosion rate of the sample in the tank. Linear polarization resistance was performed at a scan rate of 600V/hr starting at the open circuit potential and proceeding anodically to 10mV versus the open circuit potential.

The electrochemical samples were then removed from the tank into a six port electrochemical cell. The cell was filled with tank solution and care was taken to keep the sample immersed as it was being transferred from the tank to the cell. In the cell tests for open-circuit potential and linear polarization resistance were repeated as described above. Potentiodynamic scans were also performed to determine the corrosion behavior of these alloys. These scans were not performed in the tank due to the possibility of the tank being contaminated with metal ions as sample dissolution takes place. All alloys were scanned at 10V/hr. in 2mV increments. CDA 706 was scanned from -500mV to 750mV versus open circuit potential where as CDA 715, Monel 400, and Monel K-500 was scanned from -500mV to 750mV versus SCE.

A description of the set-up can be seen in figure 6. A platinum mesh was used as the counter electrode and the cell was sealed so that the ozone could be properly vented. The reference electrode was isolated from the test solution to prevent cross contamination and a salt bridge was used to electrically connect the test solution with the saturated potassium chloride solution used for the reference electrode. Fritted glass bubblers were used to deliver the gas to the cell. The sample serves as the working electrode.

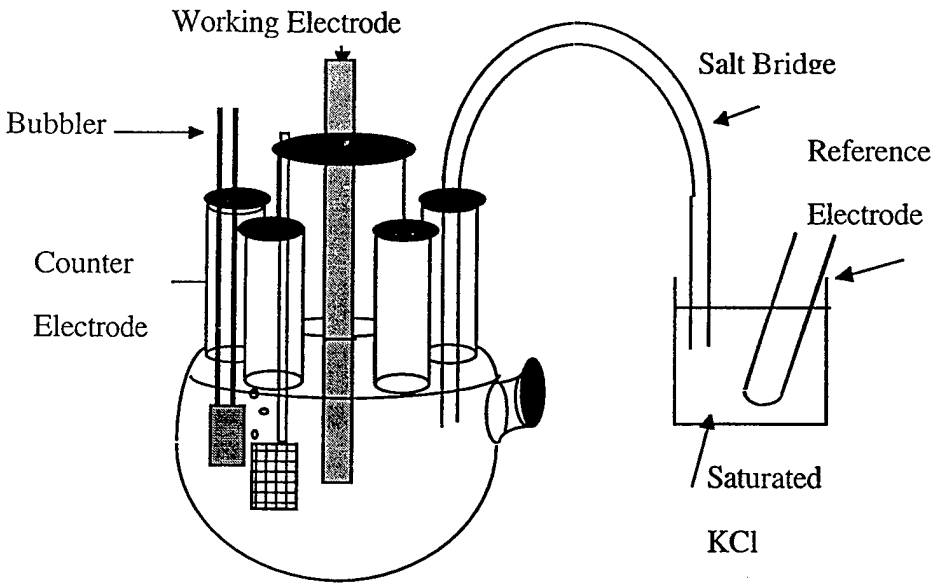

Figure 6. Schematic showing electrochemical cell set-up

After electrochemical testing has been completed the samples are removed from the cell, the waterline is marked for immersed area calculations, and the samples are rinsed and stored for later examination.

Cleaning samples

Weight loss samples collected during these experiments were cleaned to remove corrosion product, observe the extent of the damage, and get an accurate weight loss determination. The alloys were cleaned in a 10% sulfuric acid solution (H_2SO_4), scrubbed with a soft bristle brush, rinsed in water, rinsed in acetone and dried with compressed air. This process was performed repeatedly if necessary to remove all observable corrosion product. The mass of these samples was then recorded and the samples were returned to the dessiccator for storage.

Experiments performed at LaQue Center for Corrosion Technology

Seawater

Experiments were conducted at the LaQue Center for Corrosion Technology in Wrightsville Beach, N.C.. This facility is immediately adjacent to the ocean and natural seawater is continually available. For these purposes it was important to have warm seawater, allowing a window of June-mid October for testing. Experiments were conducted in natural seawater which was pumped directly from the ocean, flowed through the tanks, and returned back into the ocean. Information from the summer of 1995 was obtained for seawater from the same location and is shown in table 5. A large number of fouling organisms were also present during their season of attachment thereby providing an excellent test of the biocide abilities of ozone.[17]

pH	7.8-8.0
Salinity	33.0-37.0 g/l
Conductivity	47.8-58.7 mS
Temperature	25.8-29.8°C
Dissolved Oxygen	5.0-6.6 mg/l
Ammonia	<0.05 mg/l
Chloride	17.3-20.5 mg/l
Total Iron	0.1-0.2 mg/l
Sulfate	2.4-2.8 mg/l
Sulfide	<0.005 mg/l

Table 5. Seawater information for Wrightsville Beach, N.C. June 1995 to August 1995[17]

Biocide Delivery

Experiments at the LaQue Center for Corrosion Technology compared the biocide action of ozone and chlorine-based biocides in seawater.

Ozone was generated from an oxygen concentrated feed gas obtained from OGSI® OG-15 Oxygen concentrator running at 6.2E4 Pa (9psi) with an output of

0.37m^3/hr. (13scfh). Ozone was generated from this feed gas by an OREC®V10AR/O ozone generator at 89V and 5.5 lpm of 2.75% O_3 in the gas stream resulting in approximately 16gO_3/hr being delivered to the tanks. Ozone was delivered to the tanks through PVC and tygon™[†] tubing and bubbled into the seawater by fused alumina bubblers. Flowmeters were used to regulate air flow into the testing tanks. Each tank contained two bubblers one at the head of the tank before the samples and a second immediately in front of the recirculation pump, this was done to use the pump impeller to better disperse the ozone in the seawater. These measures resulted in a measured residual ozone concentration of approximately 0.2mg/l over the duration of the test. Ozone was again measured using the indigo trisulfonate method mentioned earlier. Refresh rates in these tank were held steady at 1.14 l/min. thus providing a continuous supply of fresh seawater. Refresh rates were another parameter used to control the amount of biocide present in solution.

The chlorine-based tanks were feed continuously during the duration of the test. The free active chlorine level averaged 0.33mg/l over the duration of the test with chlorination being provided through the injection of liquid sodium hypochlorite. Refresh rates in the chlorinated tanks were 1.9 l/min.

Both ozonated and chlorinated tanks were allowed to come to equilibrium before samples were immersed, making sure that the desired level of biocide was achieved in each tank. Solution and ozone generation parameters were recorded daily throughout the test.

[†] Tygon, trademark of Norton, Co.

Sample Preparation

Experiments conducted at LaQue Center for Corrosion Technology were designed to study crevice corrosion with a metal to metal and a metal to non-metal crevice. These were simple immersion tests lasting sixty days.

Alloys examined in these experiments were also represented in the lab experiments. The Cu-Ni and Ni-Cu alloys were obtained through Metal Samples® with the composition, as determined from mill analysis, being shown in table 6.

	C	Cu	Fe	Mn	Ni	P	S	Si	Other
Monel 400	0.090	30.90	1.460	1.020	66.18		< 0.001	0.290	Al-0.060
Monel K-500	0.150	29.72	0.590	0.720	65.39		0.001	0.150	Al-2.840, Ti-0.440
CDA 706	0.002	88.83	1.140	0.410	9.400	0.001	0.013		Pb-0.001, Zn-0.200
CDA 715	0.001	68.70	0.620	0.780	29.76	0.002	0.001		Pb-0.010, Zn-0.090

Table 6. Composition of alloys used at LaQue Center for Corrosion Technology

Plates of 10x10x0.32cm (4"x4"x1/16") were drilled the a 0.95cm (3/8") hole in the center. To create the metal to metal crevice a metal washer 3.2cm (1 1/4") diameter with a 0.95cm (3/8") hole in the center was manufactured by waterjet cutting from the same stock used to make the plate samples.

Samples were received and prepared by lapping in alumina and fuel oil. Samples were then cleaned with kerosene, and ultrasonically cleaned in a detergent solution. Samples were then polished by hand with 600 grit SiC abrasive paper. Final cleaning was done ultrasonically in distilled water and alcohol. Both plates and washers were prepared in an identical manner.

Plate samples were labeled with a three character alloy designator and numbered 1-15. Washers were labeled with two characters the first representing the alloy the second the particular sample. All metal samples were weighed prior to assembly for weight loss comparison after completion of the experiments.

Flat PTFE washers were used to create a metal-non-metal crevice with the washers. These PTFE washers have dimensions of 0.97cm (0.380") ID, 2.0cm (0.812") OD, and 0.079cm (0.031") thickness. Washers were cleaned ultrasonically in distilled water before assembly of the crevice specimens.

Sample Assembly and Exposure

Crevice specimens were created by mating the alloy plate with two washers of like metal on either side aligning the central hole, two PTFE washers were then mated to those washers. The assembly was held together with titanium washers, nut, and bolt insulated with PTFE tape to prevent galvanic effects. A schematic showing the assembly of these samples is included as figure 7. Samples of each alloy were prepared in triplicate for each environment. Therefore, there were three crevice samples of each alloy exposed to ozonated seawater and three exposed to chlorinated seawater.

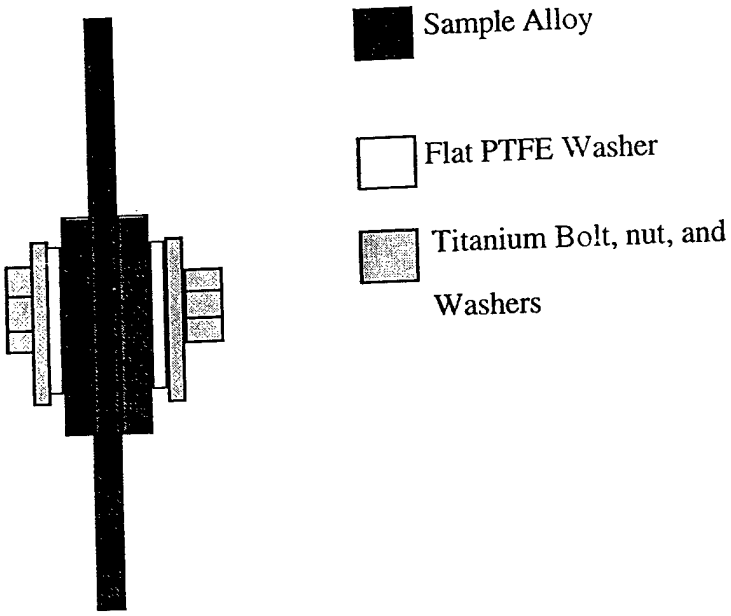

Figure 7. Schematic of crevice assembly used in N.C. experiments

Samples were aligned so that the bolt was approximately through the center of the plate and washers then tightened to 5.65 N*m (50 inch*lbs). Electric isolation of the sample alloy from the titanium bolt was checked with a multimeter.

Samples were mounted vertically on polycarbonate racks for immersion, these racks were held vertical with wooden cross members above waterline. The tanks contained approximately 400L of seawater with a refresh rate of 1.14 to 1.89 lpm as mentioned earlier. An equilibrium was maintained with a recirculating system creating a semi-quiescent environment. Tanks were covered and in the open atmosphere although protected from precipitation. Figure 8 shows a typical set-up, the tank being open so that the sample assembly can be seen.

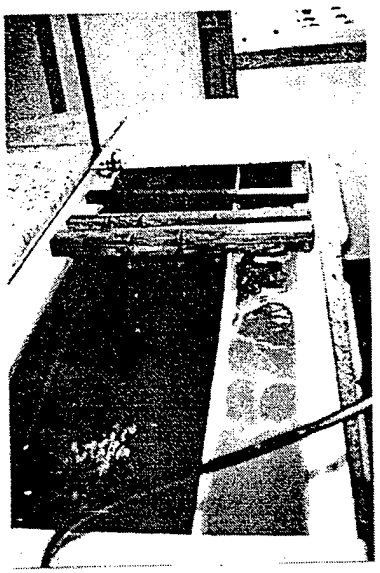

Figure 8. Photograph showing tank set-up at LaQue Center for Corrosion Technology

Samples were exposed starting 25 July 1997 for a sixty day test period ending 23 September 1997, within the warm water test window.

A brief examination after 72 hours was made by a technician at LaQue center for Corrosion Technology. After sixty days the potential of the alloys in the natural seawater was checked versus Ag/AgCl electrode for comparison with in-lab tests. The samples were then removed from the seawater and photographed while still on the rack. Two samples of each alloy were removed from the rack, disassembled, photographed, and rinsed. The third sample of each alloy was removed from the rack and stored as is for later investigation.

Water samples were also collected for titration analysis of bromide, hypohalide, and bromate for comparison with in lab water samples.

Cleaning Samples

The disassembled samples were then cleaned to remove the corrosion product allowing observation of the location and extent of corrosion damage as well as weight

loss measurements. Samples were soaked in 10% sulfuric acid for approximately one minute, rinsed in water, scrubbed with detergent on a mechanical wheel, rinsed in water, rinsed in acetone, and dried under warm air. The process was repeated until all corrosion product was removed.

After cleaning samples were again weighed, photographed, and packaged for shipment back to the corrosion lab at Rensselaer Polytechnic Institute (RPI).

Analysis

Upon returning to RPI the samples were carefully photographed. Pit density and size measurements were made at 10X using the standard rating chart for pitting corrosion as described in ASTM standard G 46-76.[18]

One of the cleaned samples was then chosen for sectioning leaving one cleaned uncut dissembled sample, and one uncleaned still assembled sample. Sections were made through the creviced section of the panel and both washers associated with that panel, cutting them in half. These sections were mounted in epoxy, vacuumed to achieve full penetration of the epoxy and remove any porosity .

Those samples left untouched after withdrawal from the seawater were cut in half and sectioned while still assembled to observe the corrosion as it occurred, leaving in place the corrosion product and all parts of the assembly. A section was made through the middle of the bolt holding the assembly together for a cut away view of the crevice. Samples were mounted in epoxy and vacuumed.

Mounted samples were then polished, first with a lapping machine in alumina and fuel oil and cleaned in kerosene. Samples were then polished by hand through 600 grit SiC abrasive paper, 15μm diamond, 9μm diamond, and 0.3μm alumina in 10% oxalic acid. Etching was performed using a bras etch with an alcohol bass consisting of 2g

potassium dichromate, 8ml sulfuric acid, 1-3 drops hydrochloric acid, and 100ml of alcohol.

Results

Laboratory Results

Solutions

The nickel-copper alloys and the copper-nickel alloys were placed in two separate tanks, labeled OTK2 and OTK4 respectively. Samples were immersed approximately two weeks after tank start up. Figures 9 and 10 show changes in pH and residual ozone concentration of the tank solutions with time. In OTK2 contained the nickel copper alloys the pH remained relatively constant at 8.28 while the ozone fluctuated between 0.07 mg/L and 0.59 mg/L with a mean value of 0.31 mg/L. In OTK4, containing copper nickel alloys the pH averaged 8.3 while the ozone concentration shows fluctuations between 0.11mg/L and 0.61mg/L with the mean being 0.36mg/L.

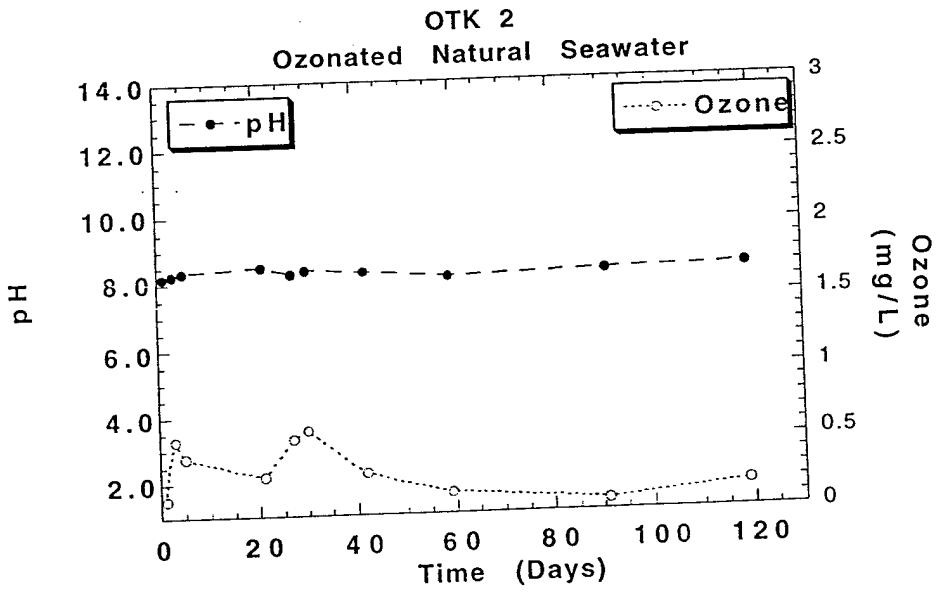

Figure 9. Change in pH and residual ozone concentration changes of solution containing nickel copper alloys.

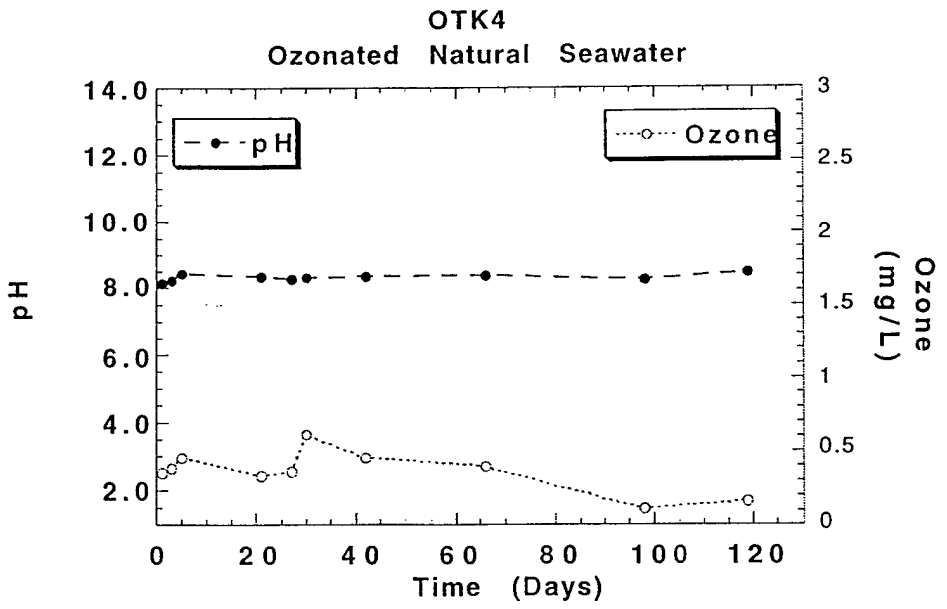

Figure 10. pH and residual ozone concentration changes of solution containing copper nickel alloys

Less than one day after sample immersion a black flocculant was seen settling in the bottom of the tank and adhering to the glass surfaces within the tank. The decrease in residual ozone concentration as time increased is believed to be due to the accumulation of this black flocculant which creates ozone demand.

Bromide species concentrations were also measured and included in the figures below as percent of total bromide. Total bromide concentration was measured at 1050μM or 84 mg/L. Figures 11 and 12 show that a majority of the bromide has been converted to the bromate ion which now constitutes 93-95% of total bromide in solution. The hypohalite ions HOBr-and OBr- form 2.3-2.8% and approximately 1% of the total bromide respectively. Free bromide is present as 2-5% of the total bromide. The concentrations of these species were relatively constant over the time of the test with these values being reached after approximately five days of ozonation.

In tanks containing aerated natural seawater, pH was the only solution parameter measured. pH remained steady at a value of 8.2 for the duration of the test in aerated seawater.

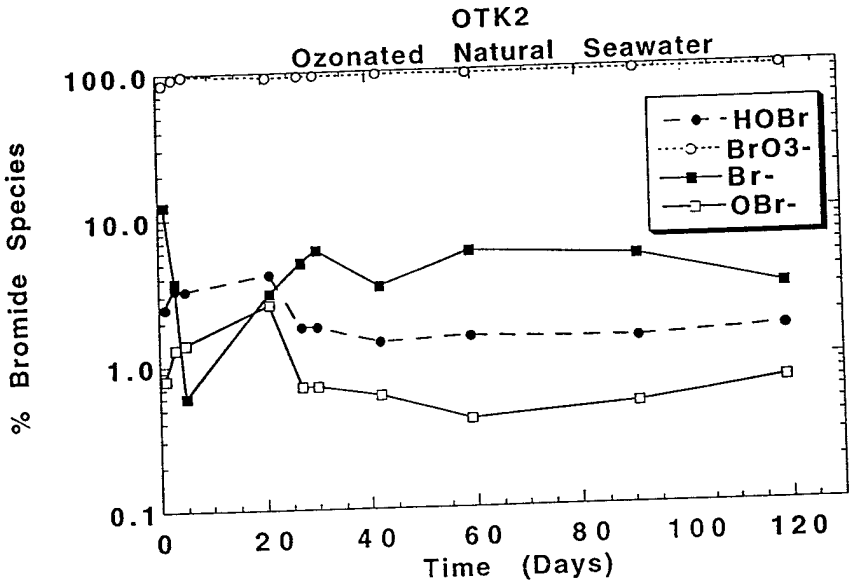

Figure 11. Change in concentration of bromide, hypohalites, and bromate with time for solutions containing nickel-copper alloys.

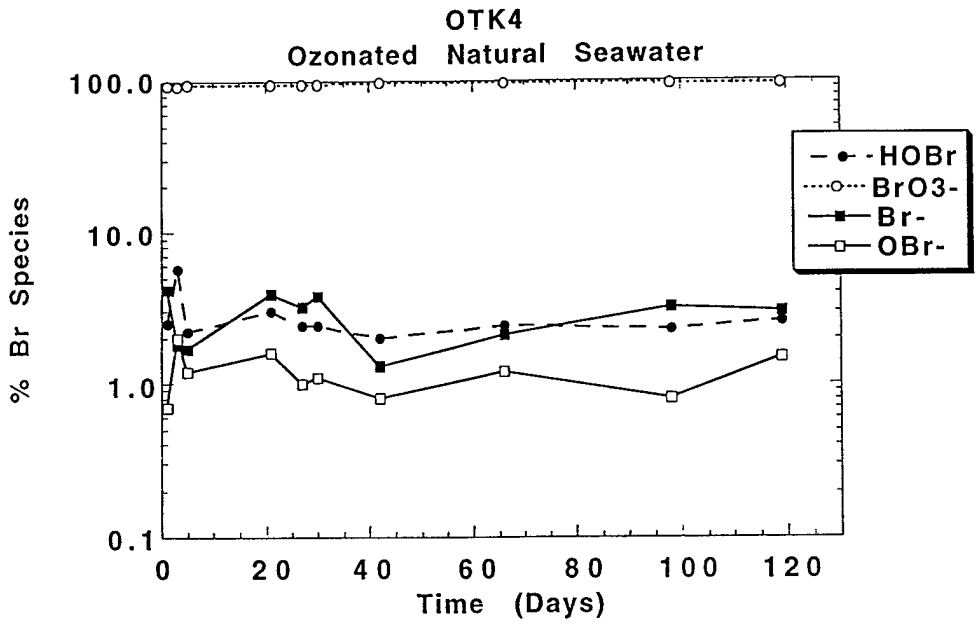

Figure 12. Change in concentration of bromide, hypohalites, and bromate with time for solutions containing copper-nickel alloys

Electrochemical results

Figures 13 through 16 show corrosion potentials comparing each alloy in ozonated and aerated seawater. Corrosion potential data was taken from electrochemical cell measurements which were found to be more stable then measurements taken while the sample was in the tank.

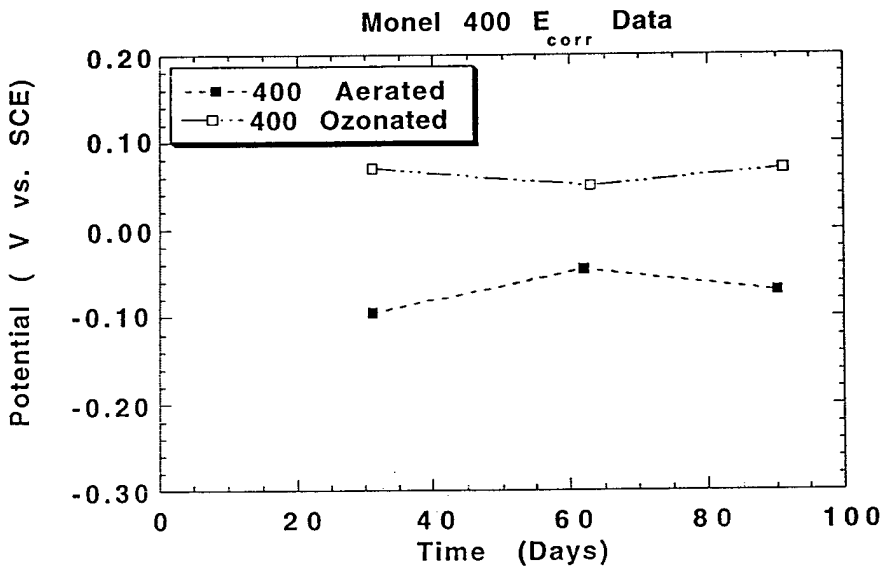

Figure 13. Corrosion Potential vs. Time for Monel 400

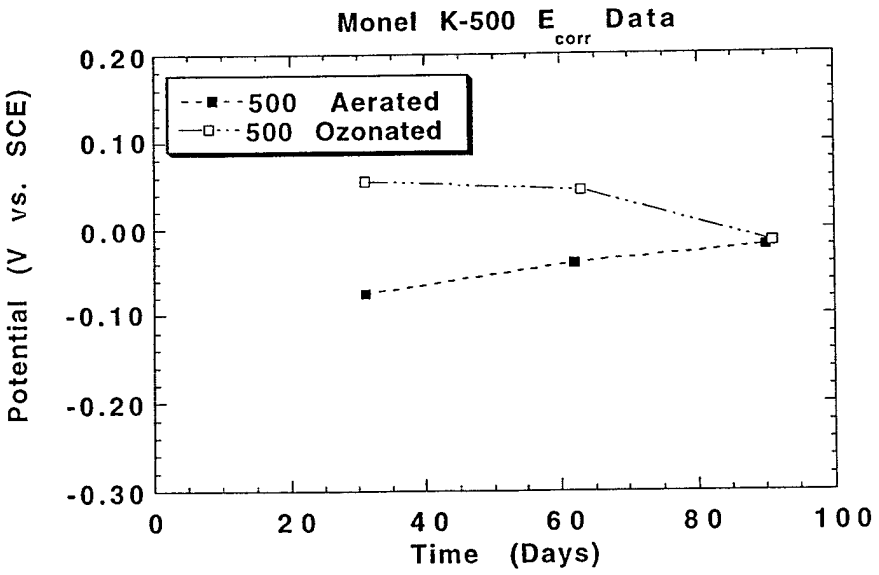

Figure 14. Corrosion Potential vs. Time for Monel K-500

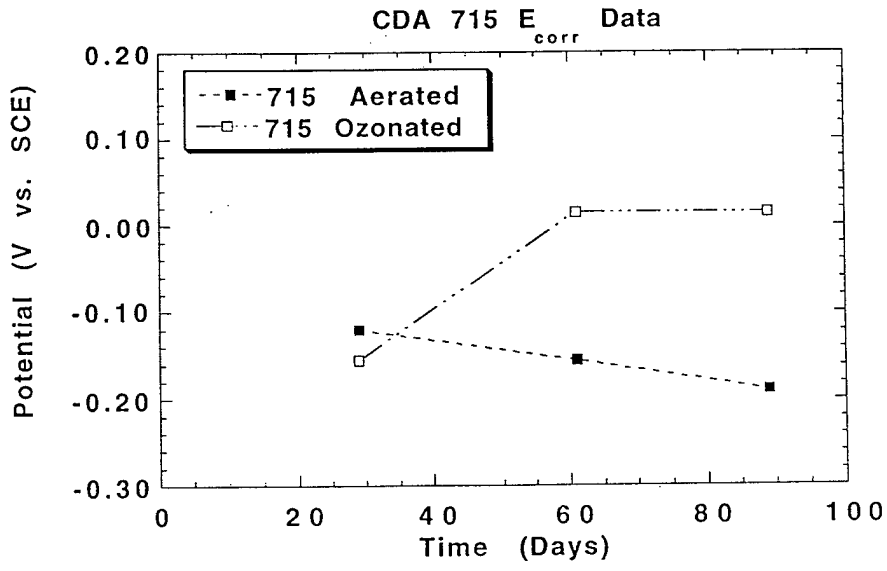

Figure 15. Corrosion Potential vs. Time for cupronickel alloy CDA 715

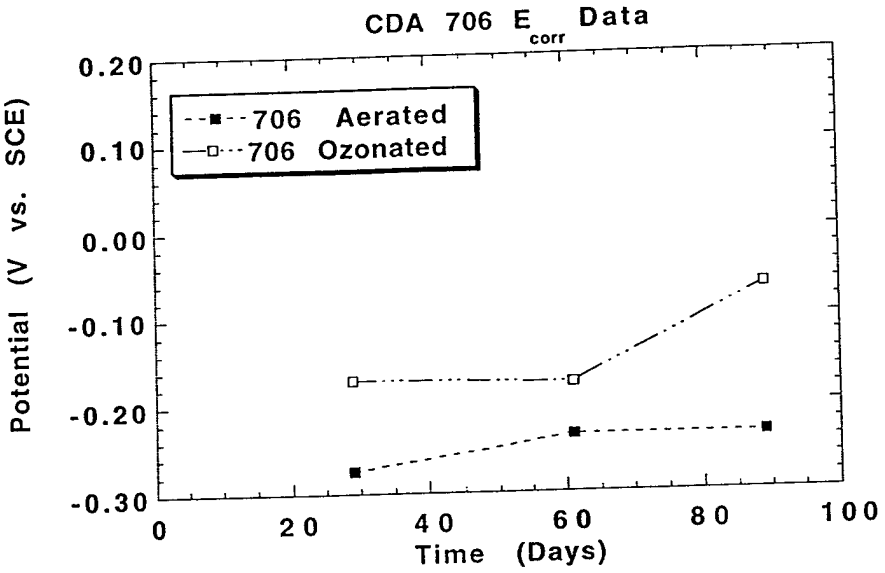

Figure 16. Corrosion Potential vs. Time for cupronickel alloy CDA 706

Each alloy shows that the corrosion potential is shifted between 0.1 and 0.2V in the noble direction in ozonated seawater when compared to the same alloy exposed to aerated seawater. As the amount of nickel in each alloys decreases the corrosion potential shifts as well. The Monel alloys have roughly the same amount of nickel (approximately 70%) whereas the CDA 715 alloy has 30% nickel and the CDA 706 alloy contains 10% nickel. This change in potential with nickel concentration occurred in both the aerated and ozonated seawater. In the Monel K-500 alloy the corrosion potential measurement in aerated seawater approaches that of the potential in ozonated seawater due. This trend is due to the increasing stability of the passive film in aerated seawater which formed more slowly than the film formed in ozonated seawater.

Potentiodynamic results are shown for each alloy in aerated and ozonated seawater as well as for time intervals of roughly thirty, sixty , and ninety days; these results are shown in figures 17 through 24.

Monel 400 shows a trait that was seen in several of the polarization scans; that is a large noble shift of the corrosion potential at the thirty day time interval. This behavior was observed in both the aerated and ozonated condition and was also seen in the aerated ninety day exposure. Those potentiodynamic curves that show the same corrosion potential seen during the steady state scan show the same noble shift of the corrosion potential in ozonated seawater. The corrosion current in ozonated seawater is greater than that seen in aerated seawater by 2-3 orders of magnitude, suggesting an increased corrosion rate in ozonated seawater. The anodic slope of the potentiodynamic scans is greater which dictates a point at more potentials at which the corrosion current of the aerated samples will be greater than that of the ozonated samples. In ozonated seawater Monel 400 shows a double corrosion potential peak at thirty days. This behavior is due to a large region of equilibrium in which the portion between the curves is actually part of the cathodic reaction. This part of the curve is shown as it is due to the computer plotting the absolute value of current.

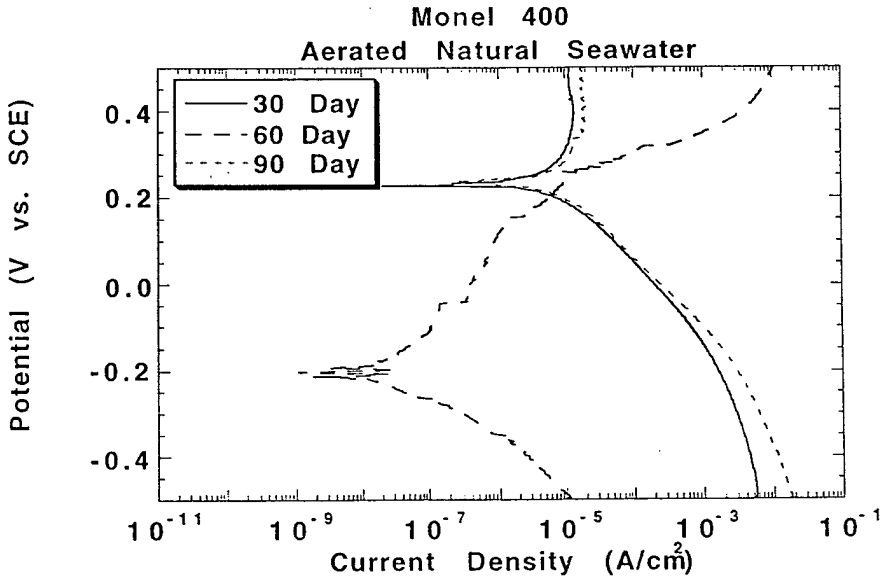

Figure 17. Potentiodynamic scans of Monel 400 exposed to aerated seawater 30, 60, and 90 days.

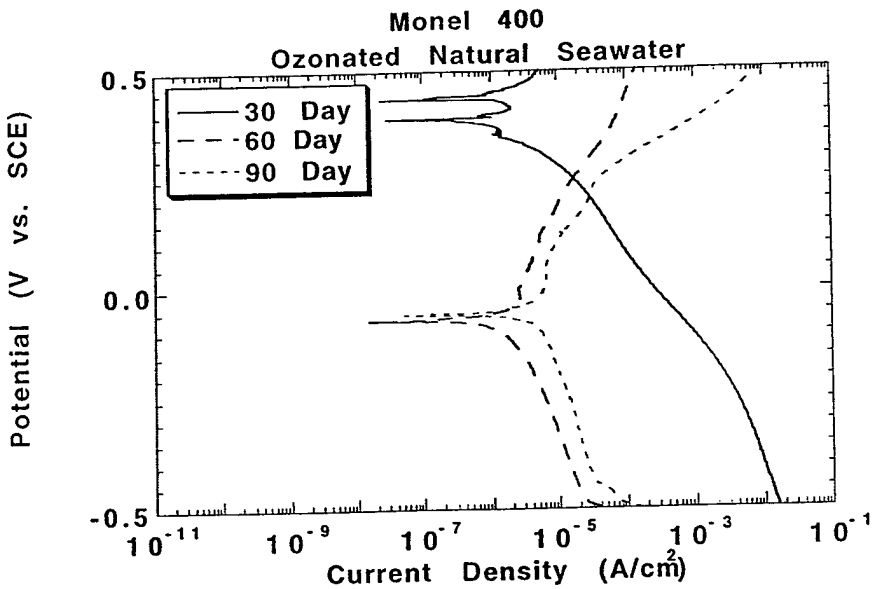

Figure 18. Potentiodynamic scan of Monel 400 exposed to ozonated seawater 30, 60, and 90 days

Monel K-500 behaves similar to Monel 400. The corrosion potential in ozonated seawater is noble to aerated seawater. At ninety days a potentiodynamic curve with a very noble corrosion potential is seen in both the aerated and ozonated seawater. When compared these ninety days curves for aerated and ozonated seawater are virtually identical in corrosion potential and current density, indicating that the corrosion mechanism may be more related to the anodic reaction than to the cathodic reactions. An odd feature is found on the thirty day curve in ozonated seawater, a bump going to lower current density which lines up with the corrosion potential found at sixty days of exposure. Coincidentally, a sharp change in current density is observed in the thirty and sixty day aerated scans at approximately 0.1V. This may suggest a pitting phenomena or an unstable film growth, in either case these anomalies were not seen on scans made in ozonated seawater.

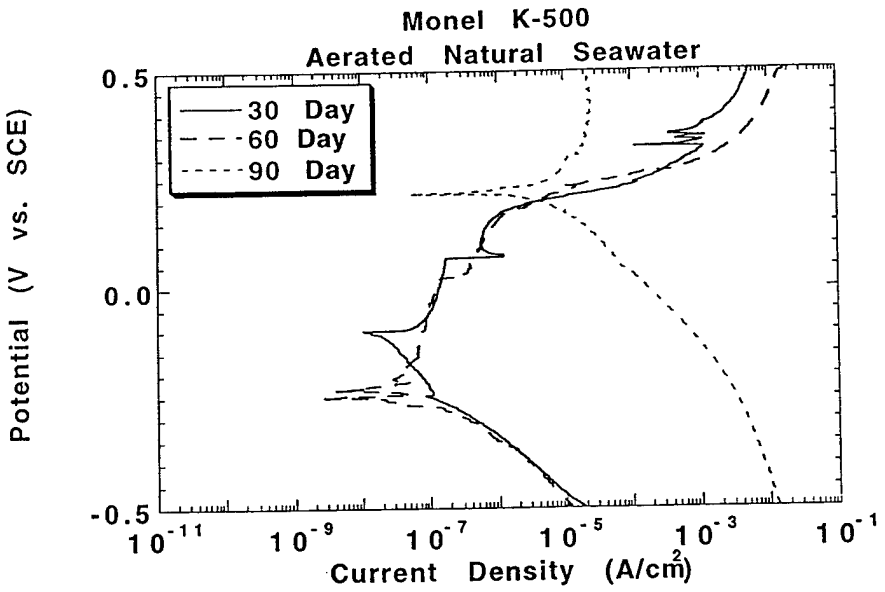

Figure 19. Potentiodynamic scan of Monel K-500 exposed to aerated seawater 30, 60, and 90 days.

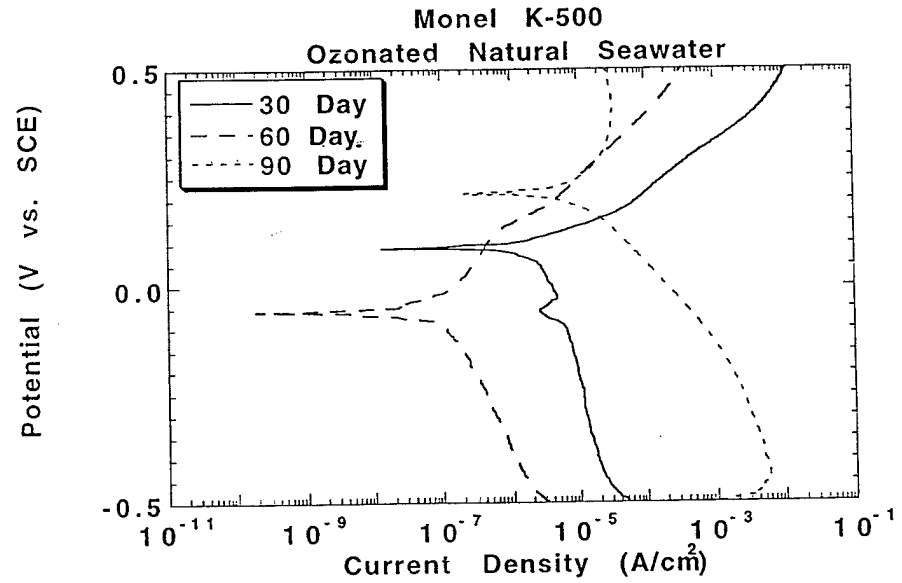

Figure 20. Potentiodynamic scan of Monel K-500 exposed to ozonated seawater 30, 60, and 90 days.

CDA 715 is an alloy that is borderline between behavior as a passive or an active alloy. The thirty percent Ni present in this alloys is at the minimum for passive protection and may or may not form a passive layer on the surface. The corrosion potential in aerated and ozonated seawater are approaching each other with only a difference of tens of millivolts separating them after ninety days. The samples exposed to ozonated seawater continue to exhibit a more noble corrosion potential. However, the difference between the aerated and ozonated corrosion potential is now small, excepting the 30 day scan which showed behavior similar to that seen in the Monel alloys. These scans also show that the corrosion current density is greater in the ozonated seawater. In ozonated seawater a change was seen between thirty and ninety days of exposure. The anodic slope became steeper suggesting formation of a more stable passive film over time. Opposite to the ozonated condition, the aerated case shows a decreasing anodic slope with time (between sixty and ninety days) which may show a breakdown of a passive film as time of immersion increases.

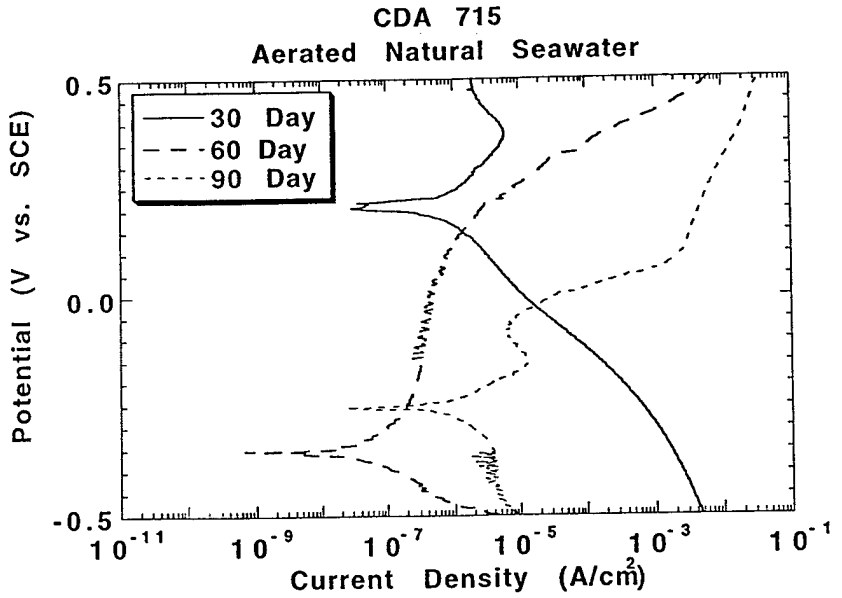

Figure 21. Potentiodynamic scan of CDA 715 exposed to aerated seawater 30, 60, and 90 days

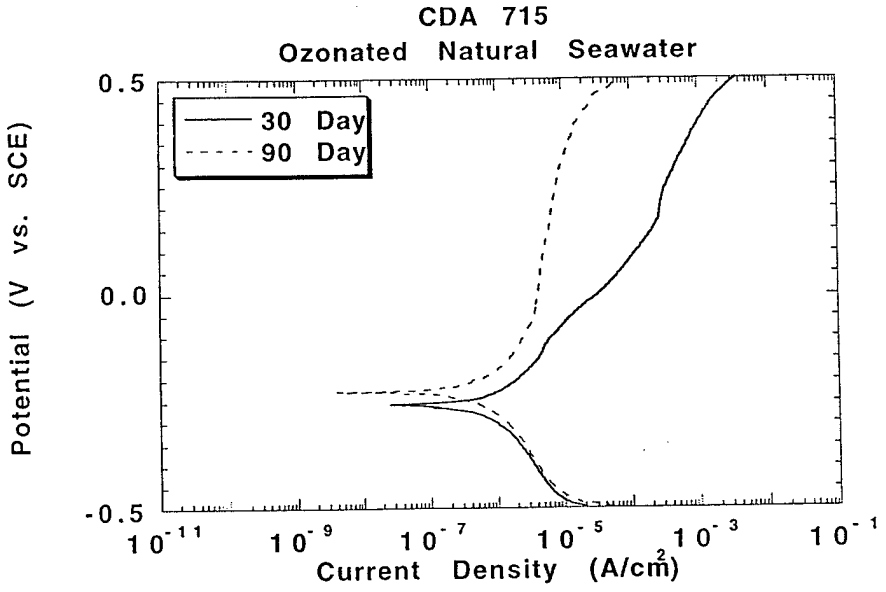

Figure 22. Potentiodynamic scan of CDA 715 exposed to ozonated seawater 30, and 90 days

CDA 706 shows the same behavior after thirty days in aerated seawater mentioned earlier. The corrosion potential shifted far noble from the value found during the steady state scan to measure corrosion potential. The potentiodynamic scans show the corrosion potential being nearly identical in both the ozonated and aerated case. The sixty day sample in aerated seawater occurs at the same corrosion potential and corrosion current density as the thirty and ninety day samples exposed to ozonated seawater. After ninety days in aerated seawater the potentiodynamic scan shows an increase in the anodic slope and a decrease in corrosion current density indicating decreased susceptibility to corrosion over time. The thirty and ninety days curves obtained from samples in ozonated seawater occur at the same corrosion current density and potential and closely follow one another as the potential is increased in the noble direction. After ninety days the sample exposed to ozonated seawater shows better resistance to corrosion at higher potentials as evidenced by a decreased current density. The ninety day ozonated curve also shows a smoothing of the thirty day curve of the transitions seen in the thirty day sample.

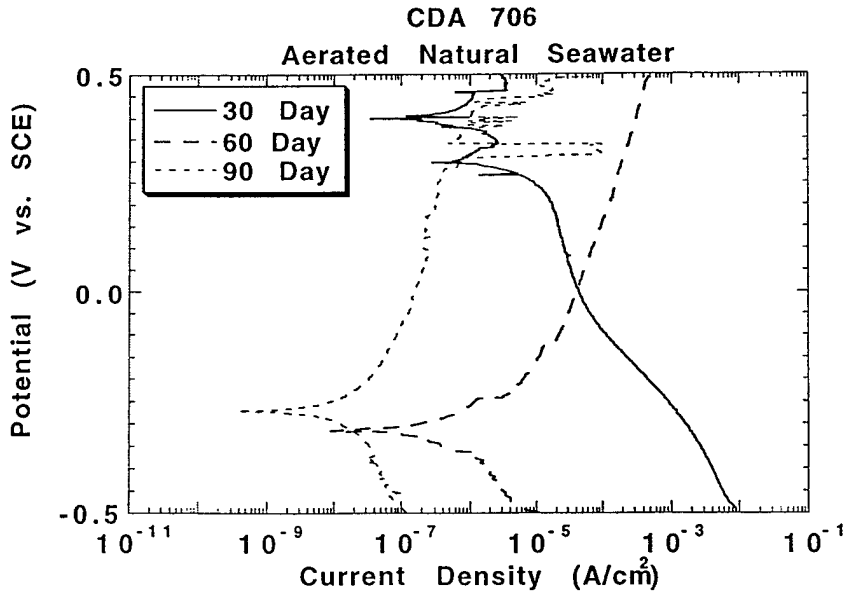

Figure 23. Potentiodynamic scans of CDA 706 exposed to aerated seawater 30, 60, and 90 days.

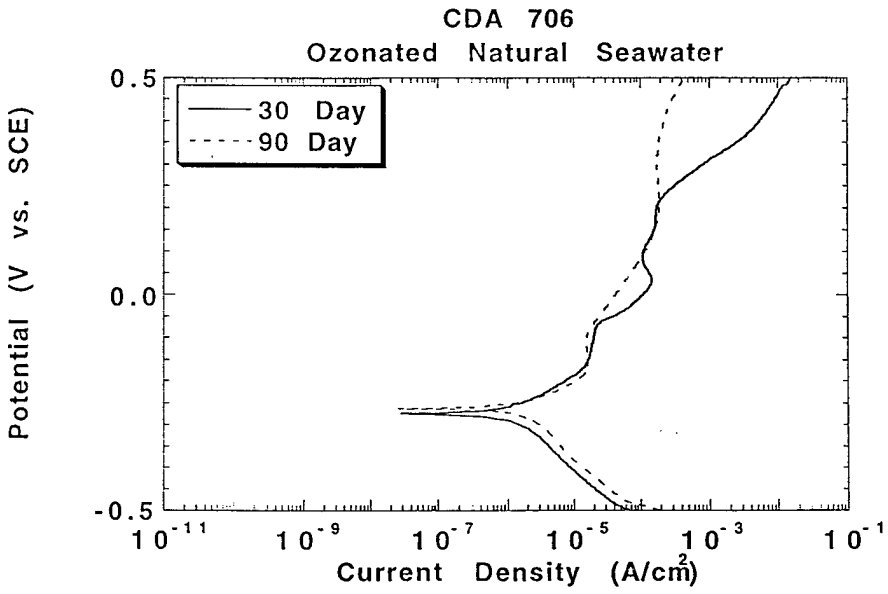

Figure 24. Potentiodynamic scan of CDA 706 exposed to ozonated seawater 30, and 90 days.

Alloy Corrosion Rate Results

A marked difference in corrosion rate was observed between those alloys exposed to aerated and ozonated seawater. Alloys exposed to ozonated seawater exhibited increased susceptibility to general and localized corrosion. Figures 25 and 26 show corrosion rates calculated from weight loss measurements.

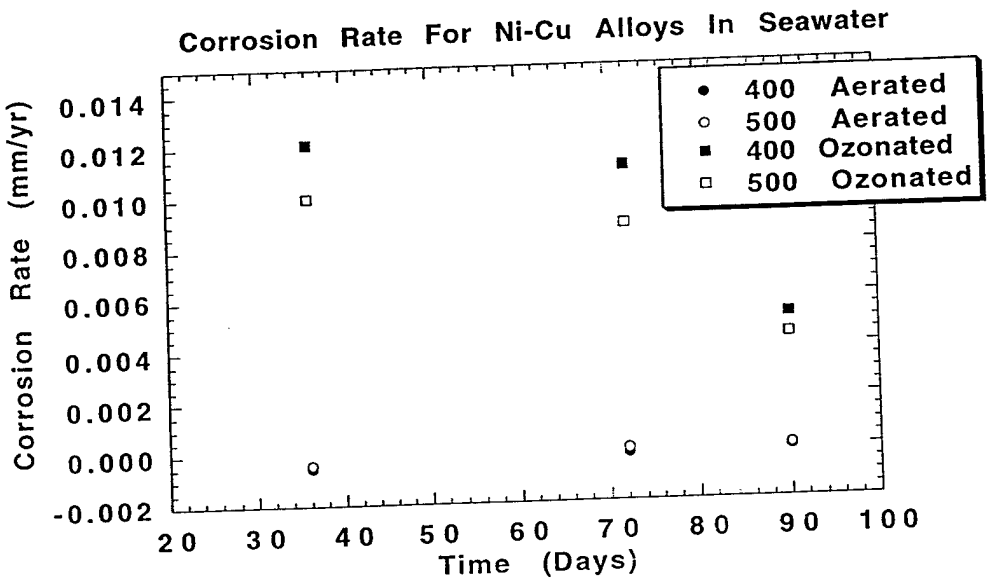

Figure 25. Corrosion rate calculated from weight loss measurements of Monel 400 and Monel K-500 in aerated and ozonated seawater.

The corrosion rates of the Monel alloys in aerated seawater remain generally constant at low corrosion rates with the maximum being only in the tens of micrometers per year. The negative value of corrosion rate indicates a mass gain due to corrosion product that was not able to be removed. Corrosion rates are higher on ozonated seawater, but decrease with time. At 0.0120mm/yr., the highest corrosion rate observed in this alloy system, these alloys reflect excellent resistance to corrosion in the ozonated seawater environment.

Alloy CDA 715 showed similar behavior to the Monel alloys with the corrosion rate decreasing with time and the aerated corrosion rate being very low, <0.005mm/yr., after sixty days. The corrosion rate in ozonated corrosion seawater is also low, the maximum being 0.013mm/yr. The CDA 706 alloy actually showed the highest corrosion rate in aerated solution at thirty days. However, CDA 706 also showed the greatest decrease in corrosion rate with time so that at ninety days it fell more into line with the other alloys studied. CDA 706 in ozonated seawater showed a steady corrosion rate of approximately 0.09 mm/yr. throughout the 90 day trial.

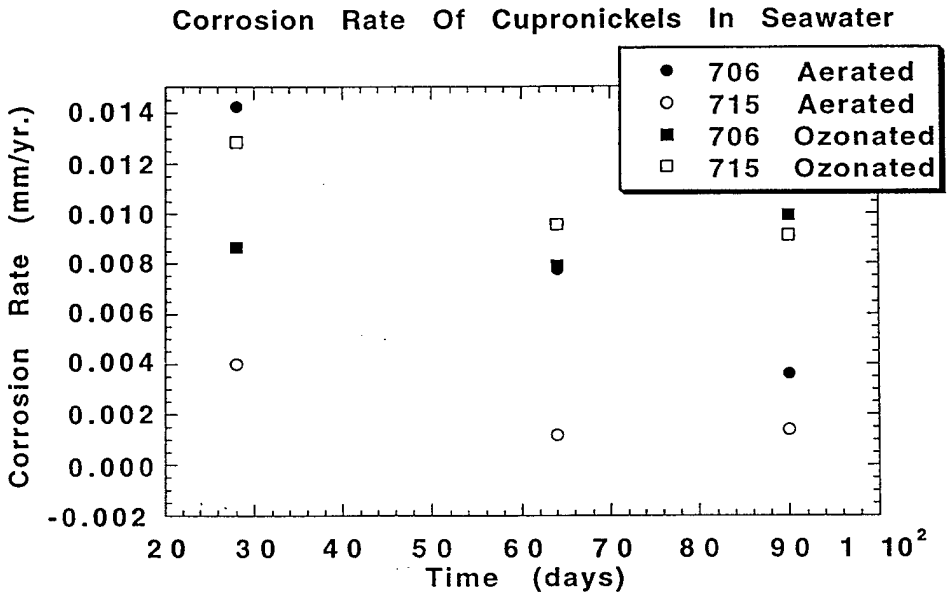

Figure 26. Corrosion rate calculated from weight loss measurements of CDA 706 and CDA 715 in aerated and ozonated seawater.

Weight Loss Samples

Of the Monel alloys, only those exposed to ozonated seawater showed signs of attack at thirty days. The Monel 400 alloy shows signs of pitting with the pits being spread randomly over the surface of the sample and filled with a green corrosion product. Monel

K-500 exhibited very little pitting. However, crevice corrosion is present on Monel K-500 where the glass rod that supported the sample was in contact with the edge of the hole through which it was threaded. Crevice corrosion at the rod sample interface on the weight loss samples continued throughout the test. After ninety days, Monel 400 exposed to ozonated seawater exhibited pitting. Pits formed after thirty days continued to grow rather than new pits forming as determined from pit density approximations according to ASTM Standard Practice G-46-76[18]. As time increased a black corrosion product is observed in the pits in addition to the green corrosion product first formed. At ninety days Monel K-500 continued to show very little pitting but continued to show corrosion at the interface between the glass rod and the edge of the hole. Those same alloys exposed to aerated seawater showed no signs of attack. Figures 27 and 28 show weight loss samples of the alloys investigated after sixty days of exposure and cleaning to remove corrosion product.

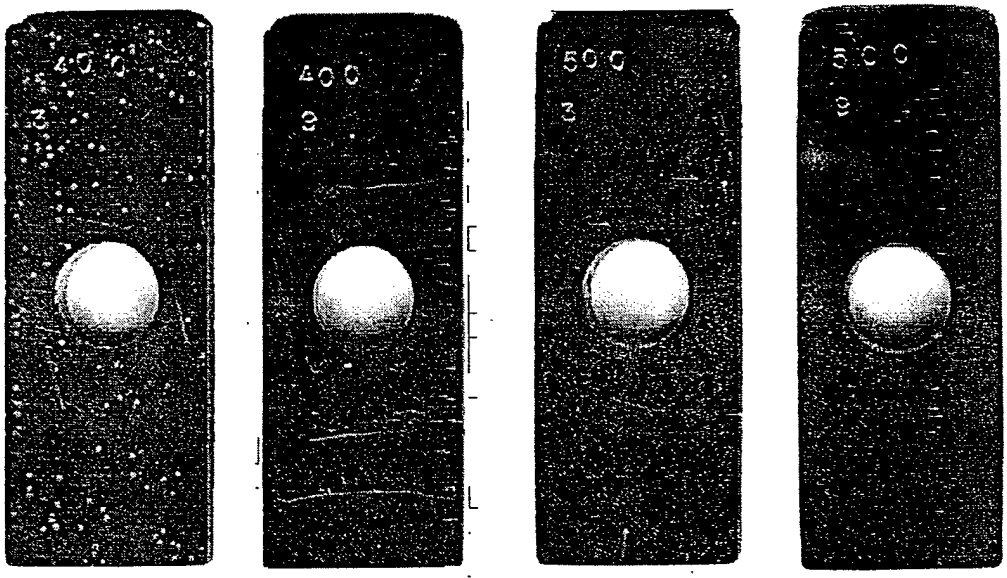

Figure 27. Monel alloys after sixty days of exposure and cleaning. From left to right Monel 400 ozonated seawater, Monel 400 aerated seawater, Monel K-500 ozonated seawater, and Monel K-500 aerated seawater.

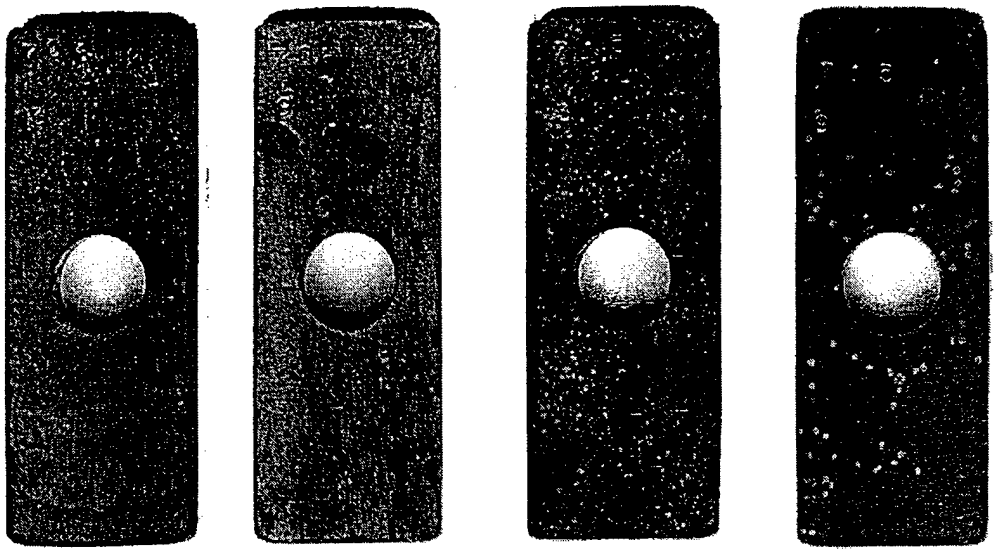

Figure 28. Cupronickel alloys after sixty days of exposure and cleaning. From left to right: CDA 706 ozonated seawater, CDA 706 aerated seawater, CDA 715 ozonated seawater, and CDA 715 aerated seawater.

The cupronickel alloys (CDA 715 and CDA 706) exhibited more signs of corrosion than the Monel alloys. The CDA 706 alloy showed a general brown corrosion product. Pits on CDA 706 were filled with a brown corrosion product after thirty days with the attack morphology being similar in both ozonated and aerated seawater, but more severe in ozonated seawater. Crevice corrosion was observed where the glass rod contacted the edge of the hole. With increased time the pits formed became larger and more numerous in both ozonated and aerated seawater. The attack was most severe in ozonated seawater after ninety days exposure.

Alloy CDA 715 showed pitting that much more dense than the pitting on CDA 706. These pits were filled with a red-brown corrosion product and the pits per unit area increased as time increased. This pitting was of the same morphology in aerated and ozonated seawater. However, the attack in ozonated seawater was much more severe, with the sample being almost completely covered with pits by the end of the ninety day test period.

Crevice Corrosion

The crevice corrosion behavior of the Monel alloys follows the same trend as the general corrosion behavior. Localized attack was more severe on the Monel 400 alloy compared to the Monel K-500 alloy in ozonated seawater after thirty days. The Monel 400 alloy shows a green over black corrosion product predominantly adjacent to the tight crevice areas. The areas within the tight crevices show little attack with only some signs of pitting. The Monel K-500 alloy shows less corrosion product in these same areas. As time increased the attack became more severe in each alloy and environment. A greater amount of black corrosion product was seen at the mouths of the corroded regions (between the tight crevices). Pits in the tight crevices did not increase in number but became broader and deeper with time.

In aerated conditions the morphology of the corrosion was the same, occurring between the tight crevice areas. However, attack, as evidenced by the amount of corrosion and appearance of the surface, was much less severe in aerated seawater. Generally, a series of refractive oxides appeared to have formed with some pitting occurring at the interface of the tight crevice.

Figures 29 and 30 show sixty day crevice results of the alloys investigated in this study in aerated and ozonated seawater.

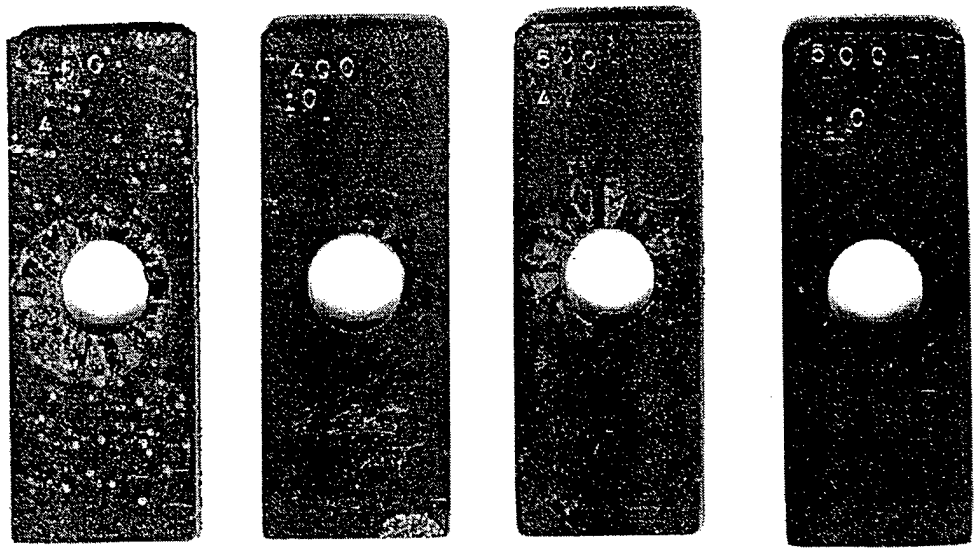

Figure 29. Crevice corrosion results after 60 days of exposure. From left to right: Monel 400 ozonated, Monel 400 aerated, Monel K-500 ozonated, and Monel K-500 aerated.

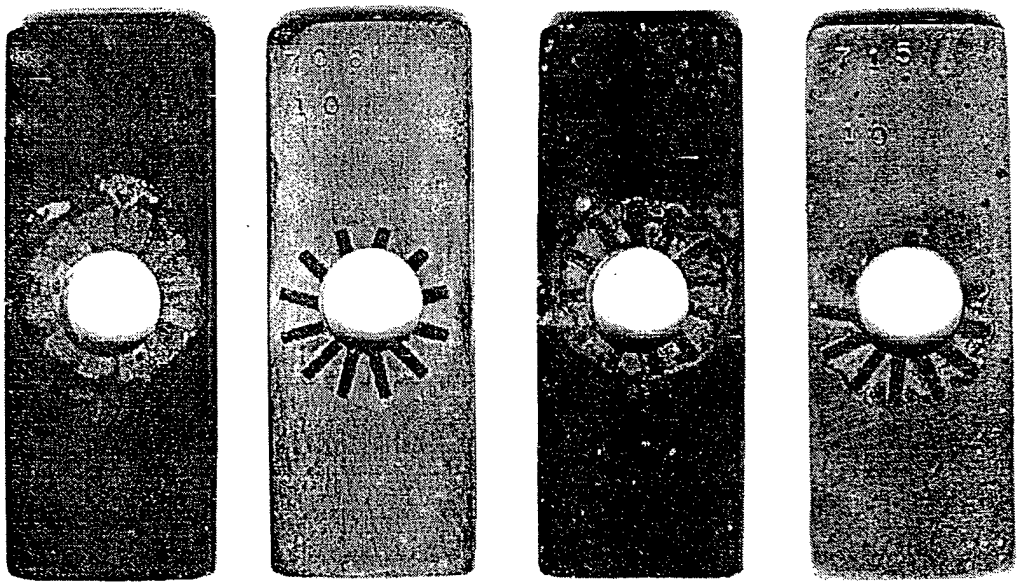

Figure 30. Crevice corrosion results after 60 days of exposure. Form left to right: CDA 706 ozonated, CDA 706 aerated, CDA 715 ozonated, and CDA 715 aerated

The cupronickel alloys differed somewhat in their corrosion behavior. In ozonated seawater the attack was similar to the Monel alloys. Localized attack occurred between the tight crevice areas. The corrosion products have a layered appearance with a red corrosion product occurring between the tight crevice areas and a green corrosion product over top of this at the mouths of these areas and immediately outside the crevice region, a dark brown corrosion product covered the rest of the sample. This morphology was generally true of both CDA 715 and CDA 706 with the overlaying corrosion product on CDA 706 being darker in appearance than that formed on CDA 715. CDA 715 also had a much larger pit density as was also observed on the weight loss samples. With time the attack becomes more severe as the corrosion begins to invade the tight crevice regions from the outside.

In aerated seawater, corrosion occurred inside the tight crevice in all excepting the sixty day CDA 715 sample which showed the same red and brown corrosion product as seen in ozonated seawater but without the large pit density and dark brown corrosion product covering the rest of the sample. Otherwise, CDA 706 and CDA 715 experienced corrosion inside the tight crevice regions. In CDA 706 this was evidenced by pitting within the crevice. The pits are filled with a dark brown corrosion product and do not appear to be particularly deep. Additionally, the pit density does not seem to increase between sixty and ninety days in this CDA 706 alloy.

The CDA 715 alloys exposed for thirty and ninety days also show corrosion within the tight crevice regions, with the attack in the tight crevice areas being quiet extensive. It appears to have begun with a pitting phenomena, however these pits appear to have coalesced, forming large areas of attack typical of crevice corrosion. The red-green corrosion product morphology is seen inside these regions occurring around the edges of the tight crevice. Because the sixty day sample did not exhibit this behavior it is difficult to consider trends. However, the attack observed on the ninety day sample is more severe than that observed after thirty days of exposure to aerated seawater. The sixty day sample exhibited attack more typical of that seen in ozonated seawater and may have occurred due

to extreme localized corrosion which set up conditions similar to that seen by the alloy exposed to ozonated seawater.

Results of Experiments Performed at LaQue Center for Corrosion Technology

Solutions

The amounts of residual ozone and chlorine were measured daily for the entirety of the test. Results are shown in figure 31. Residual ozone levels averaged 0.21mg/l in both tanks and ranged between 0.05-0.32mg/l over the sixty days of exposure. Residual chlorine levels depended upon a test being run concurrently and thus there was less control over the levels of hypochlorite in the water because this tests was monitored less often. Residual chlorine levels averaged 0.32 mg/l and ranged between 0.1 and 1.0 mg/l.

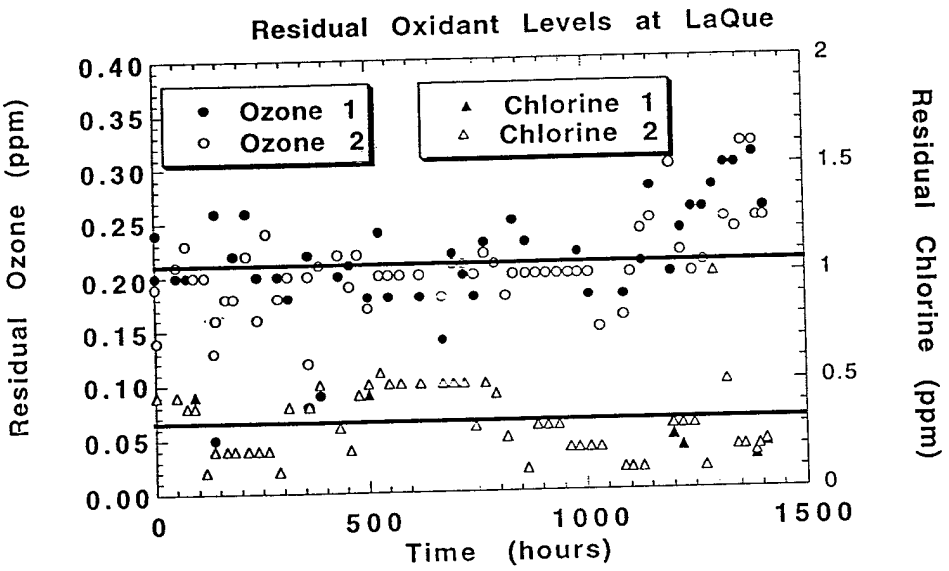

Figure 31. Residual oxidant concentration vs. time for experiments performed at the LaQue Center for Corrosion Technology.

Corrosion Potential Results from LaQue Center for Corrosion Technology

The corrosion potential of each sample assembly was measured at the end of the sixty day tests, these results are shown in figures 32 and 33 for chlorinated and ozonated seawater respectively. These figures show the data collected at the LaQue Center for Corrosion Technology, Wrightsville Beach, N.C., for each alloy (open circles) as well as the average of that data (closed circles). For comparison the corrosion potential found in sixty day electrochemical cell test in aerated seawater at Rensselaer Polytechnic Institute are also included (closed triangles).

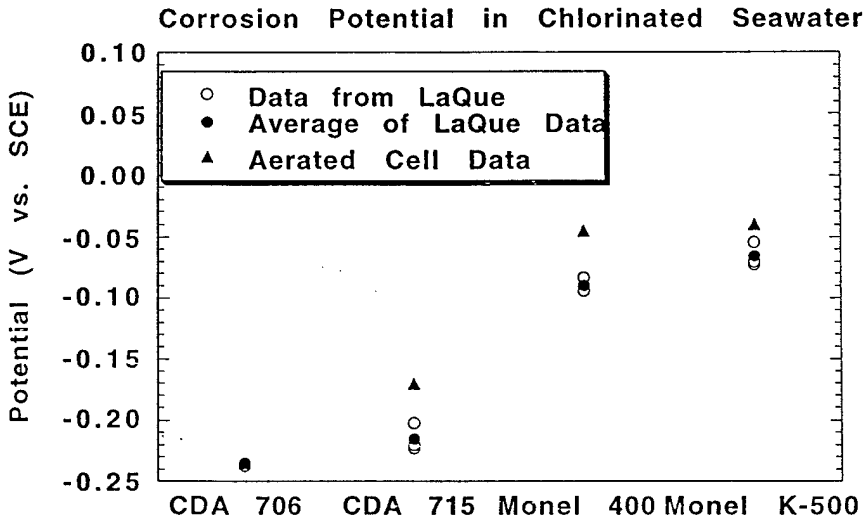

Figure 32. Corrosion potential of alloys after sixty days of exposure to chlorinated seawater at Wrightsville Beach, N.C. (open circles). The average of the N.C. data is included (closed circles), and in-lab results are shown for comparison (closed triangles).

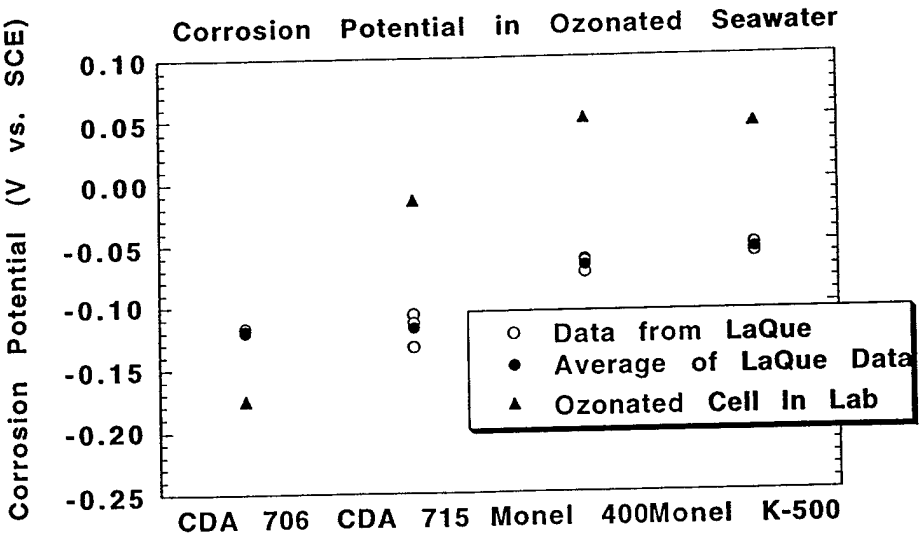

Figure 33. Corrosion potential of alloys after sixty days of exposure to ozonated seawater at Wrightsville Beach, N.C. (open circles). The average of the N.C. data is included (closed circles), and in-lab results are shown for comparison (closed triangles).

As the amount of nickel in each alloy increased (or amount of copper decreased) the corrosion potential becomes more noble. This trend was observed in chlorinated and ozonated seawater. The corrosion potential of the in lab tests was typically more noble than those measured at the LaQue Center for Corrosion Technology. In the case of chlorinated seawater a comparison is being made with aerated seawater. However, a direct comparison can be made with ozonated seawater which was used in both in the lab and at Wrightsville Beach, N.C.. This ennoblement is true for the alloys investigated here, excepting CDA 706. In chlorinated seawater CDA 706 showed a nearly identical corrosion potential when comparing aerated and chlorinated seawater. In ozonated seawater the in-lab results of CDA 706 shows a more active corrosion potential than that found at Wrightsville Beach, N.C..

Corrosion Rate From Weight Loss Measurements Of Panel Samples

Samples cleaned of corrosion product after immersion and disassembly were also weighed in order to calculate corrosion rates. The results of these measurements and calculations is shown in figures 34-40. The data presented in the figures below is for both washers and plates. These tests were designed to observe the effects of crevice corrosion, a localized form of corrosive attack. The calculation of corrosion rate shows important trends and helps to order materials in order of their resistance to a specific environment.

Figures 34 and 35 show the corrosion rate of the creviced panels in chlorinated seawater. Once again the open circles represent the data collected while the closed circles show the average of the data. In chlorinated seawater the corrosion rate is very low and is shown on the large scale for comparison with the ozonated results. Figure 35 shows an expanded scale to better make comparisons of the corrosion rate of panels in chlorinated seawater. These alloys show excellent resistance to general corrosion in chlorinated seawater as can be seen by the very low corrosion rates, <0.010mm/yr. With the passive alloys (Monel and CDA 715) showing even lower corrosion rates.

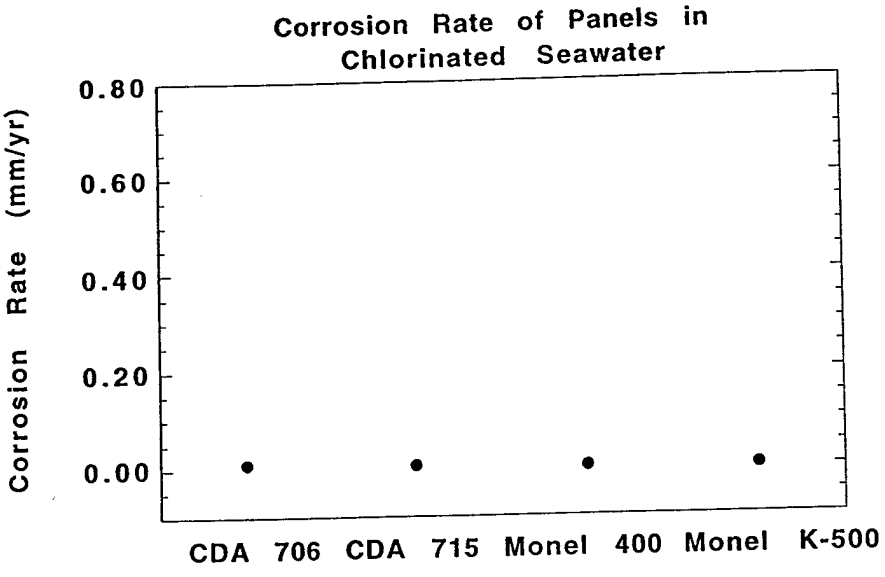

Figure 34. Corrosion rate of alloys in exposed for sixty days in chlorinated seawater at Wrightsville Beach, N.C.. Average of data in closed circles

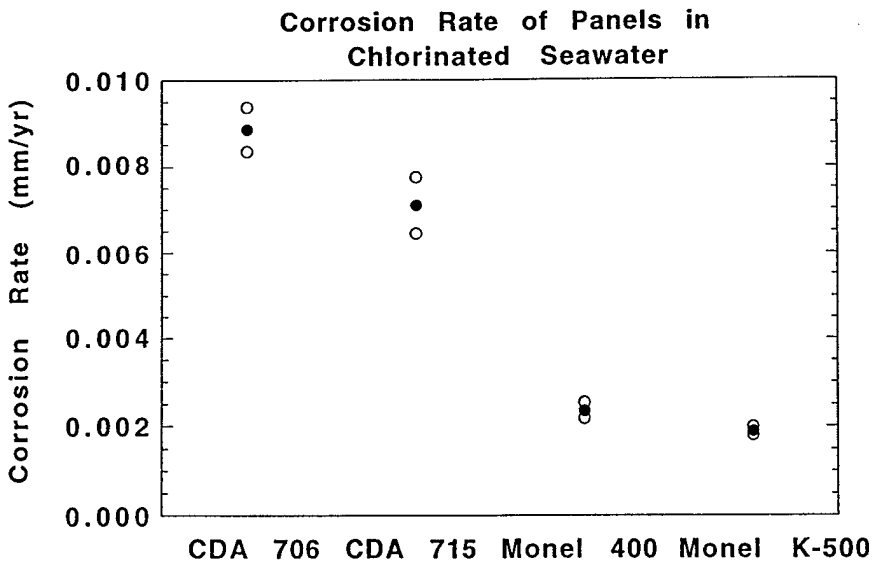

Figure 35. Corrosion rate of panels exposed for sixty days to chlorinated seawater at Wrightsville Beach, N.C.. Expanded scale for added clarity. Average of data in closed circles

In ozonated seawater the corrosion rates are higher, as can be seen in figure 36 and 37 which is added for better clarity. The corrosion rate of these alloys in ozonated seawater is also very good, at less than 0.2 mm/yr.. In chlorinated seawater the largest corrosion rate was seen in the active alloy (CDA 706) whereas in ozonated seawater the passive alloys display higher corrosion rates. CDA 715, which has borderline passivity in seawater, falls between the two extremes in each case. The larger corrosion rate and larger variation of the passive alloys demonstrates either that the passive film is breaking down and general corrosion is taking place throughout the sample at a higher rate than that seen in the passive alloy, or that localized corrosion is taking place which is very severe and is the major contributor to the high corrosion rates.

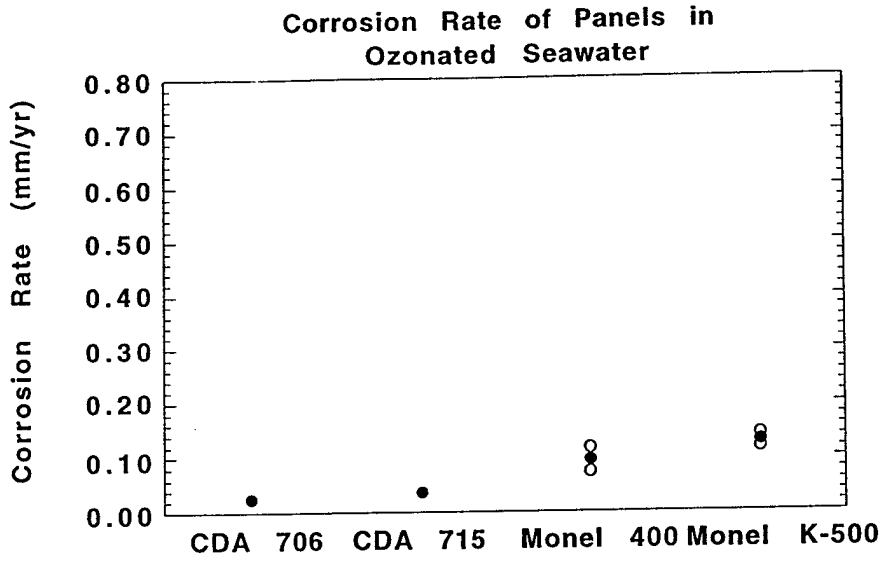

Figure 36. Corrosion rate of panels exposed for sixty days to ozonated seawater at Wrightsville Beach, N.C.. Average of data in closed circles.

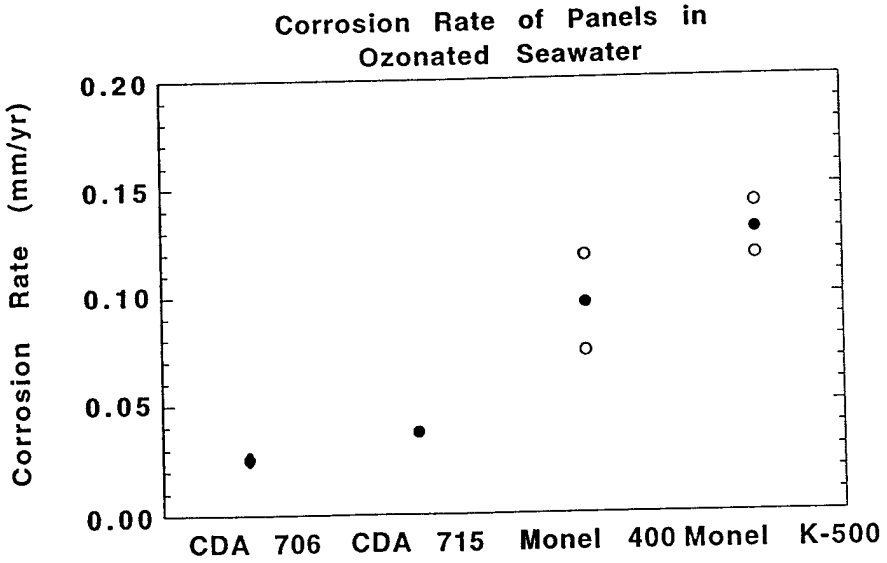

Figure 37. Corrosion rate of panels exposed for sixty days to ozonated seawater at Wrightsville Beach, N.C.. Expanded scale for added clarity. Average of data in closed circles

Corrosion Rate From Weight Loss Measurements of Washer Samples

The metal washers used for metal-metal crevice corrosion tests experienced two crevices, one on either side of the washer. A crevice was formed with a plate of the same metal and a crevice was formed on the opposite side with a PTFE washer. The corrosion rate measurements of the washers calculated by weight loss reflects this dual crevice.

The corrosion rate of the washers in chlorinated seawater is still very low, figures 38 and 39, with the largest corrosion rate being only slightly more than 0.1 mm/yr. In this case the passive alloys show the higher corrosion rate. This might possibly be due to a more classical crevice being set up with the PTFE washer. Degradation of PTFE in ozonated seawater is theorized to produce hydrofluoric acid.[19] This acid would attack under the washer and therefore set up a more classical crevice corrosion situation.

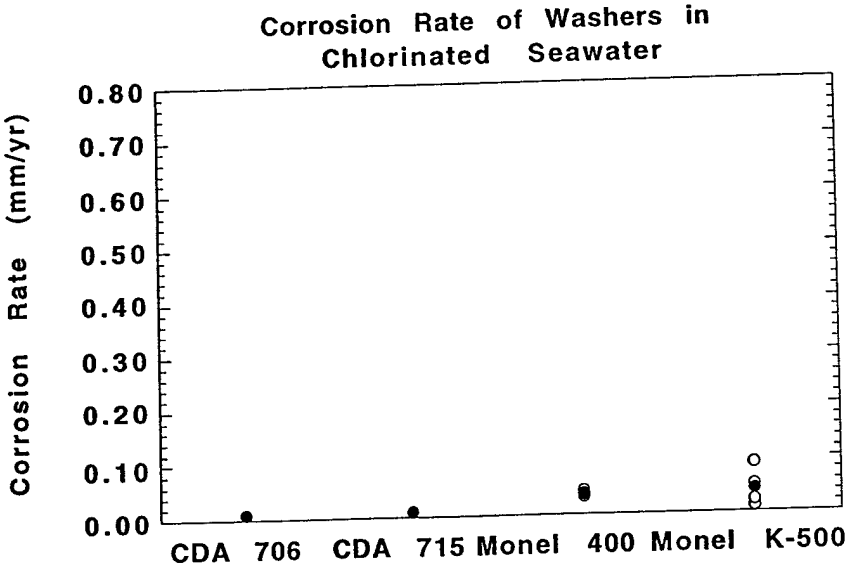

Figure 38. The corrosion rate of washers exposed to chlorinated seawater sixty days at Wrightsville Beach, N.C.. Average of data in closed circles.

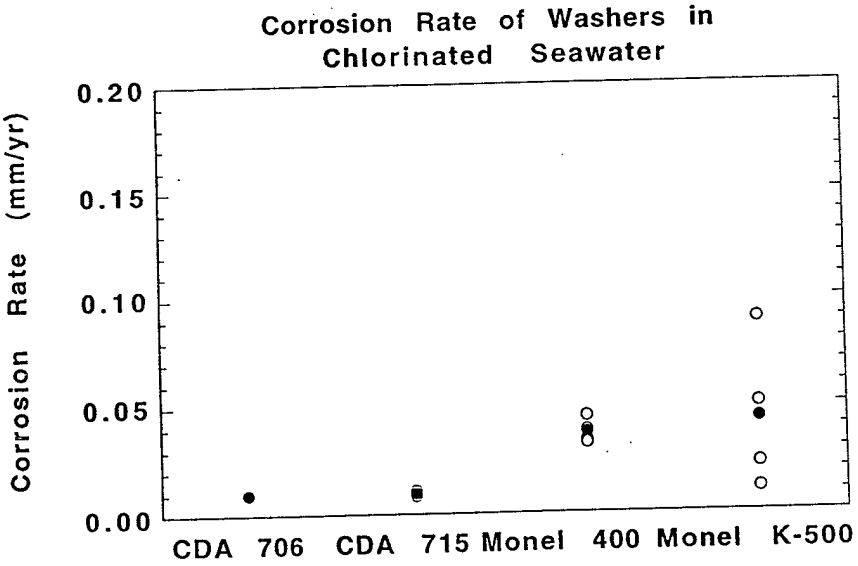

Figure 39. The corrosion rate of washers exposed to chlorinated seawater for sixty days at Wrightsville Beach, N.C.. Expanded scale for added clarity.

In ozonated seawater the corrosion rate of the washers is remarkably higher, figure 40, more than 0.70mm/yr. in the case of the passive Monel alloys. The corrosion of these washers was largely due to localized attack. This localized attack has a severe effect on the washers (and plates) corroding up to half the thickness of the passive alloys after sixty days. Also observed upon removal of the samples is preferential corrosion of one side of the assembly. The side more corroded was found to be random and is associated with the stochastic nature of localized corrosion which will protect one side of the sample by making it the preferential cathode. Therefore one washer or the other usually saw more severe corrosion. This differing attack for alternating sides of the sample is reflected in the corrosion rate of the washers which show a wide difference between maximum and minimum corrosion rates because one washer was exposed to each side of the sample.

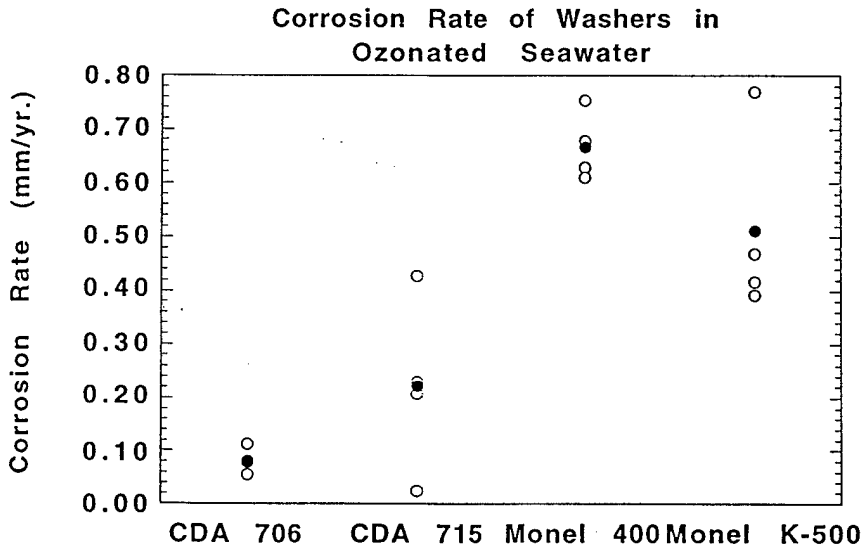

Figure 40. Corrosion rate of washers exposed to ozonated seawater sixty days at Wrightsville Beach, N.C.. Average of data in closed circles

Monel 400 Alloy Exposed To Natural Seawater At LaQue Center For Corrosion Technology.

Examples of the appearance of the Monel 400 samples after sixty days of exposure are shown in figures 41 through 48. The sample exposed to ozonated seawater was covered with a brown film with areas of a black powdery corrosion product associated with pitting. This corrosion product was concentrated around the mouths of both the nonmetal-metal and metal-metal crevices. This voluminous corrosion product also ran down the sample as can be seen below. A green corrosion product was intermixed with the large volumes of black corrosion product around the mouths of the crevices and running down the sample from the crevice. The areas within the crevice were unaffected by the exposure to ozonated seawater and show no corrosion.

Monel 400 shows large areas of corrosion and severe depth of attack after the corrosion product has been cleaned off. This is particularly true around the crevice and under the concentrated black corrosion product which extends down the sample. Large pits were found over the surface of the sample although the density of pitting was rather low.

The washers show a similar morphology, with attack concentrated around the mouth of the crevice working its way toward the center. The attack at the metal-metal crevice was much more severe than the attack at the metal-nonmetal crevice, even eating away the edges of the washers and corroding significant parts of the washer and taking it out of round. The figure below shows the sample after cleaning. A binary image showing only the areas of corrosion (in black) is included to better observe the extent of attack, figure 43.

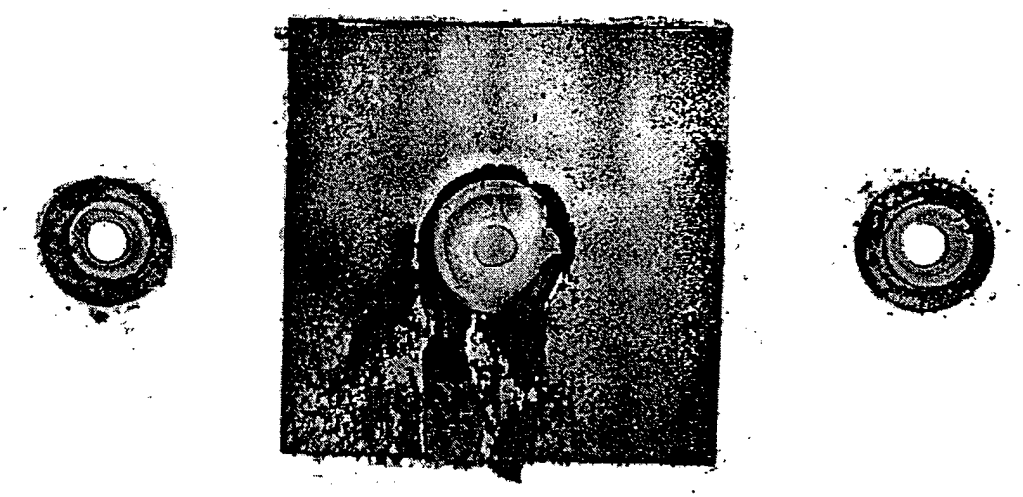

Figure 41. Appearance of Monel 400 alloy unassembled after sixty days of exposure to ozonated seawater in Wrightsville Beach, N.C.

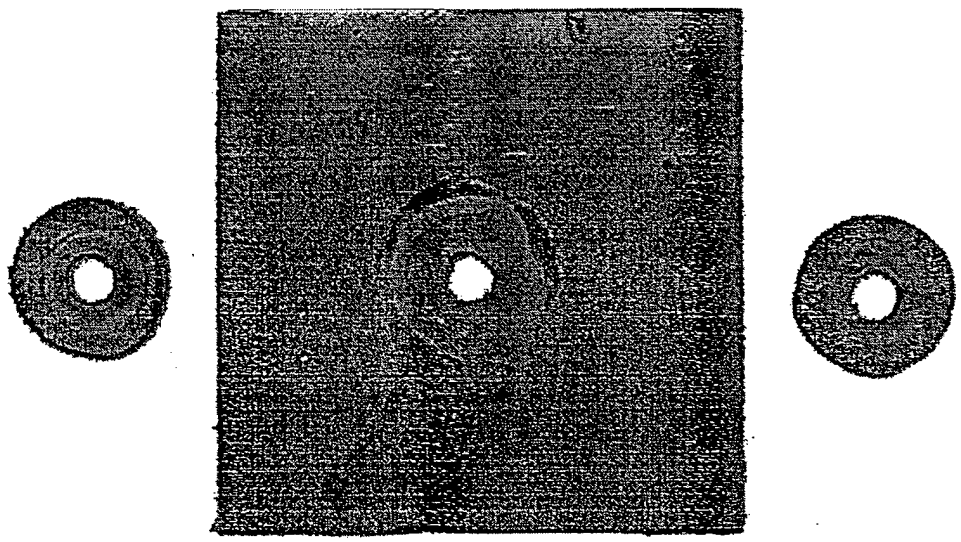

Figure 42. Appearance of Monel 400 unassembled after sixty days of exposure to ozonated seawater and cleaning.

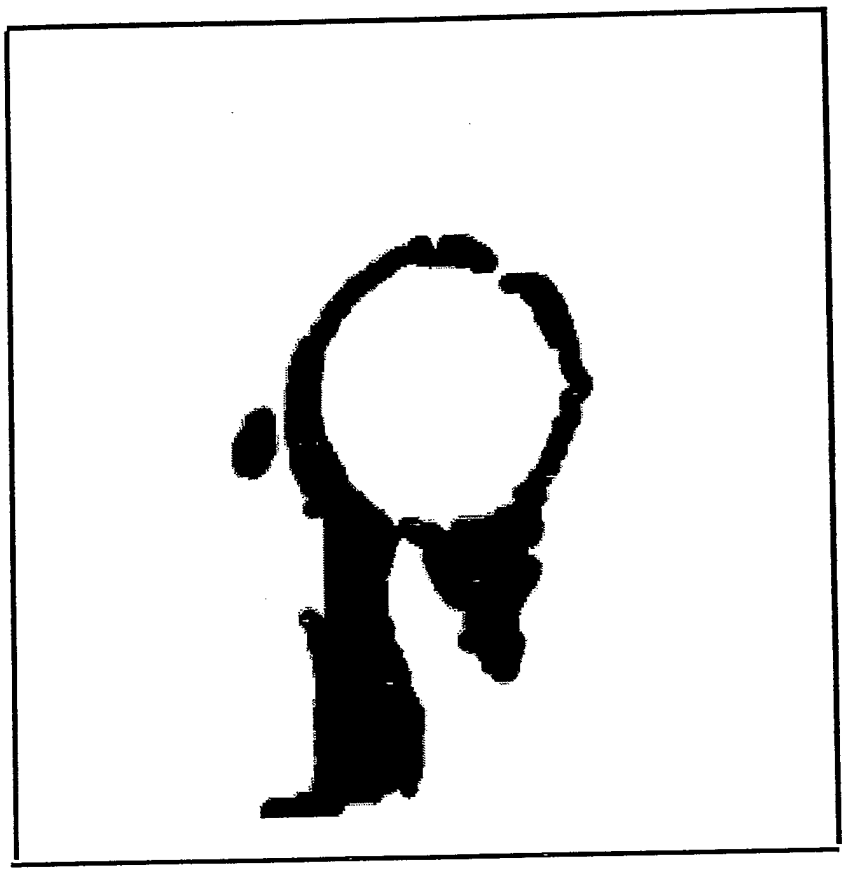

Figure 43. Binary image of Monel 400 showing corrosion areas of attack (black) after sixty days of attack to ozonated seawater

Examples of the severity of attack on the Monel 400 alloy in ozonated seawater are shown in figures 44 through 46. Figure 44 is a cross section of the plate section of the assembly. This figure shows the severe corrosion that occurred at the mouth of the crevice. It can be seen that the attack is nearly through half the thickness of the plate, which originally was 0.95cm (0.125") thick, after sixty days of exposure. Figure 45 shows a cross section of a Monel 400 washer. The edge of this washer exposed to ozonated seawater has been eaten away at the top and bottom due to corrosion at the edge of the crevice formed by the metallic washer and the metal plate. Figure 45 also shows the cold worked structure of the washers and plates as evidenced by the flow lines running

parallel to the surface. Studies by Dobb et.al., found that annealing as received sample of 70Cu/30Ni and 90Cu/10Ni had no noticeable effect on corrosion in seawater.[20]

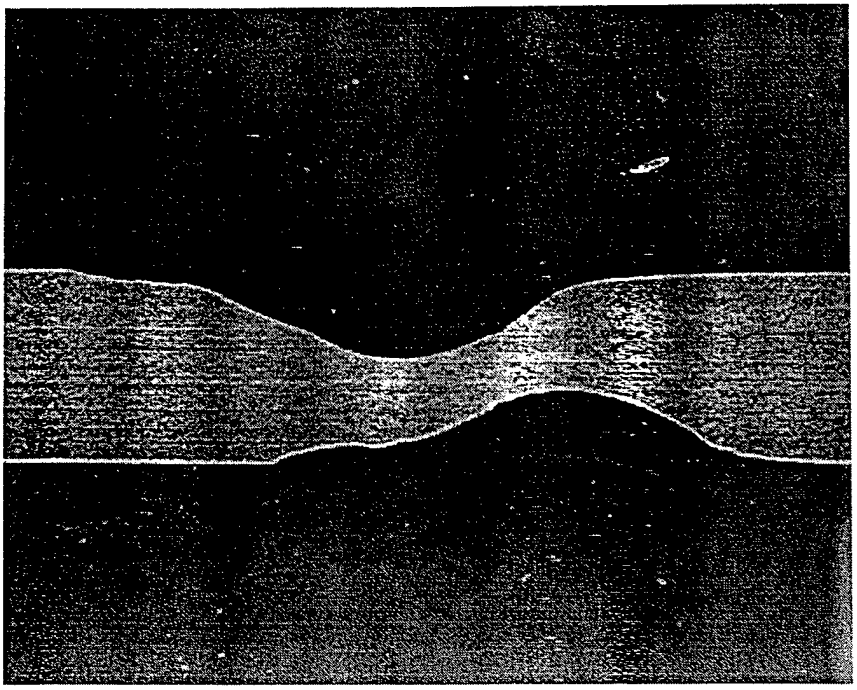

Figure 44. Photograph showing cross section of Monel 400 plate exposed to ozonated seawater sixty days and cleaned. 15X

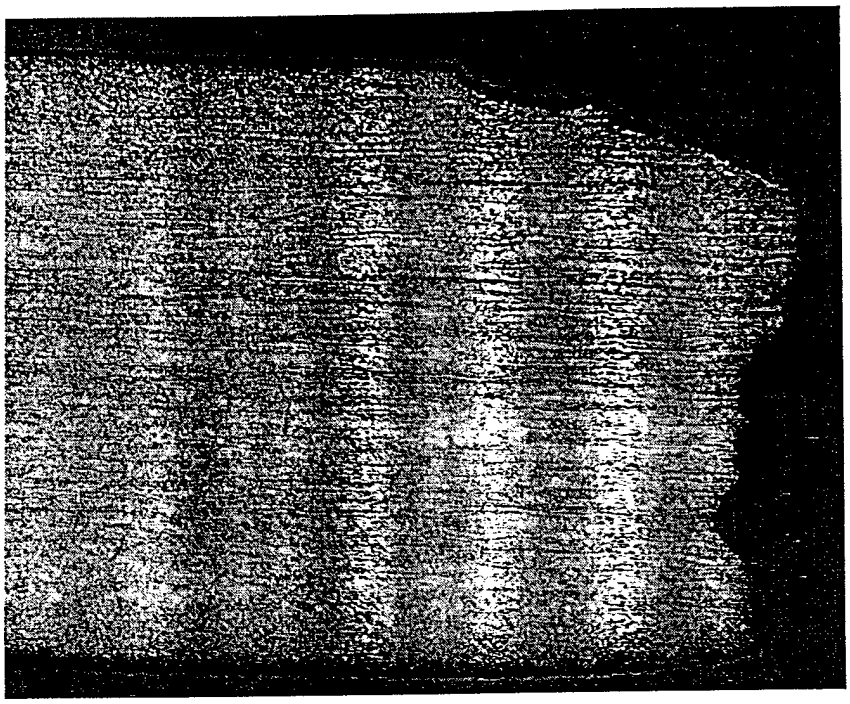

Figure 45. Edge of Monel 400 washer exposed to ozonated seawater sixty days. 50.4X, Brass Etch

To capture a crevice in-situ the sample that was not cleaned was sectioned while still assembled and the resulting cross section is shown in figure 46. The titanium bolt and washers can be seen (gray) as well as the PTFE washers and the metal washers and plate. This figure shows the attack occurring at the mouth of the crevices. The attack is seen starting at the outside and working into the crevice formed with PTFE and the metal-metal crevice . Classical crevice corrosion is also seen in this sample between the metal plates, although this behavior was not observed in other samples of Monel 400 exposed at the same time. The metal washers directly underneath the PTFE washers show a jagged appearance indicating attack due to a classical crevice corrosion mechanism.

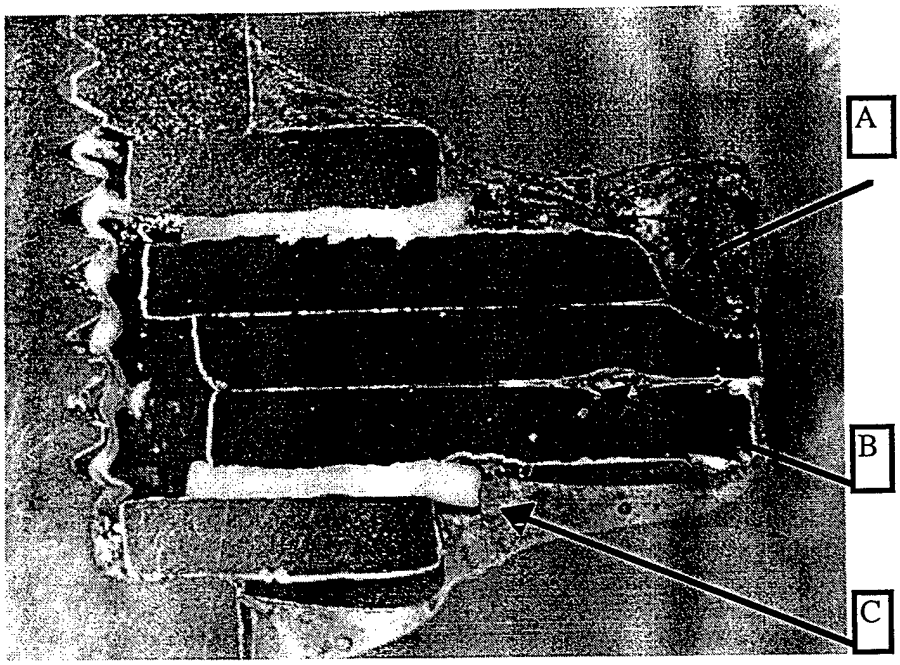

Figure 46. Cross section of crevice assembly after sixty days of exposure to ozonated seawater. 6X., A., Corrosion at the mouth of the metal-metal crevice. B., Classical crevice corrosion between the metal plate and washer. C., Corrosion at the mouth of the metal-nonmetal crevice.

The same alloy exposed to chlorinated seawater shows much less corrosion, figure 47. The black corrosion product is not present over the bulk of the sample. A thin black line of corrosion product was present around the mouth of the crevice extending further in some cases at the metal-metal crevice. The sample also shows a green corrosion product further away from the mouth of the crevice and outside the line of black corrosion product.

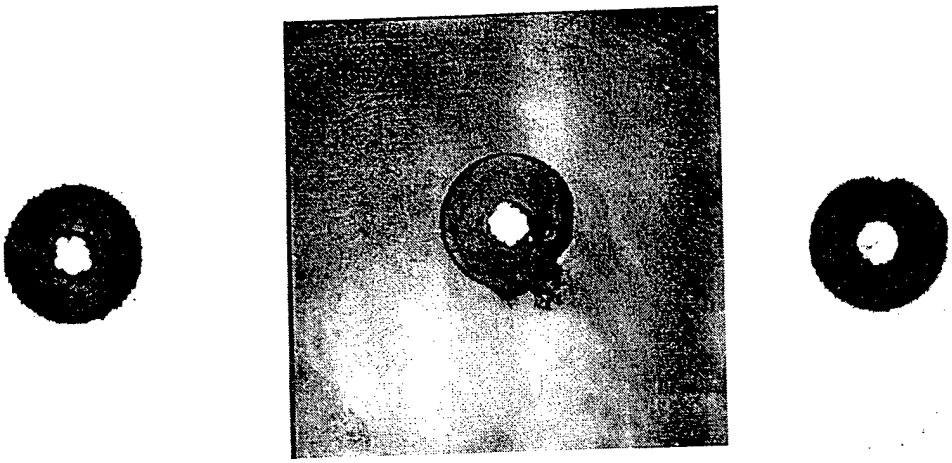

Figure 47. Appearance of Monel 400 unassembled after sixty days of exposure to chlorinated seawater in Wrightsville Beach, N.C.

Once cleaned the sample exposed to chlorinated seawater showed attack only in areas where the black corrosion product was present. The attack was not as severe as that seen in ozonated seawater and penetration was minimal. Figure 48 shows the attack at the mouth of the crevice when the Monel 400 alloy is exposed to chlorinated seawater. This photograph taken at 200X magnification shows the transgranular attack and the much smaller amount of crevice corrosion in chlorinated seawater as opposed to ozonated seawater.

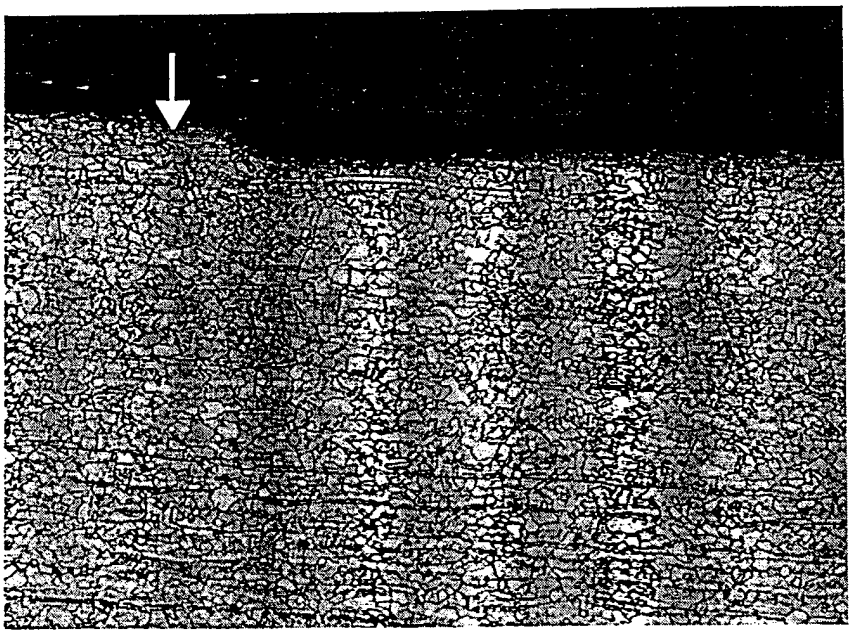

Figure 48. Cross section of Monel 400 plate exposed to chlorinated seawater sixty days. 126X, Brass etch, White arrow indicates location of the outermost edge of the washer mated to this plate.

Monel K-500 Alloy Exposed To Natural Seawater At LaQue Center For Corrosion Technology.

The Monel K-500 alloy behaved in a very similar manner to Monel 400 when exposed to ozonated and chlorinated seawater. Monel K-500 shows a brown surface film over the bulk of the sample. A black corrosion product was scattered over the surface of the sample and concentrated around the mouth of the crevice extending down the sample in the direction of gravity. The extent of this black corrosion product can clearly be seen in figure 49 still attached to the washers which have been removed from the plate. A green corrosion product was also found intermixed with the black corrosion product. This type of attack, around the mouth of the crevices, was seen on both the plate and the washer, neither showed attack within the crevice. Under the creviced area the metal appeared as the day it was immersed.

After removal of the corrosion product the attack was found to be concentrated around the mouth of the crevice. Severe attack was also found around the edge of the plate and washers which have a delaminated appearance. Large pits were observed over the surface of the sample and large areas of shallow dissolution were also found. In the bottom of the pits green and black corrosion product remained which was unable to be removed in the cleaning process. The large areas of general dissolution also show striations of black corrosion product unable to be removed. The majority of the corrosion was concentrated under the black corrosion product observed on the sample after removal from the ozonated seawater. The appearance of the Monel 500 alloy after removal from ozonated seawater can be seen in figure 50. A binary image showing areas of corrosion is shown in figure 51 to better see the morphology of the attack.

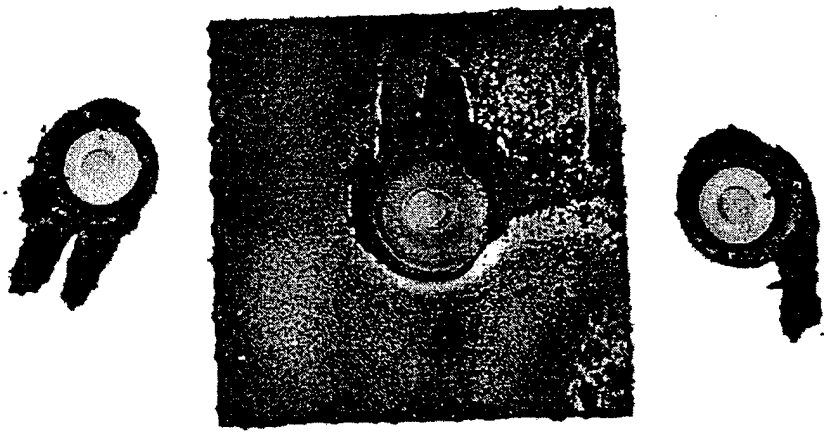

Figure 49. Monel K-500 alloy unassembled after sixty days of exposure to ozonated seawater at Wrightsville Beach, N.C.

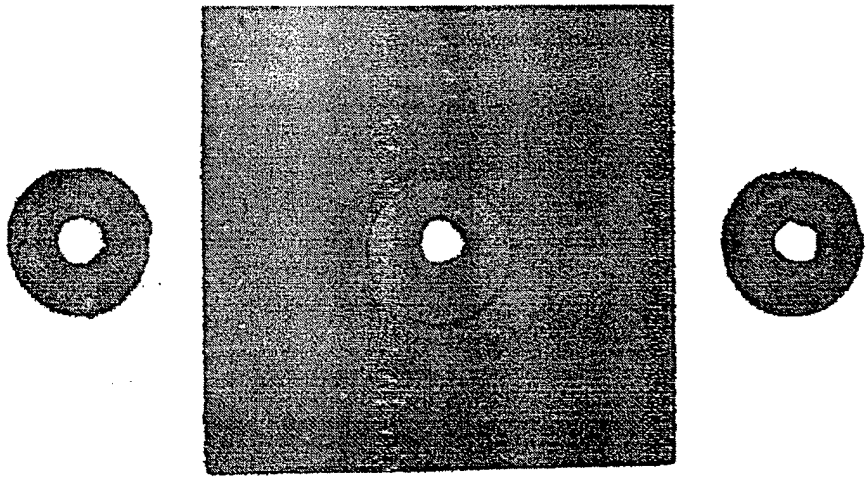

Figure 50. Appearance of Monel K-500 unassembled after exposure to ozonated seawater sixty days, and cleaning.

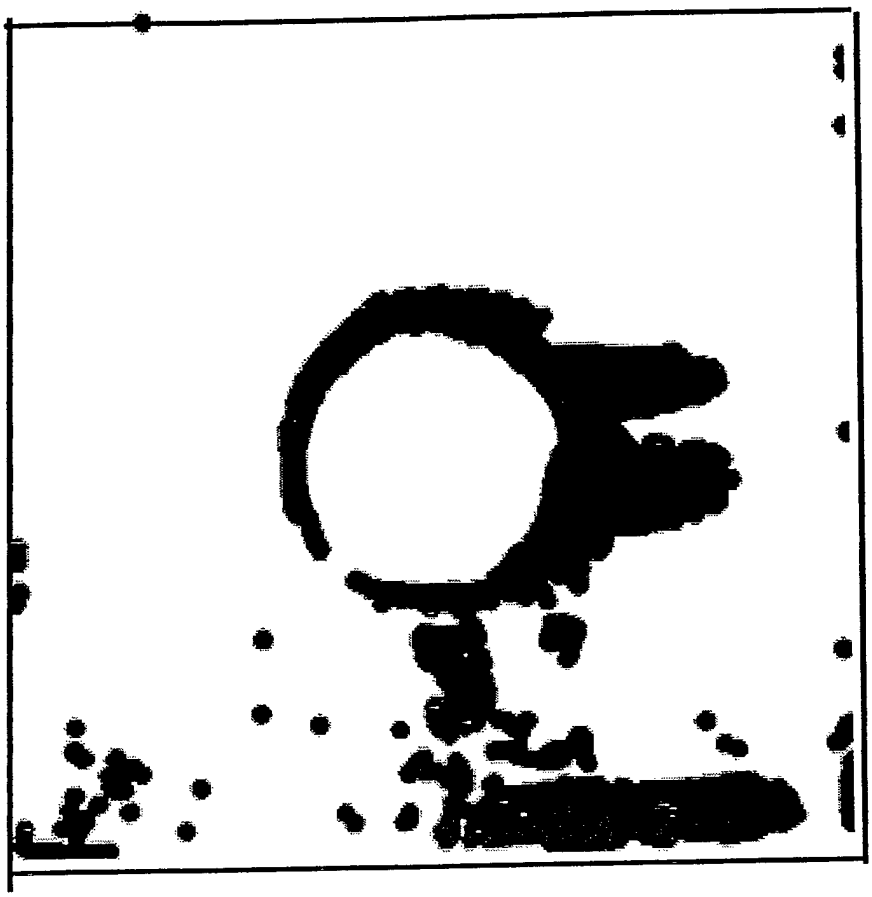

Figure 51. Binary Image showing areas of attack on Monel K-500 after sixty days of exposure to ozonated seawater

Figure 52 shows the Monel K-500 alloy sectioned through the crevice assembly. The outer-most washers are titanium, while the white washers are PTFE. The inner washers and middle plate are Monel K-500. The localized corrosion present at the mouth of the crevice is clearly visible. This attack affected not only the plate but a large area around the edge of the washer.

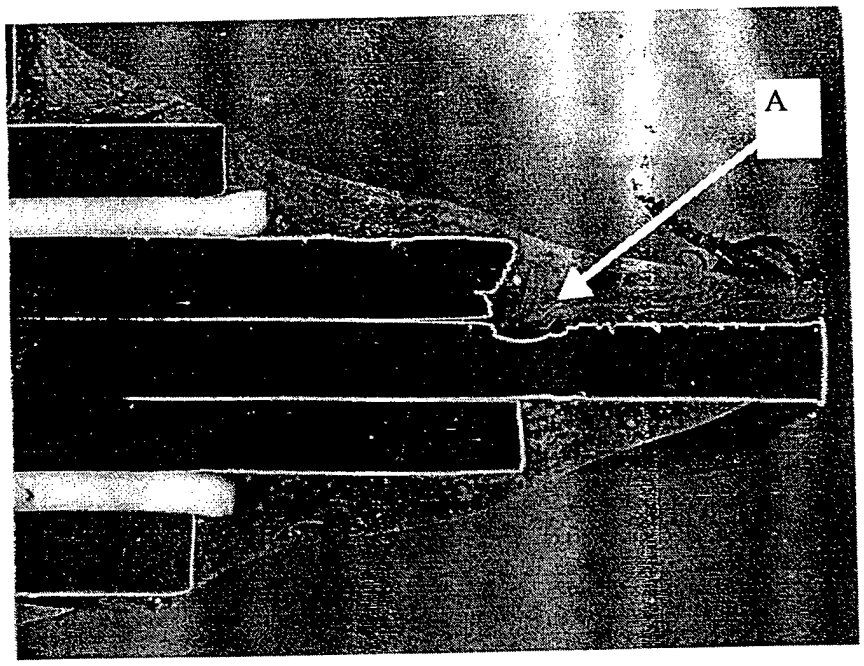

Figure 52. Cross section of Monel K-500 crevice assembly after sixty days of exposure to ozonated seawater at Wrightsville Beach, N.C. 6X. A., shows attack at the mouth of the metal-metal crevice.

Figure 53 shows a cross section of the plate immediately outside the creviced region. Shown here is the severe depth of attack experienced by this alloy after sixty days of exposure to ozonated seawater. Attack of the plate occurred from both sides with attack on one side of the plate being more severe. Having one side of the sample more severely attacked than the other was seen throughout all alloys examined in these tests. Half the thickness of the sample has been eaten away immediately outside the metal-metal crevice region, the area of attack shown in figure 53.

Washers of Monel K-500 exposed to chlorinated seawater show classical crevice corrosion with the deepest attack occurring immediately behind the mouth of the crevice and slight attack throughout the crevice. This is very similar although much less severe than the same washer alloy being exposed to ozonated seawater.

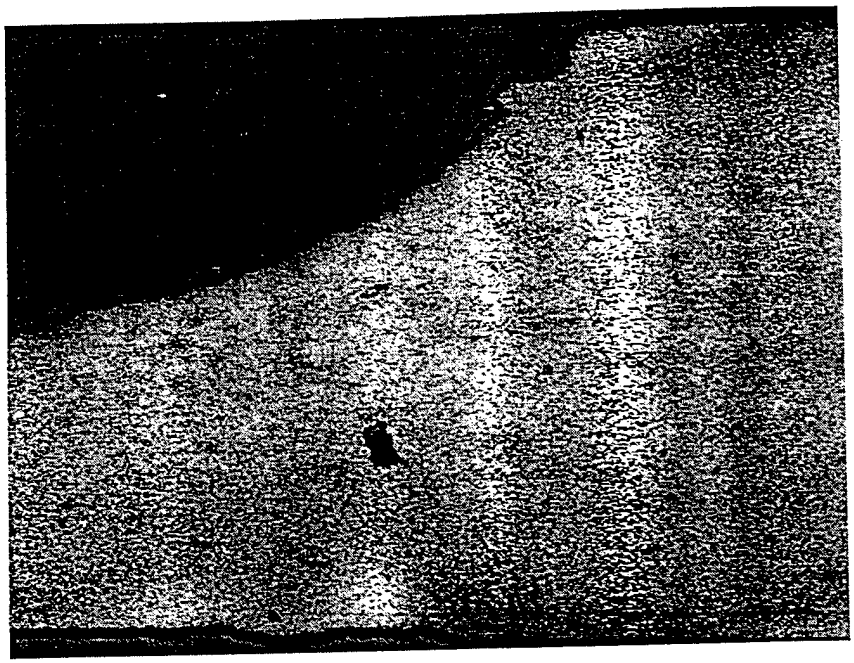

Figure 53. Cross section of plate from Monel K-500 crevice assembly exposed to ozonated seawater sixty days at Wrightsville Beach, N.C. 50.4X, Brass Etch

Monel K-500 exhibits less severe corrosion when exposed to chlorinated seawater compared to ozonated seawater. The localized corrosion is much less severe and the bulk surface of the sample appears largely unaffected. Pitting is much reduced and corrosion is largely confined to the mouth of the crevice as evidenced by a thin black line around the circumference of the mouth of the crevice and some black corrosion product extending out from the crevice, as shown in figure 54.

Upon cleaning the sample shows dissolution around the mouth of both the metal-metal crevice and the metal-non metal crevice. Pitting is still observed and the pitting density may also be slightly larger than that found in ozonated seawater. However, the size of the pits formed on Monel K-500 in chlorinated seawater is smaller than those pits seen in ozonated seawater.

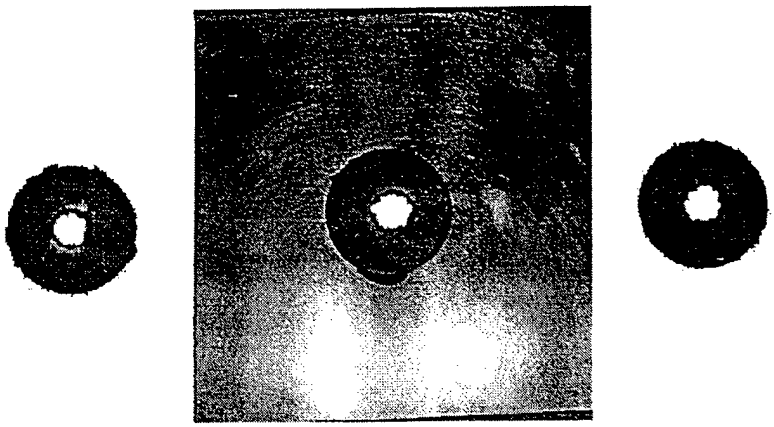

Figure 54. Monel K-500 crevice sample unassembled after sixty days of exposure to chlorinated seawater sixty days at Wrightsville Beach, N.C..

CDA 706 Alloy Exposed To Natural Seawater At LaQue Center For Corrosion Technology.

The CDA 706 alloy (90Cu/10Ni) showed largely general corrosion over the surface. The corrosion products had a layered appearance. The top most layer was a green corrosion product while under that a sparse black corrosion product was formed. Further below a thin brown corrosion product covered most of the sample, much like the brown film seen on the Monel alloys. Other areas show a more copper colored appearance with spots of a red corrosion product or film formed underneath.

Localized corrosion occurred at the mouth of the crevice, as seen in the Monel alloys, in some cases traveling down the sample slightly. Localized attack at the mouth of the crevice was not as severe or deep as that seen in the Monel alloys. Around the mouths of the crevices a red corrosion product or film was found, sometimes in conjunction with the green and brown/black corrosion product. Within the crevice some pitting was experienced. However, the pitting was shallow and not of consequence when compared with attack outside the mouth of the crevice. An example of the CDA 706 alloy after removal from ozonated seawater and disassembly is presented in figure 55.

Figure 55. CDA 706 crevice assembly exposed to ozonated seawater sixty days at Wrightsville Beach, N.C. and unassembled.

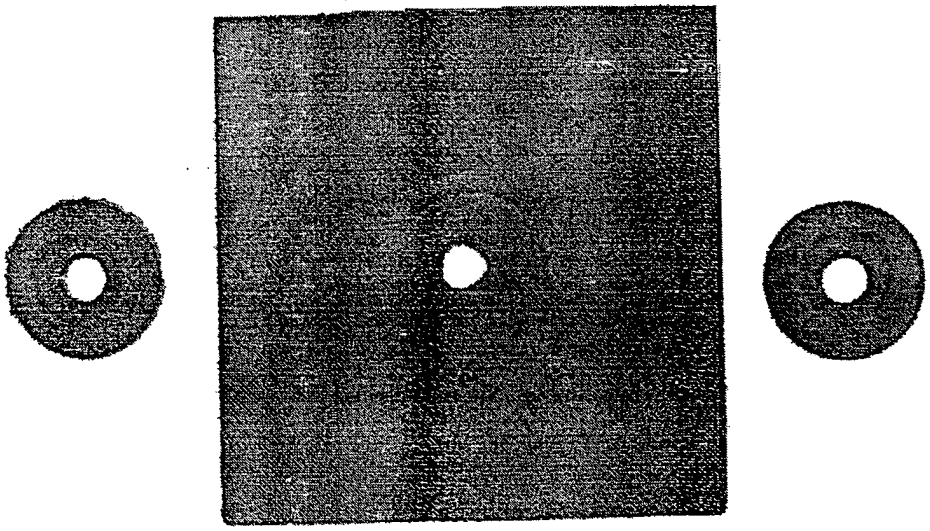

Figure 56. CDA 706 exposed to ozonated seawater sixty days at Wrightsville Beach, N.C. removed, unassembled, and cleaned to remove corrosion product.

A sample of CDA 706 is shown in figure 56 after sixty days of exposure to ozonated seawater and cleaning to remove corrosion product. Approximately half of the sample is covered with the brown film seen formed on the uncleaned sample. This film is especially present within the crevice both on the washers and plate portions of the crevice assembly. The remainder of the sample has an electropolished copper appearance concentrated outside the crevices, covering the washers, and extending over half of the bulk of the plate sample. Areas of shallow pitting or localized general dissolution also become apparent in areas covered with the brown film as evidenced by local areas of electropolished appearance.

A cross-sectional view of the crevice is shown in figure 57. Once again the mouth of the crevice shows the most significant attack. Localized corrosion at the mouth of the crevice has crept into the crevice and up the side of the washer after sixty days of exposure to ozonated seawater. A rough appearance under the PTFE washer (white) also indicates more of a classical corrosion mechanism in the metal-nonmetal crevice.

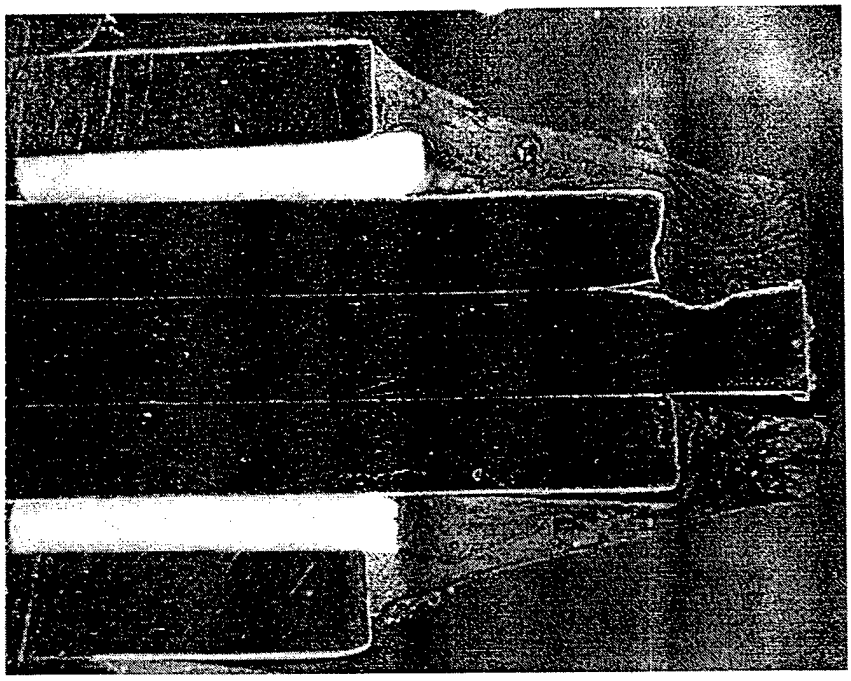

Figure 57. Cross section of CDA 706 crevice assembly after exposure to ozonated seawater sixty days in Wrightsville Beach, N.C. 8X

The same alloy exposed to chlorinated seawater for the same amount of time shows little to no attack, figure 58. The sample was covered in a thin light brown corrosion product. The only evidence of attack is a thin green film found on boundaries between areas of differing sample preparation due to bends of the plate. Additionally, a thin line of red corrosion product/film was found around the crevice just inside the mouth. Inside the crevice some superficial pitting was found however the metal in this area appeared as it did before immersion. CDA 706 exposed to chlorinated seawater did not show the large areas of corrosion product seen in ozonated seawater or the depth of attack around the mouth of the crevice.

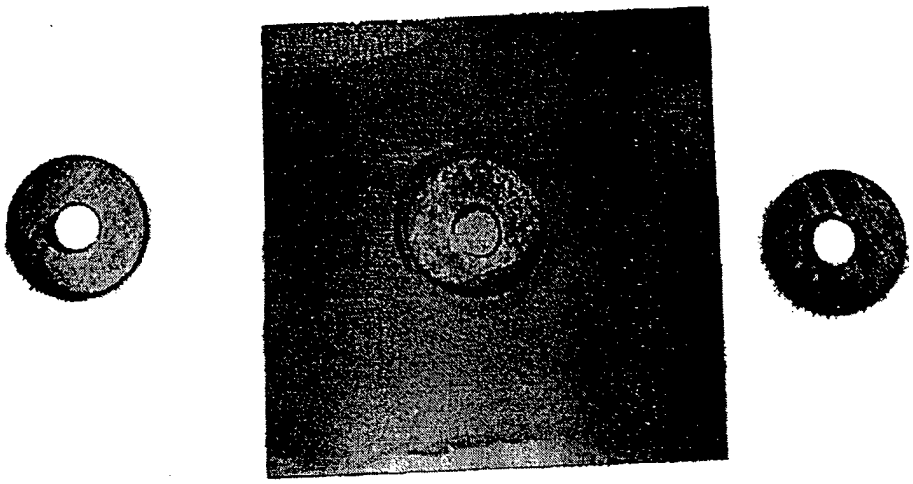

Figure 58. CDA 706 crevice assembly exposed sixty days to chlorinated seawater at Wrightsville Beach, N.C., and unassembled.

CDA 715 Alloy Exposed To Natural Seawater At LaQue Center For Corrosion Technology.

CDA 715 (70Cu/30Ni) once again exhibited a brown film over the surface of the sample. Above this film are intermixed bulky black and green corrosion product. Areas within the crevice are generally free of corrosion product but some the areas under the crevice are covered in a transparent orange film. Areas showing any variation in thickness on the washers (due to labeling of the sample or localized corrosion) were sometimes filled with a red corrosion product. The corrosion seen at the mouth of the crevice in the Monel alloys and CDA 706 is limited in CDA 715. Only a very small area seems to be attacked to any depth at all outside the crevice and certainly not to the depth seen in the other alloys considered. An example of CDA 715 crevice sample exposed to ozonated seawater is shown in figure 59.

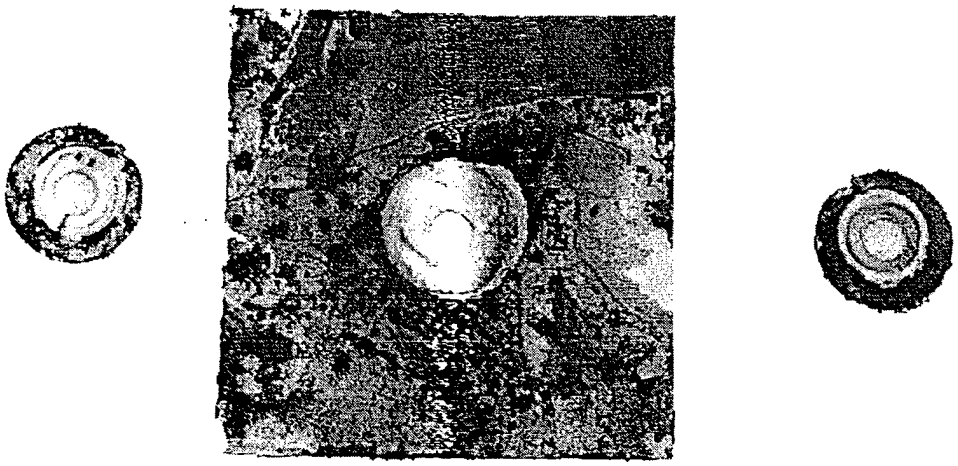

Figure 59. CDA 715 crevice assembly after sixty days of exposure to ozonated seawater at Wrightsville Beach, N.C.

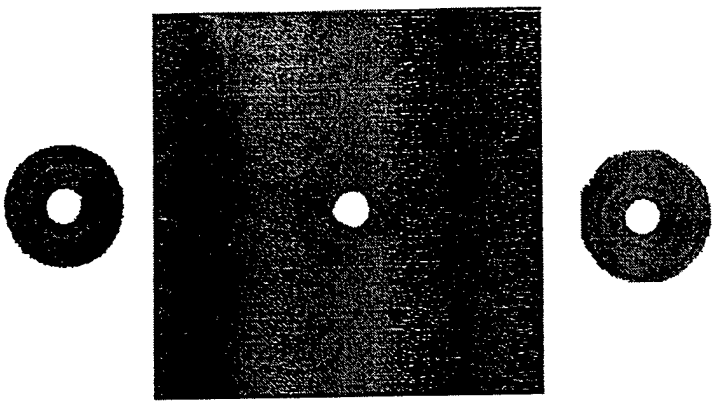

Figure 60. CDA 715 crevice assembly after sixty days of exposure to ozonated seawater at Wrightsville Beach, N.C., disassembly, and cleaning to remove corrosion product.

Cleaning this sample revealed a thin line of attack immediately outside the mouth of the crevice which appeared as coalesced pits or general dissolution. A slight gray discoloration over the surface of the sample evidences a general corrosion over the bulk of the sample. An adherent red film remained on the sample after cleaning. The washers are similar in morphology to the plate showing little attack in the creviced region, a thin area of attack immediately outside the crevice, and a discolored gray film over the remainder of the surface. Figure 60 shows a CDA 715 crevice assembly after sixty days exposure to ozonated seawater, disassembly, and cleaning to remove corrosion product.

A cross section view of the crevice assembly is shown in figure 61. The severe attack seen at the mouth of the crevice is not seen in this case replaced with a general dissolution outside the metal-metal crevice and over the entire outer surface of the metal washer in contact with PTFE. This attack is evidenced by the jagged surface in the mentioned areas and was not seen to this extent in any of the other alloys considered in this paper.

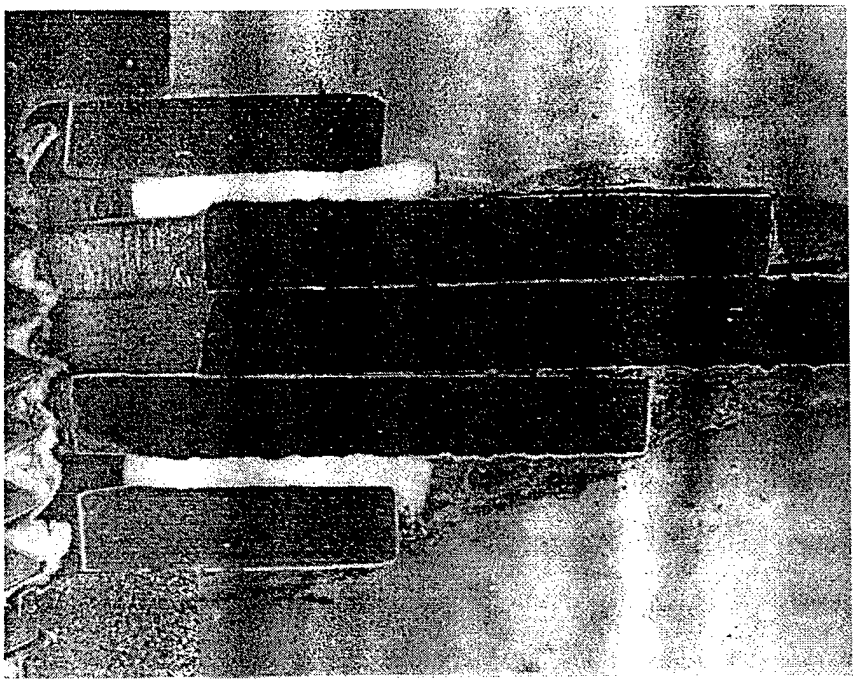

Figure 61. CDA 715 crevice assembly in cross section after sixty days of exposure to ozonated seawater in Wrightsville Beach, N.C. 6X

In chlorinated seawater, corrosion was minimal, occurring only slightly within the boundary of the crevice and in areas of differing preparation due to bends in the sample plate. around the circumference of the crevice a thin line of layered corrosion product is present in this order of color from the outside in: green, black, and red. The metal facing portion of the metal washer shows the same progression. The portion of the washer facing the PTFE washer shows attack of the same morphology although the green corrosion product was not seen. An example of this alloy after exposure to chlorinated seawater is shown in figure 62.

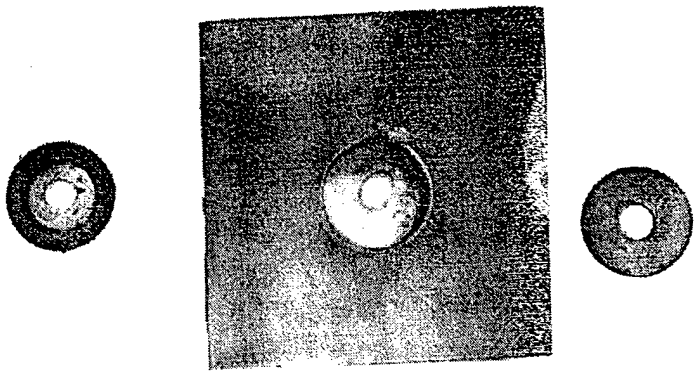

Figure 62. CDA 715 crevice assembly after sixty days of exposure to chlorinated seawater at Wrightsville Beach, N.C. and disassembly.

Discussion

Summary of Results

A black flocculant corrosion product was formed in ozonated seawater after only one day exposure. This corrosion product formed in solution and adhered to the glass portions of the tank and supporting assembly but was not found on the sample itself.

Electrochemical results indicate a noble shift in corrosion potential with ozonation. This shift is more pronounced in the passive, Monel, alloys than in the cupronickel alloys. During potentiodynamic scans a film was formed on all samples which maintained reduction on the surface of the sample to the oxygen reduction potential during polarization after thirty days of exposure. During potentiodynamic measurements the corrosion current density decreased as time of exposure increased, indicating a more protective film being formed on the surface. Also observed, was a shift in corrosion potential during potentiodynamic testing when compared to steady state tests. This indicates a kinetic factor in the corrosion process. The shift was in the active direction and was more pronounced as the nickel content of the alloy decreased. In the CDA 706 the corrosion potential seen during potentiodynamic scans was the same in aerated and ozonated seawater.

Passive alloys exposed to ozonated seawater exhibited the most severe corrosion. Attack in these alloys was concentrated around the mouth of the crevice, with pitting occurring over the remainder of the sample. The cupronickel alloys exposed to ozonated seawater formed a brown/black film over the surface and showed limited attack at the mouth of the crevice.

In chlorinated or aerated seawater attack was limited. All alloys showed little or no attack . Crevice corrosion occurred in a more classical fashion concentrating under the lip

of the crevice rather than immediately outside the crevice as seen in alloys exposed to ozonated seawater.

In Lab

Solutions

The black flocculant found in the ozonated tanks in lab tests after one day of immersion was not seen in North Carolina tests due to continuous refreshment of the tanks in North Carolina. Brown[8] has reproduced this black flocculant by exposing a sample of pure Ni to ozonated distilled deionized water, pH adjusted to 10 with NaOH. Using a potential-pH diagram it was found that the black flocculant is composed of Ni_2O_3 and Ni_3O_4 both of which are decomposition products of NiO_2. NiO_2 and Ni_2O_3 are described as being black by Pourbaix.[21] Brown goes on to state that the black flocculant is a mixture of calcium oxide, sodium chloride, hydrated nickel chloride however the components of seawater are not necessary to form the precipitate.

Electrochemical Results

A noble shift of approximately 100mV in the corrosion potential was observed in ozonated seawater when compared with aerated seawater. This shift in corrosion potential was observed in experiments performed in the lab and in Wrightsville Beach, N.C. and is due to the higher oxidizing potential of ozone compared to oxygen or hypochlorite.

The corrosion current density observed during the potentiodynamic tests lies approximately an order of magnitude greater than the limiting current density due to concentration polarization as estimated according to equation 1.

$$i_l = \frac{D_{ozone} n F C_{ozone}}{\delta} \qquad (1)$$

Where i_l is the limiting current density, D_z is the diffussivity of the oxidant in seawater (estimated to be 10^{-5} cm^2/sec)[22], n is the number of equivalents exchanged, F is Faraday's constant (96500 C/equivalent), C is the concentration of oxidant (0.2 mg/L), and δ is the boundary layer thickness (estimated to be 0.005 cm[23]). Using these values (chosen to simulate the largest reasonable limiting current density) the limiting current density for ozone in seawater is 4.25E-6A/cm^2 below the limiting current density shown in the polarization curves obtained. This indicates that the cathodic reaction is not only due to oxygen reduction. There is another, separate, reduction process occurring.

The polarization curves show anomalous behavior typically seen in the thirty day test. Evidenced by a noble corrosion potential (approximately 0.3 V vs. SCE) and a higher corrosion current density (10^{-5}A/cm^2) this behavior was seen in most alloys and in both environments after thirty days of exposure and again at ninety days in the Monel alloys. A sluggish passivation reaction is a possible cause for this behavior. Corrosion potential values were relatively constant throughout the test at thirty, sixty, and ninety days. This large deviation between the potential seen at thirty days and the corrosion potential measured moments earlier suggests that the cathodic portion is influencing the film formed on the surface of these alloys. The film continues to be reduced until a zero current potential is reached for the oxygen reduction reaction.

$$O_2 + 4H^+ + 4e^- \leftrightarrow 2H_2O$$

Using thermodynamic data[22] the oxygen reduction potential in water was found to be 0.509V vs. SCE with ozone as the feed gas (pO_2=0.95) and 0.499V vs. SCE during aeration (pO_2=0.21). Seawater or kinetic factors, may shift these values slightly reducing the reduction potential to that seen in the polarization curves (about 0.3V vs. SCE).

The steady corrosion potential tests showed the corrosion potential to be shifted between 0.1 and 0.2 V noble in ozonated seawater when compared to aerated seawater. However, in the potentiodynamic tests the corrosion potential in ozonated seawater

approached that of aerated seawater as the amount of nickel in the alloy is reduced. The Monel alloys exhibited corrosion potentials in the potentiodynamic test similar to the steady state test in ozonated seawater. CDA 706 showed that, when the potentiodynamic test was performed in ozonated seawater, the potential was shifted to virtually the same value as that seen in the steady state test performed in aerated seawater. CDA 715 shows an intermediate value, with the corrosion potential observed during potentiodynamic tests shifted active to that found during the steady state tests in ozonated seawater but slightly noble to the values seen in aerated seawater. Corrosion potentials in aerated seawater remained roughly constant between the steady state and potentiodynamic tests.

This shift, with polarization, in corrosion potential in the active alloy (CDA 706) and the alloy with borderline passivity (CDA 715) indicates that the corrosion process is developing a film which limits the anodic portion of the corrosion reaction. The oxidation of copper and/or nickel forms a film which technically would not be considered passive. However, it reduces the corrosion rate by limiting the transport of ions away from or toward the surface of the sample through the film. Dhar et. al[24] have studied the 70Cu/30 Ni alloy in synthetic seawater and state that corrosion current is generated by flux of Cl- or CuCl- toward or away from the electrode surface. Likewise, R.J.K. Wood et. al.[25] have studied the Cu-9.4Ni-1.7Fe alloy (CDA 706) in 3.4%NaCl under rotating conditions proposed that the rate determining step was ionic transport through the electrolyte in the film.

Alloy Corrosion Behavior

Weight loss samples of Monel K-500 show reduced susceptibility to localized corrosion when compared to Monel 400. In aerated seawater the Monel alloys show little attack, protected by a passive film formed on the surface of these alloys due to the high nickel content. In ozonated seawater the Monel K-500 alloy continues to be protected where as the Monel 400 alloy shows significant signs of pitting. This difference is

probably due to an alloying additions of aluminum and titanium which will further stabilize the passive film on Monel K-500. Aluminum alloys have been found to perform well in ozonated seawater due to fast repair of any defects formed in the passive aluminum oxide film because of the high reactivity of ozone.[26] Titanium has been found to be virtually immune to attack in ozonated seawater due to the tenacious passive film which readily forms on the surface. Monel 400 also contains more iron than Monel K-500. Iron remains in the active state and leaves the alloy in a state of active corrosion.[27]

Monel 400 suffered pitting due to localized breakdown of the passive film on the surface in the presence of ozone and chloride. The chloride will initiate breakdown localized breakdown of the film and once started a differential aeration cell will set up with active and passive sites on the surface of the sample. Because of the high oxidizing power of ozone a larger potential difference between the passive and active areas will drive the cell and cause severe localized corrosion. Monel alloys have been found susceptible to pitting due to their passive film, any breaks in the film passive will create this active/passive situation.[28]

The cupronickel alloys show pitting on all samples and in each environment. CDA 706 generally exhibits general corrosion although a film of corrosion product will form which protects the surface by controlling diffusion through the film. Pitting that was found in this alloys may be due an active/passive situation due to protection from the film formed on these alloys.

Pitting was more severe in CDA 715 than CDA 706. CDA 715 is a borderline alloy, at the limit of protection due to formation of a passive nickel oxide film. This film is prone to localized breakdown leading to pitting due to differential aeration as described for Monel 400. M. Reda et. al., have found that 90Cu/10Ni corrodes uniformly and usually avoids pitting attack where as 70Cu/30Ni protects itself with a passive film.[29] Pitting on CDA 715 was seen in both aerated and ozonated seawater indicating susceptibility to

breakdown of the film in either environment and demonstrating the instability of the film formed on CDA 715. Pitting in aerated seawater was less severe possibly due to the reduced driving force of oxygen reduction compared to ozone or to a larger cathode area needed to drive the pit in aerated seawater (related to a the potential difference between ozone and oxygen). In ozonated seawater a larger number of pits per unit area was observed, again, due to the higher driving force in the presence of ozone.

Corrosion rates from weight loss measurements show increased corrosion in ozone of CDA 715 compared to CDA 706 although the opposite is true in aerated seawater. This may indicate that the film formed on CDA 706 due to the corrosion process in ozonated seawater is more stable than the passive film found on CDA 715. This comparison may also indicate the severe localized corrosion found in CDA 715, even though CDA 706 experiencing pitting corrosion and probably general corrosion these do not meet the rate of corrosion found on CDA 715.

CDA 706 shows a corrosion rate that is higher at thirty days in aerated seawater than in ozonated seawater- contrary to what is typically seen. The film on CDA 706 that protects the alloy from corrosion may take some time to form and be fully protective. The higher oxidizing power of ozone may increase the rate of film formation and thus show a lower corrosion rate at shorter times. As time increases the film becomes more protective and the corrosion rate decreases. A decreasing corrosion rate was seen for the CDA 706 alloy over the entire ninety day test period in aerated seawater where as in ozonated seawater the corrosion rate remained relatively constant.

Crevice Corrosion Behavior

Samples exposed in-lab for crevice corrosion testing showed results similar to weight loss samples exposed concurrently. Monel samples exhibited crevice corrosion in ozonated seawater but show no signs of corrosion in aerated seawater. Crevice corrosion in ozonated seawater occurred between the tight crevice spaces on both Monel 400 and

Monel K-500. Crevice attack on Monel 400 was more severe than attack on Monel K-500 as was seen in the case of pitting on weight loss samples as described earlier. Again this difference in behavior between the two alloys is due to alloying differences- or the presence of tenacious oxide formers in Monel K-500 such as aluminum and titanium.

The most interesting feature is that crevice corrosion took place between the tight crevices of the crenelated washers and not in the tight crevice as would be expected in the case of classical crevice corrosion. This type of corrosion has been observed on several nickel- base alloys and some highly alloyed stainless steel alloys in ozonated seawater.[5, 30] This crevice corrosion in the regions between the tight crevice has been described by Brown[8] as Boundary Layer Corrosion (BLC) in nickel-based alloys. Boundary layer corrosion is a result local acidification due to dissolution and subsequent oxidation of nickel which cases local acidification and a lack of mass transport of solution away from the crevice. Additionally a high oxidizer is needed to diffuse into this zone, ozone being a strong oxidizer fulfills this role. This phenomena has been demonstrated in nickel systems and has also been described for copper. Wood et. al.[24] describes local acidification occurring due to Cu_2O precipitation and transfer of H^+ ions into the pore as copper dissolution takes place in order to preserve electroneutrality.

Cupronickel alloys experienced crevice corrosion in both aerated and ozonated seawater. In aerated seawater alloys CDA 706 and CDA 715 experienced classical crevice corrosion with attack occurring beneath the tight crevices formed with a crenelated washer. Pitting within the crevice indicates film breakdown which may be the result of local acidification as a result of crevice corrosion or the presence of chloride in the crevice. The two process occurring together would be expected for a crevice.

In ozonated seawater these cupronickel alloys showed attack similar in morphology to the Monel alloys with the corrosion occurring between the tight creviced areas. It is assumed that the mechanism is the same as that found in the Monel alloys. Boundary

Layer Corrosion is again the dominant mechanism for corrosion here at the crevice. As time went on the corrosion attacked enough metal so that it could begin to attack areas under the crevice from the interface moving in.

Crevice corrosion in aerated seawater was not as severe as that seen in ozonated seawater. In aerated seawater crevice corrosion occurred in a more typical manner (underneath the crevice former). Crevice corrosion in aerated seawater was less severe because a large oxidizer (such as ozone) was not present in solution. The large driving force was not present to continue dissolution and drive local active/passive cells such as was the case in ozonated seawater.

Wrightsville Beach, N.C. Studies

Solution Performance

The corrosion behavior of engineering alloys in ozonated waters has been studied for several years at Rensselaer Polytechnic Institute. These tests have been in sodium chloride solutions as well as artificial seawater but not in water containing the biofouling organisms that ozone was designed to control. The residual ozone concentration of 0.2-0.3mg/l was chosen after discussions with managers of large aquariums where ozone is used to keep the tanks clean. The studies at LaQue Center for Corrosion Technology allowed ozone to be tested in seawater containing organic organisms to determine if the levels used in these previous tests were adequate to prevent biofouling. Testing in ozonated seawater was compared to chlorinated seawater to compare the performance of these two biocides side-by-side. After sixty days of exposure neither tank showed any signs of biofouling. Indicating that continuous ozonation at 0.2mg/l and continuous chlorination at 0.33mg/l will prevent biofouling of these surfaces by micro- and macro-organisms.

Corrosion Potential Comparison

Corrosion potential results between in lab test and test in North Carolina differ noticeably. Corrosion potential results obtained from in lab tests are typically noble to those measurements taken on samples exposed to ozonated seawater in North Carolina. This was particularly true in ozonated seawater where a difference of up to 150mV was seen. The more active values from N.C. tests may be due to increased ozone demand of the natural seawater solution. Microorganism in the seawater, which ozone is used to control, would create a large ozone demand. It was found that ozone did control the biofouling, therefore, ozone demand was created by organisms in the seawater. The exception to this is the CDA 706 alloy, an active alloy which benefited from the increased oxidizer activity to form a more protective film faster limiting corrosion by limiting diffusion as discussed earlier.

In chlorinated seawater the shift in potential was similar to the shift observed in ozonated seawater when those values are compared to aerated seawater tests performed in lab. This shift is due to the larger chlorine concentration which will breaks the passive film, lowering the potential by shifting these passive alloys into the active state. Again the exception is the CDA 706 alloys in which the corrosion potential values between chlorinated and aerated seawater are virtually identical. These similar values indicate that the CDA 706 alloy does not depend on the passive film for corrosion resistance and that the corrosion rate is controlled by the anodic reaction.

Of interest also is that the corrosion potential of the Monel alloys in chlorinated seawater and ozonated seawater are nearly identical. The destabilization of the passive film formed on these alloys due to excess chlorine present could again explain this phenomena and the agreement between the ozone (which sees a higher reduction potential) and chlorinated (which sees increased chloride concentration) seawater. The corrosion rate of these two alloys is also similar differing by only 0.1mm/yr..

Crevice Corrosion Behavior

A second focus of tests conducted in North Carolina was the observation of crevice corrosion effects in ozonated seawater. Studies were first conducted in lab to better understand crevice corrosion under more controlled circumstances. The morphology of corrosion was the same between in lab and N.C. tests, however, attack was much more severe on samples exposed to ozonated seawater in N.C.

Contributing to this large difference in corrosion severity between the in-lab and N.C. studies can be found in the black flocculant found in solutions containing these alloys in lab studies. In this situation the black flocculant was allowed to accumulate where as in the N.C. studies the tanks were continually refreshed, flushing away the black flocculant. This black flocculant has a certain ozone demand, reacting with the ozone before it is able to react on the surface of the metal samples immersed. In the continuously refreshed tanks the ozone could immediately react with the samples, which thus saw a larger concentration of oxidizer and therefore show increased corrosion when compared to the study conducted in lab. Introduction of ozone into the tank was done immediately ahead of the samples (with respect to seawater flow) and thus fresh ozone was allowed to react on these alloys, possibly still in a gaseous form.

A second contributor to the large difference in corrosion severity is the flow present in the tanks. Flowing seawater reduced the boundary layer over the sample which would allow faster transport of ions to and from the sample, assuming the same diffusion constant. It has already been hypothesized that the corrosion process is controlled by transport of ions to or away from the electrode surface, a thinner boundary layer would only increase the corrosion process. The flow also aided in the creation of stagnant layers adjacent to the crevice which was a factor in the boundary layer corrosion seen in ozonated seawater

The corrosion morphology of alloys exposed to ozonated seawater in N.C. is similar to that found in lab tests. Voluminous corrosion product formed on the Monel alloys further aggravated already severe corrosion. As the corrosion continued at the mouth of the crevice this porous corrosion product formed around the area of attack further protecting that area from mass transport and thus solution refreshment. Acidification occurred is this area breaking down the film and exposing the area underneath for further corrosion. Because of density differences between this acid and seawater, the acid solution traveled down the sample forming this same voluminous corrosion product during the descent. Essentially this process formed an occluded cell which started at the mouth of the crevice. Attack was severe, consuming half the thickness of the sample (0.159cm, 0.0625"). The nonmetal-metal crevice exhibited the same sort of attack however, it was not as severe as the attack seen at the metal-metal crevice mouth. The PTFE is more stable in this environment than the alloyed metals and not as prone to local acidification although the breakdown of PTFE in ozonated seawater has been observed.[19] The area within the metal-metal crevice showed little sign of attack exhibiting no signs of attack due to seawater and only a slight spottiness, the result of the early stages of pitting.

In chlorinated seawater little attack was observed other than some corrosion product accumulation immediately inside the crevice. This indicates the initiation of attack, however, no depth of attack was observed.

The cupronickel alloys showed less corrosion than the Monel alloys with CDA 715 (70Cu-30Ni) showing less corrosion than CDA 706 (90Cu-10Ni). These alloys show less corrosion than the Monels because of lack of protection from an adherent passive film. The cupronickel alloys are more susceptible to general corrosion than the Monel alloys. CDA 706 showed some evidence of the boundary layer type of attack at the mouth. However, the depth of attack is not as severe as that seen in the Monel alloys. Attack is seen at the mouth of the crevice, extending slightly into the metal-metal crevice and attacking the edge of the washer. Large areas of the sample took on an electropolished appearance due to

large areas of dissolution. This became evident upon removal of the corrosion product indicating that the corrosion process continued to take place slowly underneath the film. Areas inside the crevice (both the metal-metal and metal-nonmetal crevices) show some superficial pitting with the metal remaining largely as it appeared before immersion.

The CDA 715 sample showed the least corrosion when exposed to ozonated seawater than the other three alloys investigated. This is most likely due to its unique combination of passive and active characteristics. A passive film is allowed to form, slowing corrosion. However, this film may quickly breakdown leaving the sample in a state of active corrosion. The cross section of the crevice in this sample (figure 61) shows general corrosion along in the crevice and outside the crevice- not the BLC corrosion seen in the other alloys. Some BLC was found in other samples of CDA 715 showing that it is susceptible to this type of attack however the depth of attack was less than that seen in CDA 706. The appearance of the BLC (a thin line of pits around the mouth of the crevice) may shed some light on the initiation of this process. BLC may form by the coalescing of several localized corrosion sites around the mouth of the crevice where acidification and thus corrosion are most severe.

In chlorinated seawater the results of the cupronickel alloys are more similar to the Monel alloys. No depth of attack was seen, indicating that the film formed in chlorinated seawater at an average concentration of 0.33mg/L on these alloys is capable to protect the metal surface. Whether the film is the result of a stable passivating process or a corrosion process it appears to be stable, limiting corrosion in chlorinated seawater.

Conclusions

Samples immersed at the LaQue Center for Corrosion Technology in ozonated seawater show that continuous ozonation at 0.2mg/l is sufficient to prevent biofouling in seawater. Continuous chlorination at an average of 0.33mg/l also proved sufficient to prevent biofouling in seawater.

Although the type of attack seen in the lab and at LaQue Center for Corrosion Technology was identical, the severity of attack was vastly different. Crevice samples exposed at North Carolina in ozonated seawater exhibit more severe corrosion, primarily occurring at the mouth of the crevice, then samples exposed in-lab to ozonated seawater. The increased severity of corrosion is due to the lack of black flocculant and the flow present in LaQue tests. This black flocculant was found shortly after immersion and is produced by the transpassive dissolution of nickel. The flocculant (which creates ozone demand) was not found in North Carolina tests because of continuing refreshment of seawater.[8] The increased ozone demand of the flocculant reduces th amount of ozone reacting on the surface of the sample, decreasing the amount of corrosion. The flow present in the North Carolina tests also contributed to the severe corrosion of these alloys by reducing the thickness of the boundary layer over the surface of the sample, increasing ion transport and creating stagnant areas due to the geometry of the crevice.

The corrosion behavior of copper-nickel and nickel-copper alloys is largely dependent on the type of film formed over the surface. Those alloys that are passive (Monel 400 and Monel K-500) show increased corrosion due to the development of active/passive sites which are caused by local breakdown of the passive film due to chloride ions. With the increased oxidizing power of ozone, corrosion would occur rapidly at the active sites. Severe corrosion was also seen, on these alloys, at the mouth of the crevice due to a boundary layer corrosion effect. Boundary layer corrosion is described by Brown[8] and is the result of metal dissolution and oxidation which produces

a local acidic environment combined with a geometrical situation which limits mass transport near the mouth of the crevice.

The additional alloying elements present in Monel K-500 (aluminum and titanium) help to form a more tenacious and faster forming film on the surface which slightly reduces the corrosion compared to Monel 400. Monel 400 also has an increased iron concentration which can accelerate corrosion in nickel alloys.

The cupronickel alloys also show this boundary layer corrosion effect but to a lesser extent than that seen in the Monel alloys. These alloys generally are more active with the corrosion rate being controlled by a film of corrosion product which limits migration to and from the surface of the sample and thus limits the corrosion rate by controlling the anodic reaction.

In conclusion, ozonation of seawater increases the severity of attack compared to both aerated seawater and chlorinated seawater as was observed in lab tests at Rensselaer Polytechnic Institute and in studies conducted the LaQue Center for Corrosion Technology. General corrosion rates in ozonated seawater remain acceptable, being below 0.2mm/yr., but are larger than those found in aerated or chlorinated seawater. In the Monel alloys up to half the thickness of the sample was consumed at the mouth of the crevice after sixty days of exposure to ozonated seawater. Therefore, crevices should be avoided considering the extent of attack seen at the mouth of the crevice

Appenidix 1

RESULTS OF CREVICE CORROSION STUDIES IN OZONATED AND CHLORINATED SEAWATER OF NI-BASE ALLOYS.

Introduction

As interest has grown in using ozone as a biocide in marine heat exchanger systems, so has concern over the corrosive effects of ozone on the materials in those systems. As an alternative to chlorine based biocides, ozone offers the ability to be produced on site, a short half-life, and a higher oxidizing potential that hypochlorite. For these reasons ozone is also favored environmentally. It is not necessary to store large volumes of chemicals and with its decomposition product being oxygen ozone is relatively benign to the environment.

This study investigates the crevice corrosion effects of ozone on IN625®[‡], Hastelloy C-22™, C-276, an C-2000™[§].Crevice corrosion studies were carried out at LaQue Center for Corrosion Technology, Inc. in Wrightsville Beach, North Carolina. Studies compare ozonated and chlorinated seawater as well as metal-metal and metal-PTFE crevices. This work was sponsored by the Office of Naval Research and special thanks to Haynes International for their donation of materials.

[‡] Inconel is a trademark of the Inco family of companies.

[§] Hastelloy, C-22, and C-2000 are trademarks of Haynes International, Inc.

Experimental

Composition

The nominal chemistry of the nickel-base alloys used in this study are shown in table 7.

	C (a)	Cr	Fe	Mo	Ni	Si (a)	W	Other
Alloy 625	0.1	21.5	5.0 [a]	9.0	62	0.5	-	Nb-4.0
C-22	0.015	22.0	3.0[a]	13.0	56	0.08	3.0	
C-276	0.01	15.5	5.5	16.0	57	0.08	4.0	
C-2000	0.01	23	-	16	bal.	0.08	-	Cu-1.6

Table 7. Nominal composition of nickel-base alloys used in LaQue tests.[31,32]

(a) represents maximum acceptable

Etching Solution

Samples from this group of alloys that were prepared for metallographic analysis were etched with 0.5g CrO_3 in 100ml HCl . To etch, samples were immersed in this solution for 10-30 seconds.

Results

Potential Measurement results

Potential measurements were performed after sixty days of exposure before withdrawal of samples from the tanks. Results are shown in the figures below. The corrosion potential in chlorinated seawater is nearly the same for the four alloys investigated at approximately 0.32V versus SCE. Not only is the potential nearly the same throughout the four alloys but the individual measurements show little variability (a maximum range of 0.03V). In ozonated seawater the potential measurements show more variability between the alloys and within the alloy.

Average potential measurements in ozonated seawater were 0.454V, 0.590V, 0.756V, and 0.765V vs. SCE for IN625, C-2000, C-22, and C-276 respectively. IN625 showed the largest range in values, varying between 0.23V and 0.585V vs. SCE. The Hastelloy C alloys showed less variability. Potential measurements in ozonated seawater are noble to those found in chlorinated seawater by as much as 0.35V. Alloys C-22 and C-276 showed the largest difference (0.35V) and highest potential (0.78V vs. SCE). Alloy 625 showed the smallest difference (a noble shift of 0.14V compared to chlorinated seawater) and most active potential in ozonated seawater (0.46V vs. SCE). Alloy C-2000 falls between these two extremes at 0.60V vs SCE.

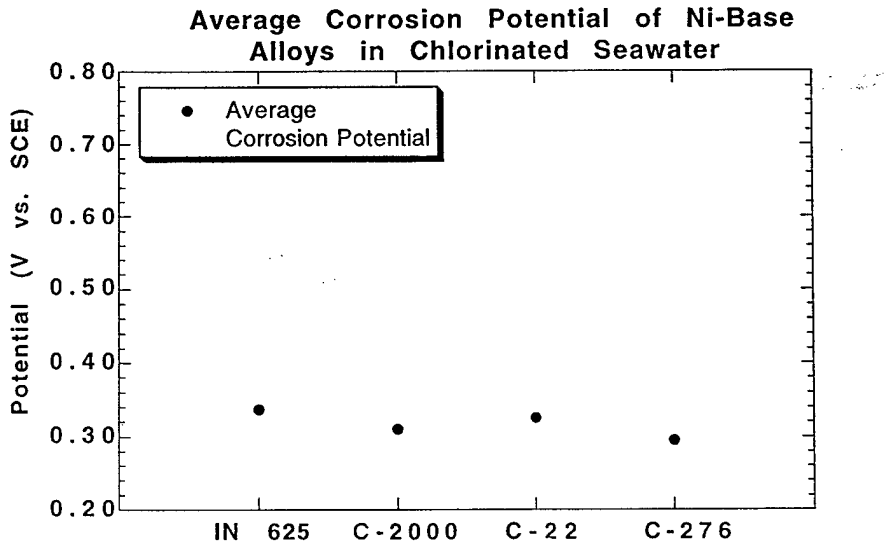

Figure 63. Corrosion potential of nickel base alloys in chlorinated seawater at Wrightsville Beach, N.C.

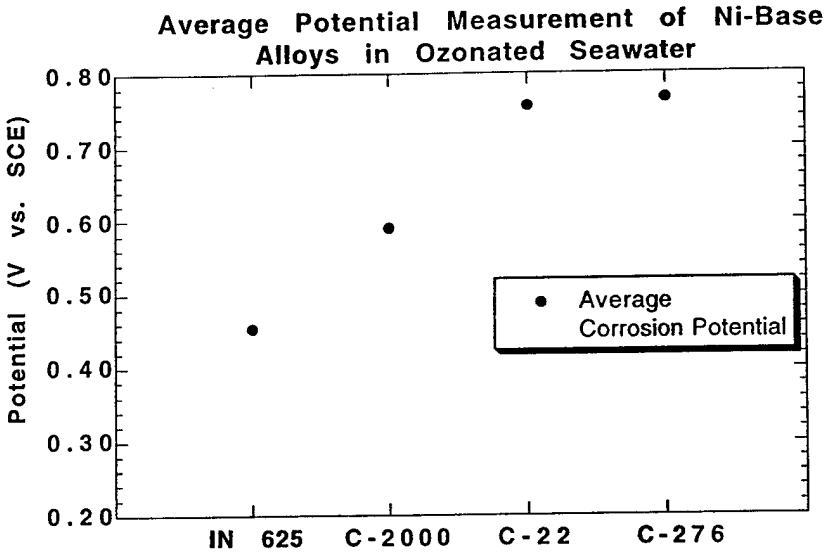

Figure 64. Corrosion potential measurements of nickel base alloys in ozonated seawater at Wrightsville Beach, N.C..

Corrosion Rate Measurements

Corrosion rate was calculated from weight loss measurements after disassembly and cleaning of the sample . Measurements were made separately for the washers and plates in chlorinated and ozonated environments, results are shown in the following four figures.

The plate portion of the sample shows a corrosion rate an order of magnitude higher in ozonated seawater compared to chlorinated seawater. Alloy C-2000 shows the highest corrosion rate (0.036mm/yr.) in chlorinated seawater, yet ties with alloy 276 for the lowest corrosion rate in ozonated seawater. In ozonated seawater alloy 625 shows the largest corrosion rate, 0.23mm/yr.. Alloy C-276 shows the lowest corrosion rate in ozonated and chlorinated seawater (0.002 mm/yr. and 0.000505 mm/yr. respectively) of the four alloys investigated here. Despite the higher corrosion rate in ozonated seawater

these alloys display excellent resistance to corrosion as determined from weight loss measurements (figures 65 &66).

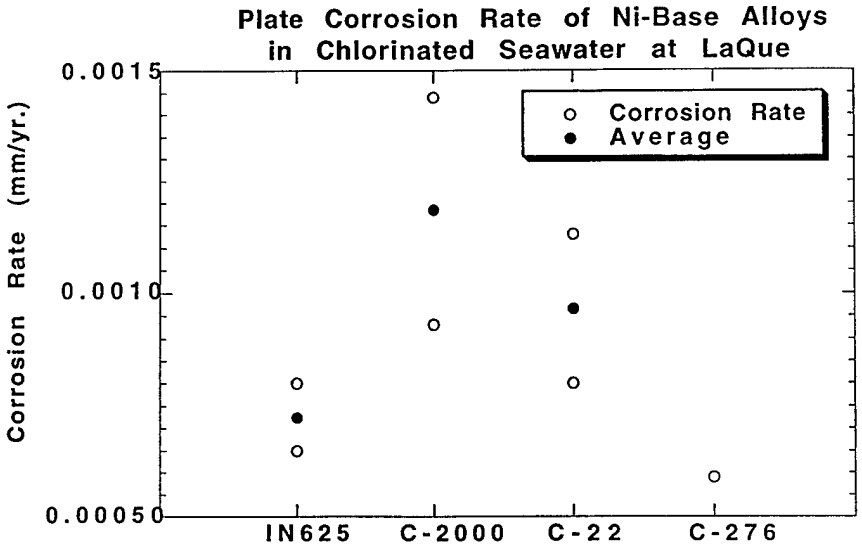

Figure 65. Corrosion rate of plate nickel-base alloys exposed to chlorinated seawater for sixty days at Wrightsville Beach, N.C.

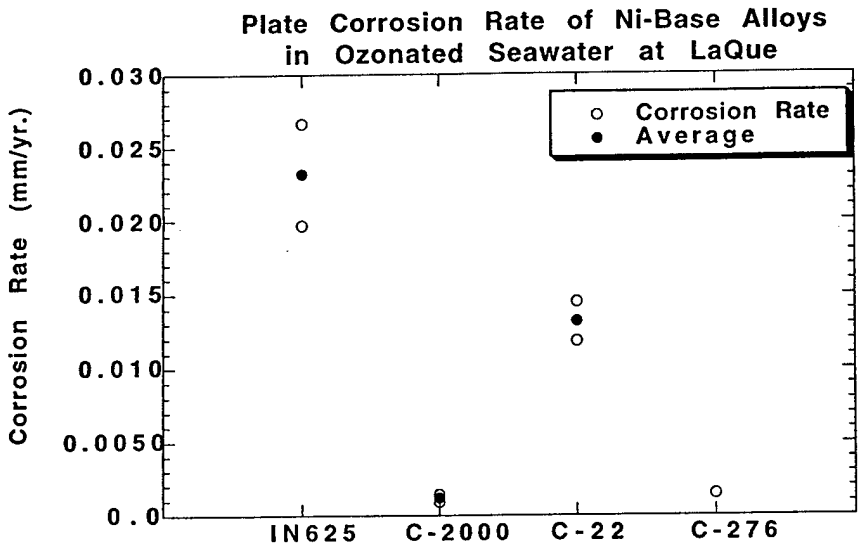

Figure 66. Corrosion rate of plate nickel base alloys exposed to ozonated seawater for sixty days at Wrightsville Beach, N.C.

The washers from the disassembled crevice samples show much larger corrosion rates in ozonated seawater and approximately the same corrosion rate in chlorinated seawater. In ozonated seawater alloy 625 once again shows the highest corrosion rate with an average of 0.30mm/yr and reaching up to 0.60mm/yr. with a washer that shows a large amount of attack within the crevice. Once again, alloy C-276 shows the lowest corrosion rate in ozonated and chlorinated seawater (0.02mm/yr. and 0.00070mm/yr. respectively). The results are plotted in figures 67 and 68.

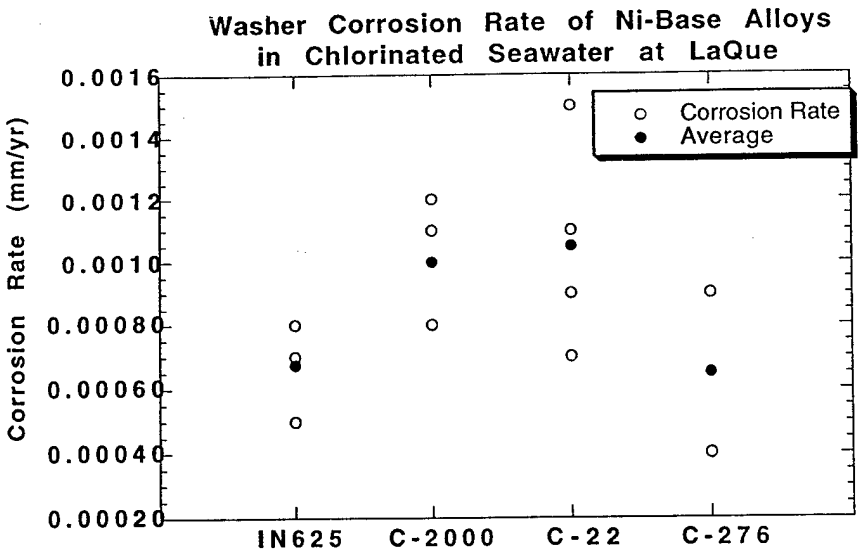

Figure 67. Corrosion rate of washer nickel base alloys exposed to chlorinated seawater for sixty days at Wrightsville Beach, N.C..

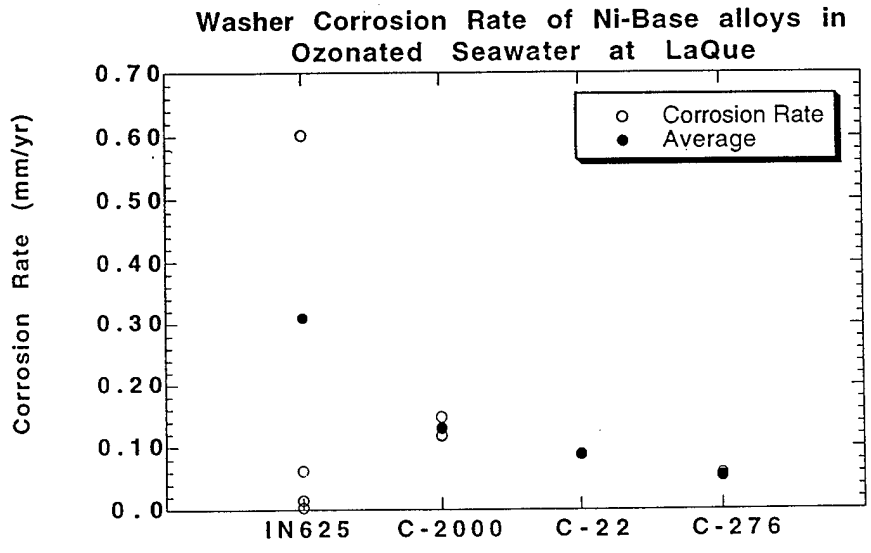

Figure 68. Corrosion rate of washer nickel base alloys exposed to ozonated seawater for sixty days at Wrightsville Beach, N.C.

Corrosion Results

Corrosion results for the Hastelloy C alloys are similar in ozonated seawater. All three of these alloys exhibit an electropolished appearance concentrating outside the mouth of the crevice and appearing over other sections of the sample. At the outside of the crevice these alloys also show a small trench formed by localized corrosion after exposure to ozonated seawater. In all of these alloys a black corrosion product was present on the sample during and after removal from the tanks. The corrosion product was loosely adherent and quickly came off. These alloys also showed a transparent brown corrosion product covering parts of the sample not necessarily occurring with the black corrosion product.

In chlorinated seawater the Hastelloy C alloys show little attack, the only visible sign of exposure is a thin line of dark brown/black oxide corrosion product at the outside of the crevice.

Alloy 625 showed both, severe classical crevice corrosion in one case, and the trench like feature found in the Hastelloy alloys when exposed to ozonated seawater. Alloy 625 also showed a black corrosion product over the entire surface of the sample which overlaid a brown discoloration also over the surface of the sample after exposure to ozonated seawater. Exposure in chlorinated seawater resulted in only the transparent brown corrosion product.

Results will be shown by alloy in the following pages.

Alloy 625 Corrosion Results

Figures 69 and 70 show alloy 625 after sixty days of exposure to ozonated and chlorinated seawater- disassembly and cleaning to remove corrosion product. In both ozonated and chlorinated seawater a brown oxide film formed over the surface of the sample; excluding the creviced regions which appeared as immersed. The one exception

to this, is a sample exposed to ozonated seawater. Here, one side of the sample showed severe classical crevice corrosion underneath the washer, as can be seen in the figure below. Otherwise in ozonated seawater alloy 625 showed the attack at the mouth of the crevice and electropolished appearance over the surface of the sample. The washers mated to these plates show attack identical in morphology. Other than the brown oxide film no attack was observed on those sample exposed to chlorinated seawater.

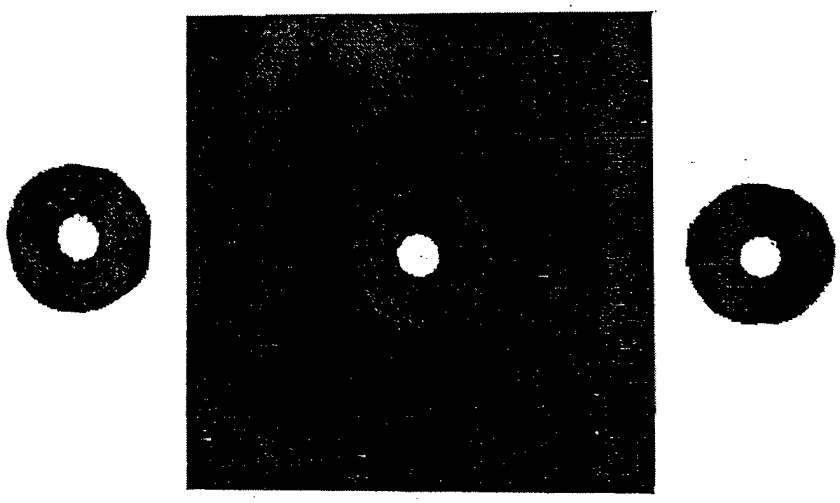

Figure 69. Alloy 625 after sixty days of exposure to ozonated seawater, disassembly, and cleaning at Wrightsville Beach, N.C.

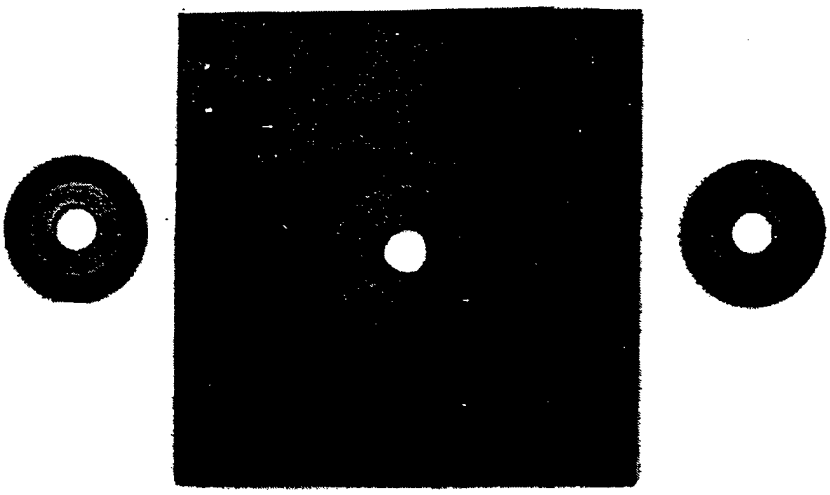

Figure 70. Alloy 625 after sixty days of exposure to chlorinated seawater, disassembly, and cleaning at Wrightsville Beach, N.C..

That plate showing extensive attack was cross-sectioned, the results is shown in the figure 71. Up to half of the plate thickness was corroded away during sixty days of exposure to ozonated seawater, the corresponding washer was also severely attacked. Otherwise, only a small amount of attack was observed in ozonated seawater at the mouth of the crevice.

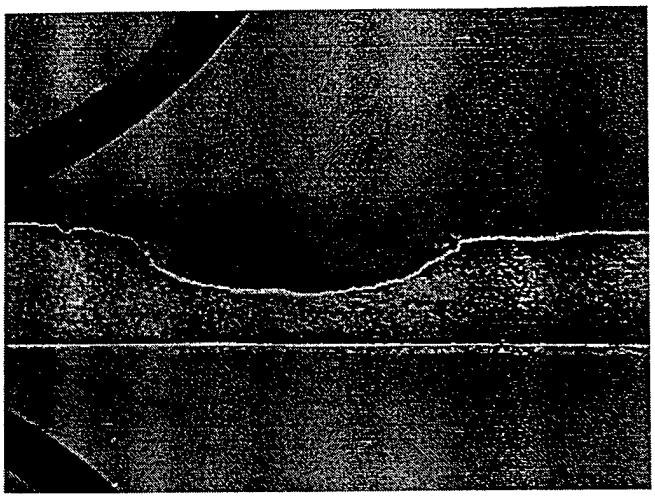

Figure 71. Cross section of Alloy 625 plate exposed for sixty days to ozonated seawater at Wrightsville Beach, N.C.. Sample is shown after disassembly and cleaning.

C-22 Corrosion Results

Hastelloy C-22 and the other Hastelloy alloys show similar results. C-22 exhibits a random eletropolished appearance concentrated around the mouth of the crevice, but is distributed over other areas of the sample. In chlorinated seawater this alloy shows little attack, only a slight discoloration over the surface of the sample is visible. Figures 72 and 73 show these samples after exposure to ozonated and chlorinated seawater.

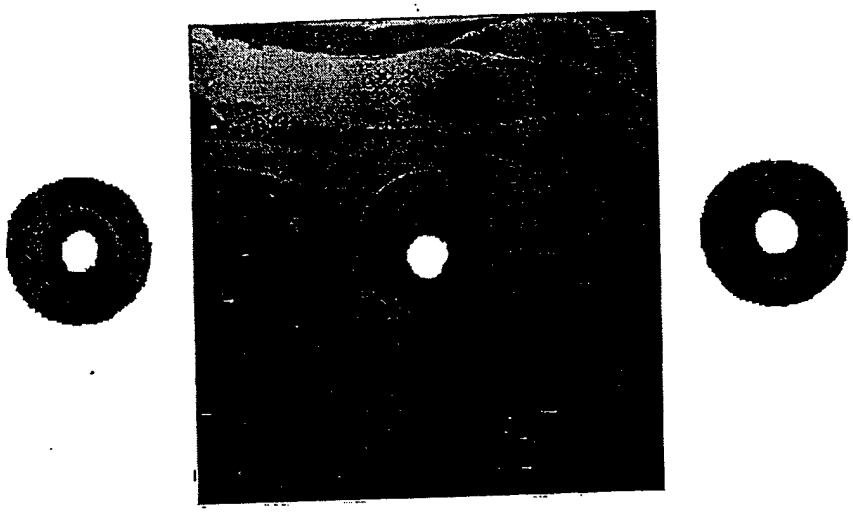

Figure 72. Hastelloy C-22 after sixty days of exposure to ozonated seawater in Wrightsville Beach, N.C. Sample shown disassembled and cleaned to remove corrosion product.

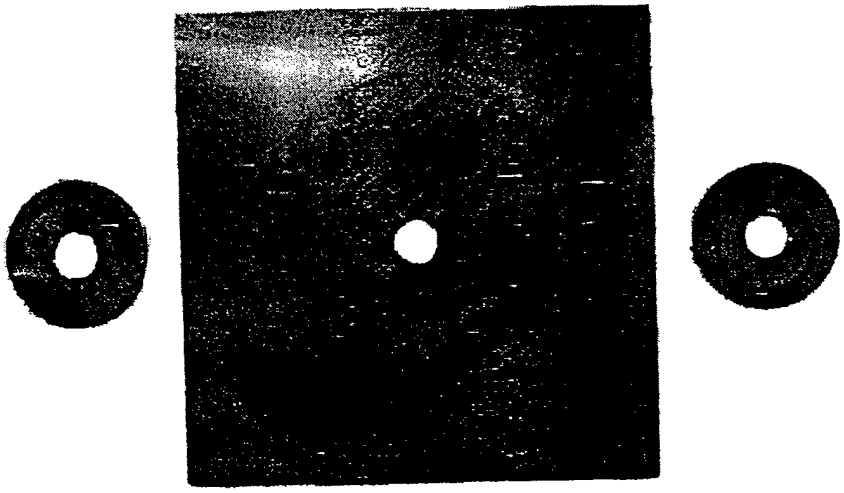

Figure 73. Hastelloy C-22 after sixty days of exposure to chlorinated seawater in Wrightsville Beach, N.C. Sample shown disassembled and cleaned to remove corrosion product.

Figure 74 shows the attack typically seen on this alloy, and other alloys in this group. The small trench, at the mouth of both the metal-metal and metal-nonmetal

crevice, seen in this alloy is typical of the localized attack seen in this group of alloys. The white areas are the PTFE washers used to create the metal-nonmetal crevice and isolate the crevice assembly from the bolt and nut, preventing galvanic attack.

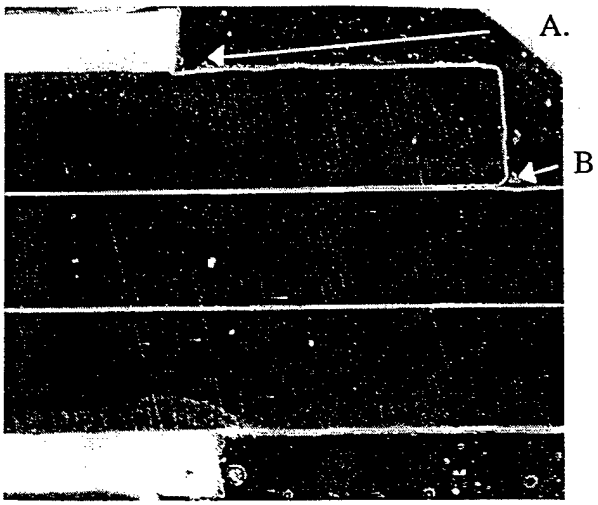

Figure 74. Cross section of C-22 crevice assembly exposed for sixty days to ozonated seawater. White areas are PTFE washers while the rest of the areas shown are C-22. A. and B. show attack at the mouths of the crevice. 14X

Hastelloy C-2000 Corrosion Results

Like C-22, C-2000 exhibits little attack after exposure to chlorinated seawater, After exposure to ozonated seawater C-2000 exhibits localized attack at the crevice mouth along with an electropolished appearance over the surface of the sample. The washers exposed with the plate samples show a similar morphology as the plates with which they were immersed. This behavior can be seen for ozonated seawater in figure 75.

A cross section is also shown of a washer section in order to exhibit the extent of attack seen in these alloys after exposure to ozonated seawater. The attack occurred at the mouth of the crevice, immediately outside the crevice interface.

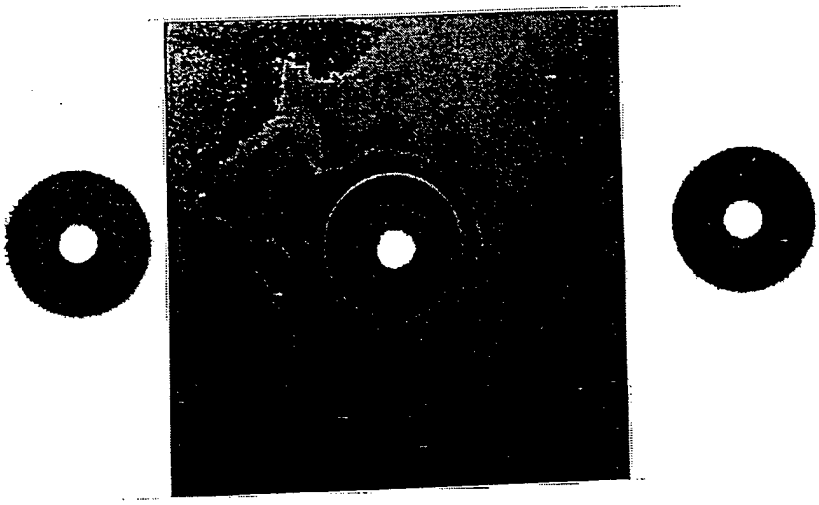

Figure 75. Alloy C-2000 after sixty days of exposure to ozonated seawater at Wrightsville Beach, N.C., Sample is shown after disassembly and cleaning.

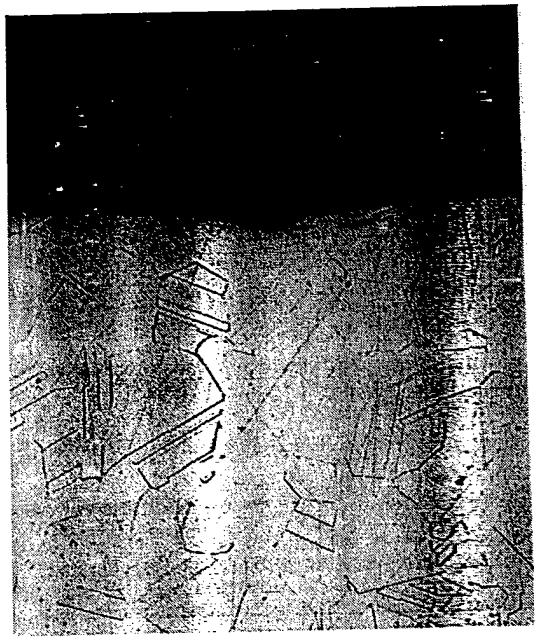

Figure 76. Cross-section of washer after sixty days of exposure to ozonated seawater. sample is shown after disassembly, cleaning, etching with 0.5g CrO_3 in 100ml HCl, and magnification of 126X.

C-276 Corrosion Results

As mentioned before, the attack for all the Hastelloy C alloys is very similar. The difference here is that alloy C-276 shows a black corrosion product within the crevice. Although the black corrosion product was over the surface of the sample, as seen in the other alloys, C-276 was the only alloy to exhibit the presence of this corrosion product within the metal-metal crevice after exposure to ozonated seawater.

Once again, exposure to chlorinated seawater resulted in little to no attack of the sample.

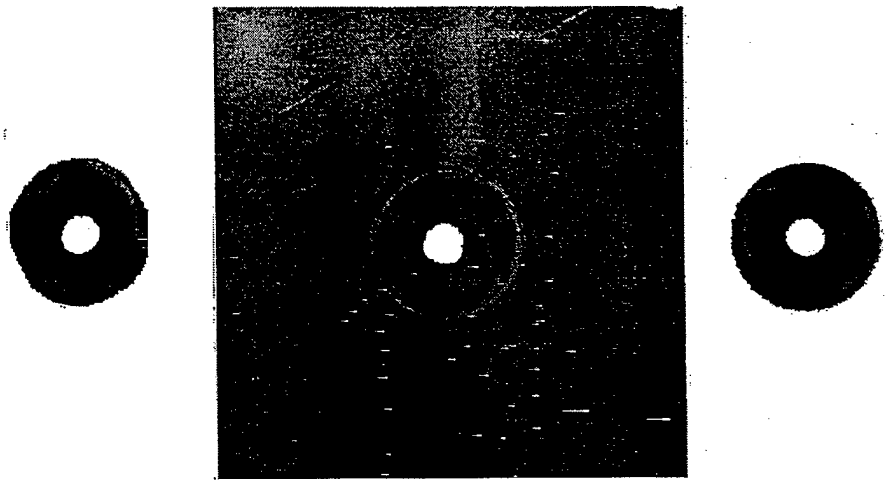

Figure 77. Alloy C-276 after sixty days of exposure to ozonated seawater at Wrightsville Beach, N.C.. Sample is shown after cleaning and disassembly.

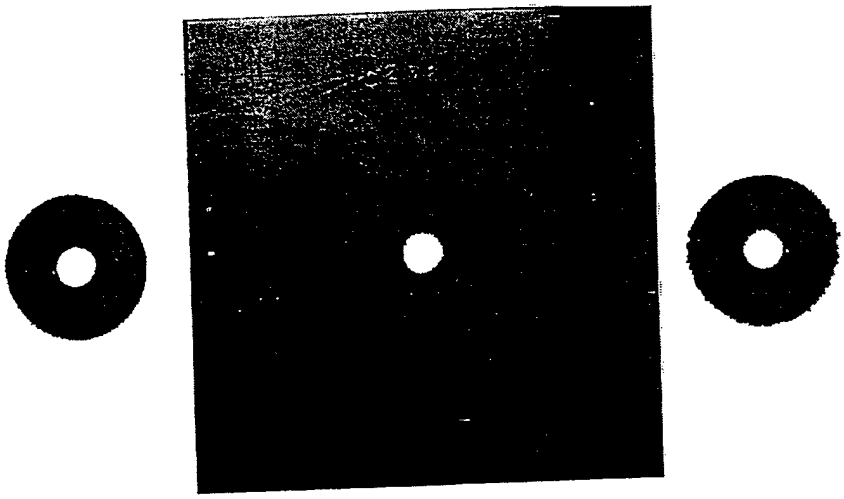

Figure 78. Alloy C-276 after sixty of the exposure to chlorinated seawater at Wrightsville Beach N.C.. Sample shown after disassembly and cleaning.

In a cross-sectional view of a C-276 washer, the extent of attack experienced by this alloy during exposure to ozonated seawater can be seen. This is shown in figure 79.

Figure 79. Cross-sectional view of a C-276 washer exposed to ozonated seawater for sixty days at Wrightsville Beach, N.C.. Sample is shown after disassembly, cleaning, etching with 0.5g CrO_3 in 100ml of HCl, and magnification of 126X.

Discussion

Virtually no corrosion was found to occur on any of these nickel-base alloys with exposure to chlorinated seawater. However, with exposure to ozonated seawater a troughing was found immediately outside the tight crevice formed by the metal washer and the PTFE washer. This troughing behavior and electropolished appearance was found throughout the Hastelloy alloys which all behaved in a very similar manner. Alloy 625 displayed this troughing behavior but also exhibited severe classical crevice corrosion after exposure to ozonated seawater.

Brown[33] has already given an extensive review of these alloys in this environment. It has been found that the troughing seen around the outside of the crevice, and the corresponding electropolished appearance is due to what is termed Boundary Layer Corrosion (BLC). BLC occurs due to transpassive dissolution of nickel ions. These ions react with ozone forming oxides and producing hydrogen ions. This reaction causes acidification at the surface. Due to the geometry at the crevice, concentration of ions is occurring because of a stagnant boundary layer which limits mass transport. While concentration is occurring ozone is also diffusing into this region. Therefore, a region is set-up adjacent to the crevice the is acidic, due to the concentration of hydrogen ions, and oxidizing, due to the diffusion of ozone. This mechanism accounts for the rapid attack seen at the mouth of the tight crevices.

Alloy 625 exhibited classical crevice corrosion behavior and BLC behavior, in contrast to the Hastelloy alloys which exhibited only the BLC behavior. This borderline behavior between the two mechanisms can be explained using the pitting resistance equivalence number (PREN)[34,35]. PREN examines these alloys with respect to the sum their content of Cr, Mo, and W, with Mo and W being weighted 3 and 1.65 times respectively. The higher the PREN, the greater the susceptibility to BLC. The PREN for

alloy 625 is approximately 48, which appears to be near a critical value between classical and BLC crevice corrosion.

Appendix 2

THE EFFECTS OF DISSOLVED OZONE ON STAINLESS STEEL ALLOYS 316, AL6XN, AND FERRALIUM 255

Introduction

Results are presented in two parts; the first group of experiments were carried out in the corrosion lab at Rensselaer Polytechnic Institute, the second group of experiments were performed at the LaQue Center for Corroson Technology, Inc. in Wrightsville Beach, N.C. The background for both of these tests was covered earlier in the report entitled "The Effect of Dissolved Ozone on the Corrosion Behavior of Monel 400, Monel K-500, CDA 706, and CDA 715 in Seawater" by John Stevens. Differences in procedure from this earlier report will be mentioned in the Experimental section.

Experimental

Alloy Composition

The composition of these alloys used in lab tests is listed in table 8.

	C	Cr	Fe	Mn	Mo	Ni	P	S	Si	Other
316 SS	0.040	16.13	bal.	1.780	2.100	10.42	0.025	4E-4	0.570	
AL6XN	0.021	20.76	bal.	0.260	6.350	24.65	0.021	4E-4	0.430	Cu-0.240 N-0.220
F255	0.040	17.49	bal.	1.690	2.070	11.90	0.027	0.024	0.400	Co-0.100 Cu-0.600 N-0.040

Table 8. Composition of stainless steel alloys used in lab test.

At the LaQue Center for Corrosion Technology alloys 316SS and AL6XN were donated by Allegheny Ludlum, the composition was not included but the nominal composition is expected to be similar to that listed in table 1. The composition of F-255 is shown in table 9.

	C	Cr	Fe	Mn	Mo	Ni	P	S	Si	Other
F255	0.020	24.7	bal.	1.000	3.100	5.800	0.021	0.004	0.400	Cu-1.900 N-0.100

Table 9. Composition of F255 used in tests at LaQue Center for Corrosion Technology

Cleaning and Etching Solutions

To clean the corrosion product from stainless steel samples a 30% nitric acid solution was used. Samples were immersed in the acid for approximately a minute, removed, scrubbed, rinsed in acetone, rinsed in water, and dried with forced air. The procedure was repeated as necessary to remove all of the corrosion product.

To etch the samples two different etching solution were used. To etch 316SS a solution of 50% HCl and 50% 3% H_2O_2 was used. 316 SS samples were immersed and swished for 10 sec. To etch AL6XN and F255 an electrolytic etch in 10% oxalic acid was used. Etching was run between 2 and 3 V for approximately one minute.

Results

In Lab Studies

Tank Chemistry

Tank chemistry was again mesaured using the titration method mentioned earlier in the copper-nickel report. As seen in several previous tests, over 95% of the free bromine is

converted to the bromate ion by ozone. The remaining species (OBr-. Br-, and HOBr) each consititue 1-2% of the bromine present inthe seawater system. These resutls can be seen in figure 80.

The pH of the tanks remained relatively constant at approximately 8.2 in both aerated and ozonated seawater. The resdual ozone level fluccuated around an average of 0.56 mg/l. The residual ozone level was higher than that seen in other tanks due to the lack of the black flocculant which was seen in tanks which held alloys containing a large amount of nickel. Figure 81 shows a plot of pH and ozone of the ozonated seawater tank over time.

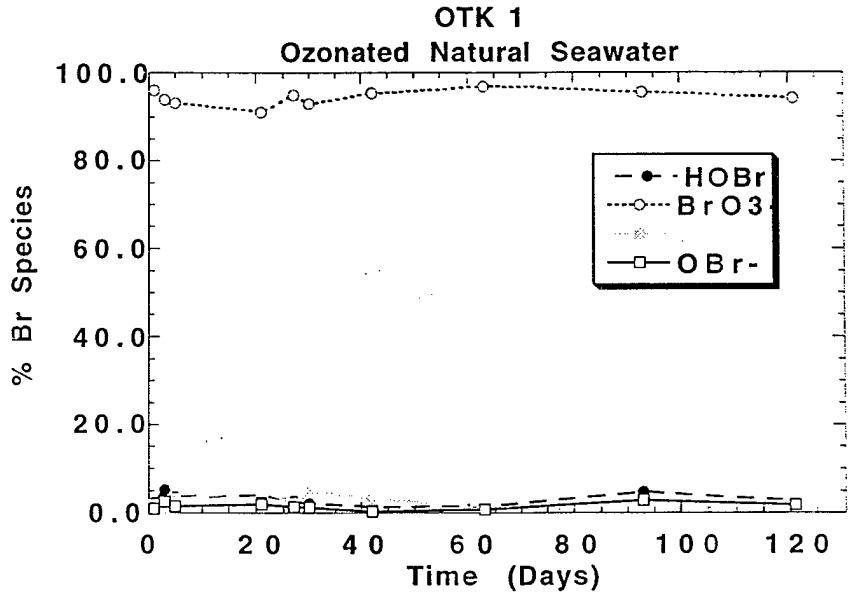

Figure 80. The change in bromine species of seawater with ozonation over time.

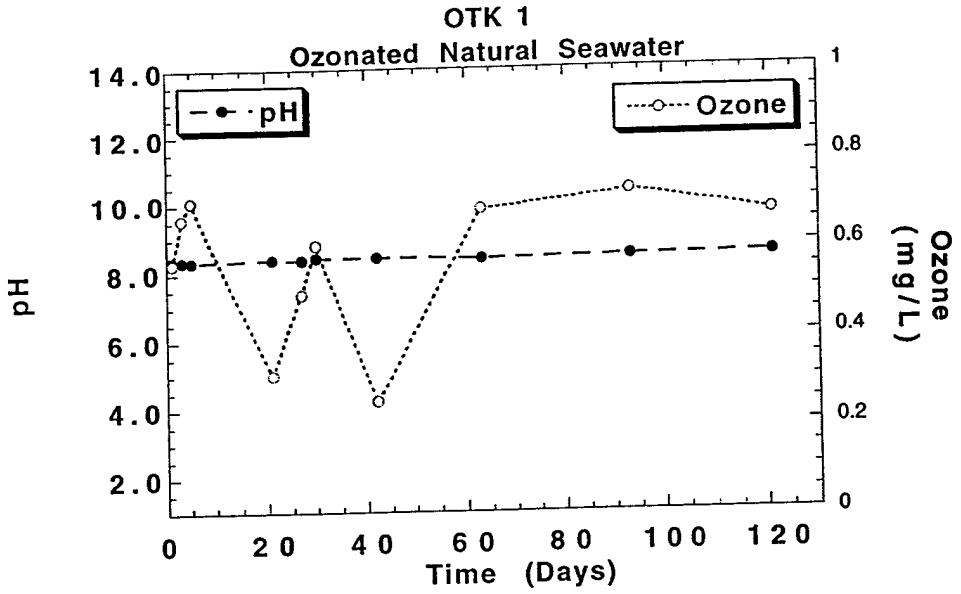

Figure 81. Change in pH and residual ozone concentration with time during ozonation of seawater.

Electrochemical Studies

Electrochemical studies were also carried out on these alloys during in lab testing, corrosion potential was measured.

Corrosion potential measurements were performed both in the tank and in an electrochemical cell. The values recorded in the cell are presented here because they were generally found to be more consistant. The three figures below show the corrosion potential results, in aerated and ozonated seawater, for the three stainless steel alloys.

Corrosion potential measurements show a steady value for aerated seawater.The corrosion potential measured for aerated seawater is not only steady over the time period but also similar between alloys at a value of about 0.1 V versus SCE.

The corrosion potential measured in ozonated seawater is not as consistant. At thirty and sixty days the corrosion potential is very similar to the value found in aerated

seawater. The corrosion potential in ozonated seawater becomes increasingly noble at ninety days. In ozonated seawater F-255 becomes active to that value found in aerated seawater, however, the value recorded in the tank (0.55V vs. SCE) is more consistant with the other data reorded and better represents the situation with ozonated seawater. This results in a potential shift of approximately 0.4V after ninety days in 316SS and F-255. Alloy Al6XN is more noble than both 316SS and F-255 in ozonated seawater with a final potenital differences of almost 0.8V between aerated and ozonated seawater after ninety days exposure. These results are shown in figures 82, 83, and 84.

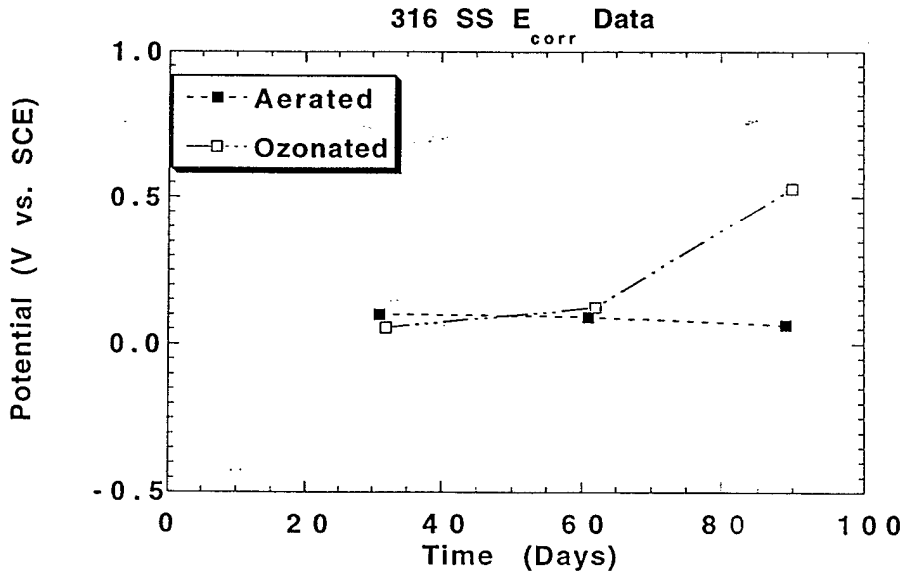

Figure 82. Corrosion potential results for 316 SS, measurements were made in an electrochemical cell.

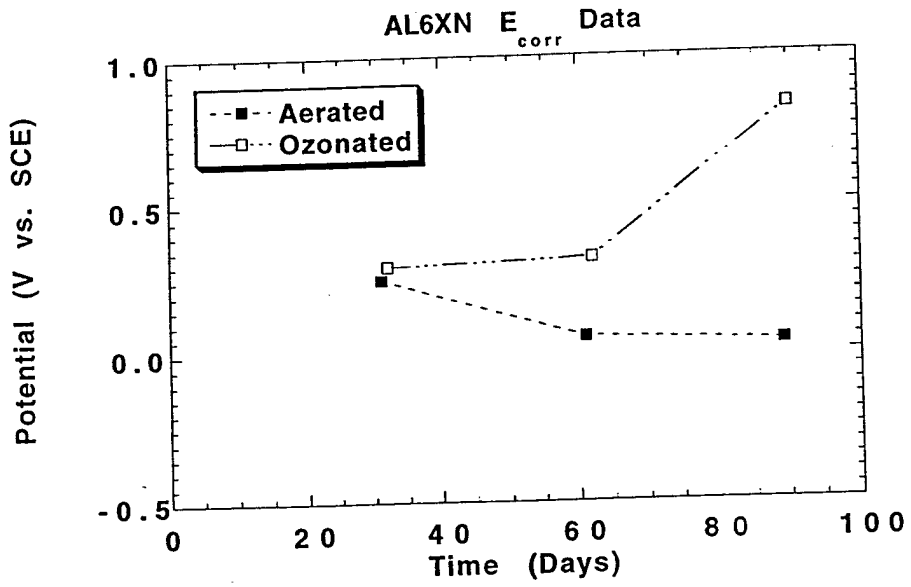

Figure 83. Corrosion potential results for Al6XN, measurements were made in an electrochemical cell.

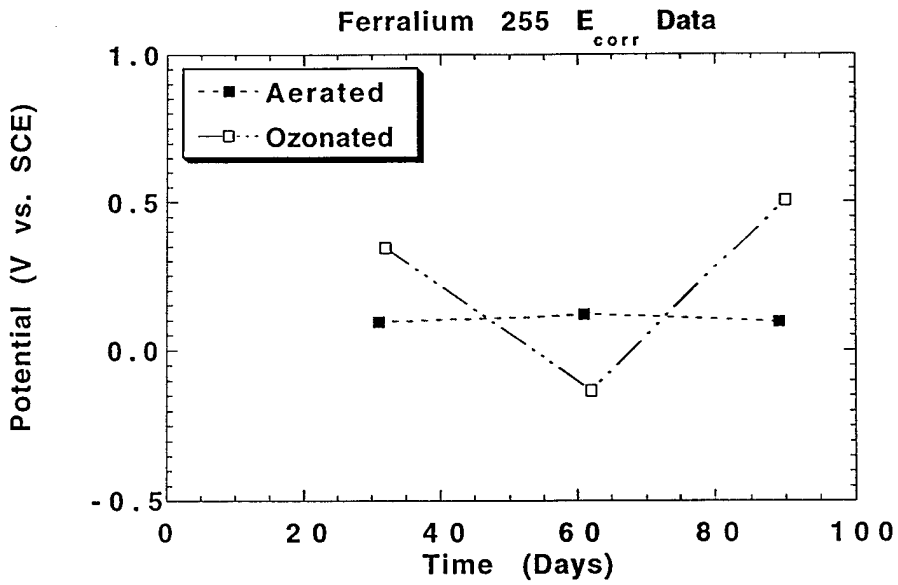

Figure 84. Corrosion potential results for F-255, measurements were made in an electrochemical cell.

Corrosion Rate

The corrosion rate of these alloys was calculated from weight loss measurements after cleaning. Samples exposed to aerated seawater exhibited no intial attack. The corrosion rate was often nearly zero, or slightly below (which would indicate weight gain). The only alloy showing any appreciable corrosion is 316 SS which peaked at 0.40mm/yr after 69 days of exposure. These alloys offer excellant and outstanding resistance to corrosion as calculated from weight loss measurements.

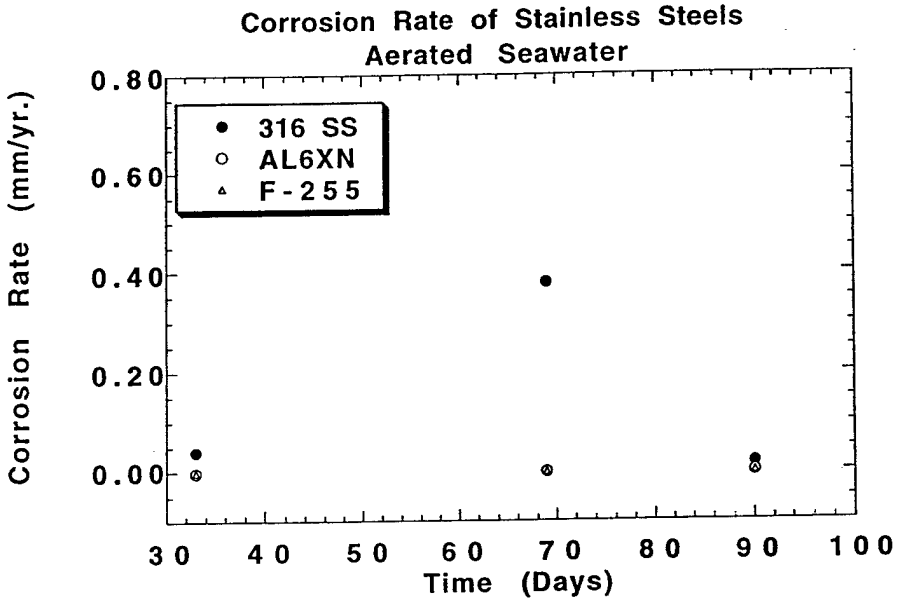

Figure 85. Corrosion rate, calculated from weight loss measurements, in stainless steel alloys in aerated seawater.

In ozonated seawater corrosion rates were higher, (figure 86) although still very low, showing excellent resistance to corrosion for 316 SS. The corrosion rate of 316 SS decreased as time went on, eventually matching that found in the other two stainless steel alloys. AL6XN and F-255 continue to have an extremely low corrosion rate, nearly zero.

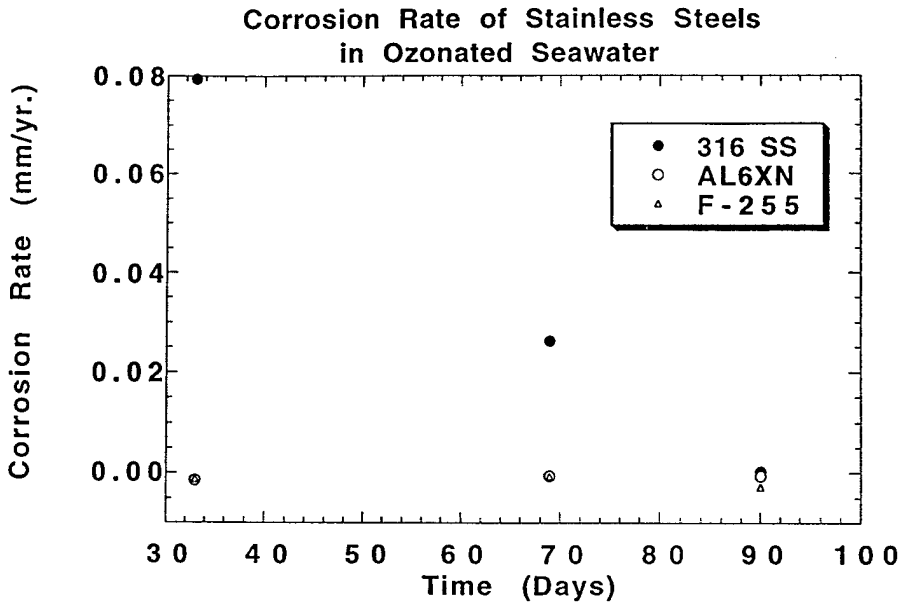

Figure 86. Corrosion rate, as calculated from weight loss measurements, of stainless steel alloys in ozonated seawater.

Weight Loss Samples

These samples, when exposed to aerated seawater, exhibited no macro signs of corrosion. Under a low power microscope some pitting was observed over the surface of the sample. The pits are broader than they are flat giving a superficial appearance. In ozonated seawater these alloys show little to no macro corrosion. Under a microscope pitting can again be seen with little difference from samples exposed to aerated seawater. These attributes are true through all the stainless steel alloys investigated in this test, figures 87 and 88 show these results after cleaning of the samples.

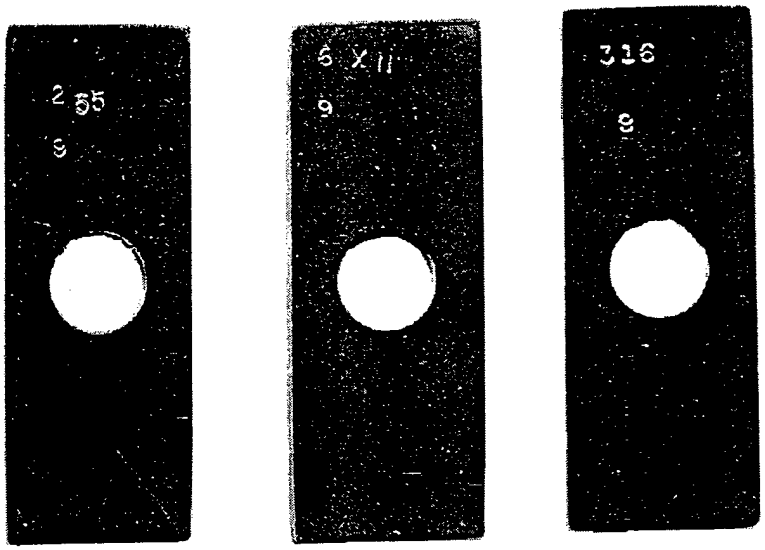

Figure 87. Weight loss stainless steel alloys Ferralium 255, Al6XN, and 316SS after sixty days of exposure to aerated seawater and cleaning.

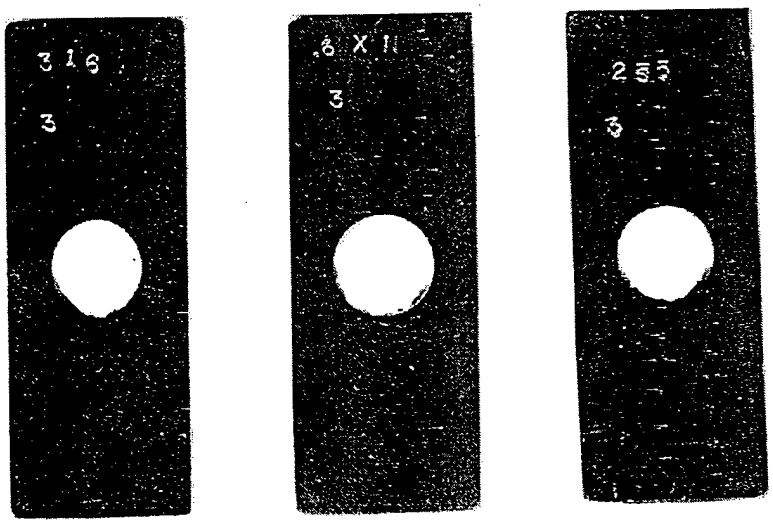

Figure 88. Weight loss stainless steel alloys 316, AL6XN, and Ferralium 255 after sixty days of exposure to ozonated seawater.

Crevice Corrosion

In aerated seawater creviced samples closely reflect concurrently exposed weight loss samples. No evidence of corrosion was found in or out of the creviced area. However, in ozonated seawater crevice corrosion was observed beneath the tight crevices. Corrosion in the crevice was characterized by an orange or black corrosion product. The black corrosion product was seen more toward the outside of the crevice, the orange corrosion product extending beneath most of the tight crevice. 316SS exhibited the most extensive corrosion as can be seen by the loss of metal near the outside of the tight crevice and under several of the sights created by the crenelated washer. Ferralium 255 shows the corrosion product seen in all the stianless steel alloys but no depth of attack was observed. Likewise, Al6XN shows visible metal loss beneath only one of the tight crevices formed by the creneleated washer. AL6XN also contains the corrosion product underneath the crevice seen in the other stainless steel alloys. Figure 89 and 90 show these crevice corrosion results after sixty days of exposure to aerated and ozonated seawater.

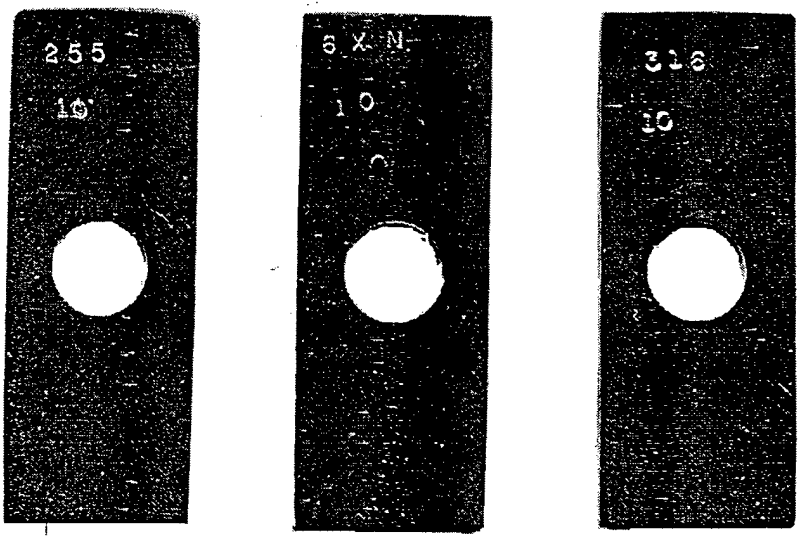

Figure 89. Creviced stainless steel corrosion samples Ferralium 255, Al6XN, and 316SS exposed to aerated seawater for sixty days

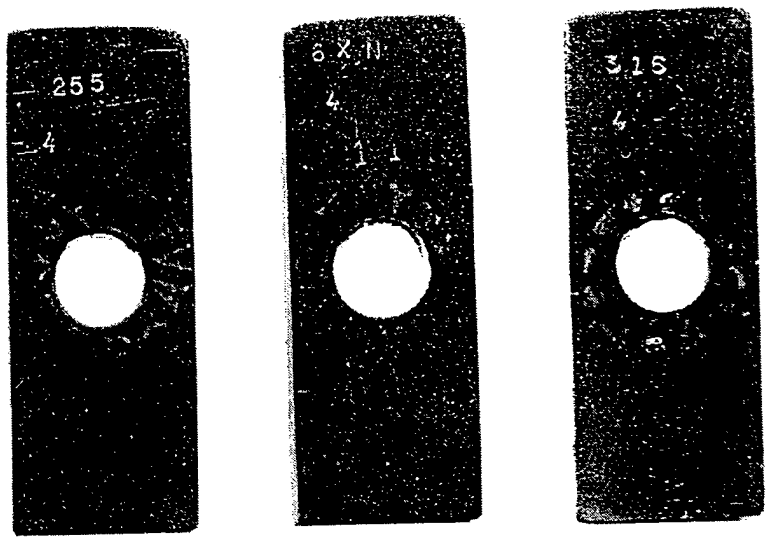

Figure 90. Creviced, stainless steel corrosion samples Ferralium 255, AL6XN, and 316SS exposed for sixty days to ozonated seawater.

Results from LaQue Center for Corrosion Technology, Inc. Wrightsville Beach, N.C.

Corrosion Potential Results

Corrosion potential measurements, at the LaQue Center for Corrosion Technology, were made at the end of the test, after sixty days of exposure to chlorinated or ozonated seawater. Corrosion potential was measured on the crevice samples, no samples were immersed as electrochemical samples. This creviced situation may account or some of the differences in results between in lab and LaQue experiments.

In chlorinated seawater (figure 91) the stainless steel alloys no longer show the constancy found in these alloys when exposed to aerated seawater during in lab testing. The three alloys testes, 316SS, AL6XN, and F-255 exhibited an average corrosion potential of -0.136V, 0.468V, and 0.306V vs. SCE respectively. Al6XN and F-255 exhibit a noble shift compared to in lab tests in aerated seawater in corrosion potential of 0.3V and 0.2V respectively. 316SS shows an active shift of over 0.2V. The active shift is due to thte breakdown of the passive film on this steel. AL6XN and F-255 are more highly alloyed with Cr and Mo and therefore have a more stable passive film. The noble shift of these alloys is due to the larger oxidizing potential of chlorine in seawater (compared with oxygen).

Average values for potential measurements in ozonated seawater are -0.054V, 0.595V, and 0.136V vs. SCE for 316SS, AL6XN, and Ferralium 255 respectively (figure 92). In ozonated seawater 316SS and AL6XN show a noble shift of approximately 0.1V compared to results in chlorinated seawater. Ferralium 255 undergoes an active shift in corrosion potential of approximately 0.2V. The noble shift in corrosion potential is due to the higher oxidizing potential of ozone when compared to chlorine. The active shift of F-

255 may be due to active crevice corrosion which was found after dissassembly of the samples.

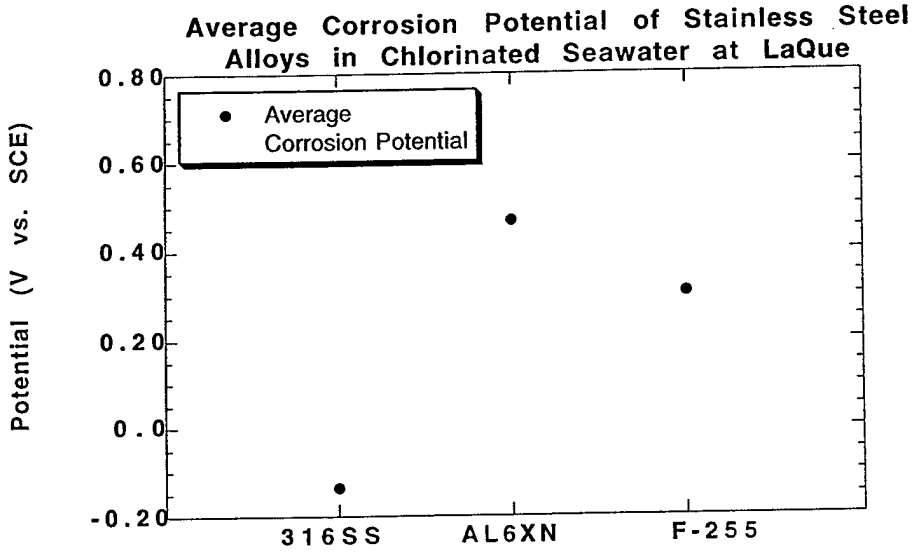

Figure 91. Average corrosion potential measurement of stainless steel alloys exposed to chlorinated seawater for sixty days.

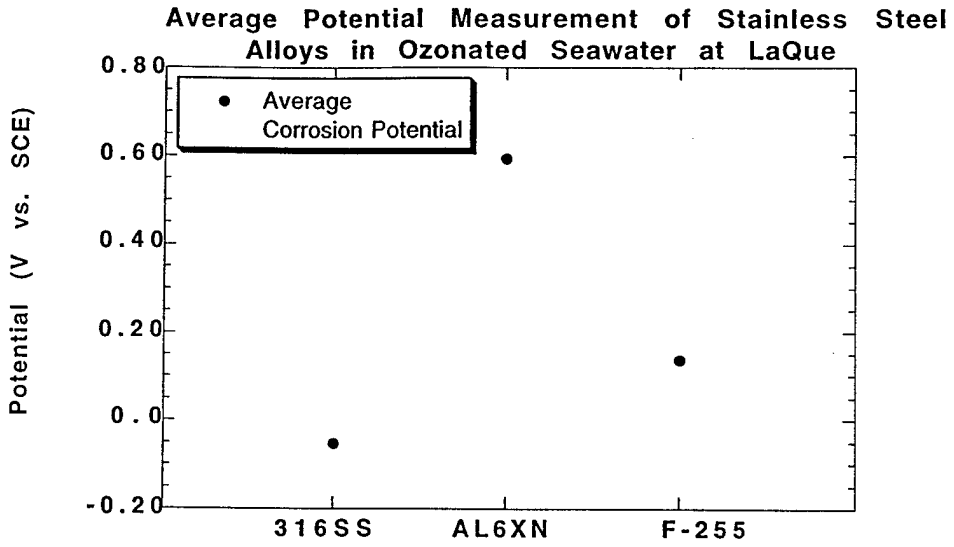

Figure 92. Corrosion potential measurements at LaQue of stainless steel alloys exposed to ozonated seawater for sixty days.

Corrosion Rate From Panels

After sixty days of immersion, these samples were removed, dried, and disassembled. The samples were then cleaned to remove corrosion product and weighed to determine corrosion rate. Corrosion rate measurements determined from the weight loss of the panels is shown in figre 93 and 94.

In chlorinated seawater the corrosion rates are very low. Even after extensive cleaning a net weight gain in mass was observed. The stainless steel samples show no signs of corrosion after sixty days of immersion in chlorinated seawater. This lack of visible corrosion is corroborated by the low corrosion rates found in chlorinated seawater.

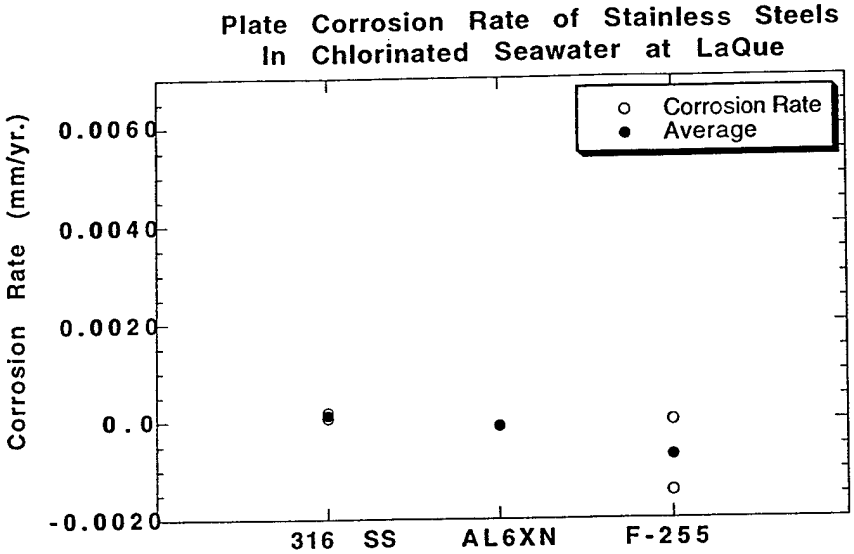

Figure 93. Corrosion rate of stainless steel panels exposed for sixty days to chlorinated seawater.

In ozonated seawater alloys 316 and F-255 did show crevice corrosion which was reflected in the corrosion rate for these alloys. Figure 94 shows the corrosion rate for these stainless steel alloys in ozonated seawater. 316SS shows the highest corrosion rate, largely due to localized crevice corrosion. F-255 underwent a small amount of crevice corrosion and therefore has a slightly higher corrosion rate. Al6XN did not show visible local or general attack and exhibits a corrosion rate of nearly zero.

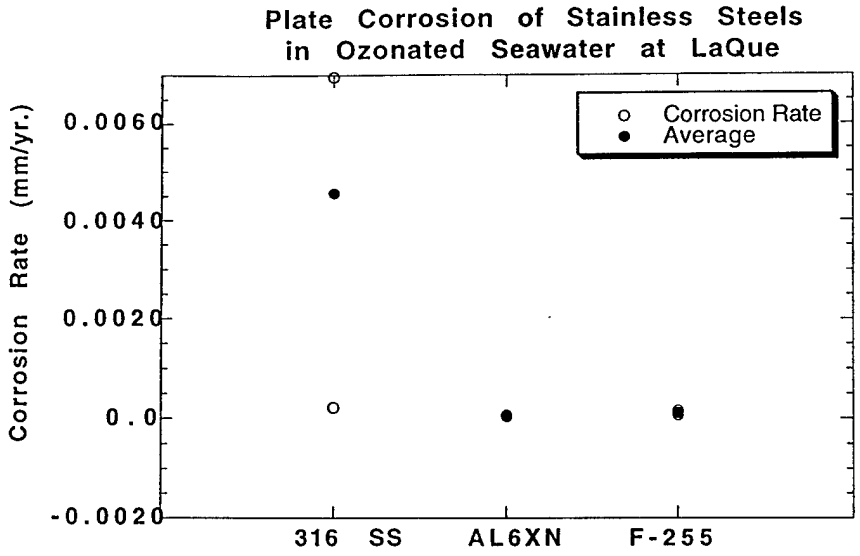

Figure 94. Corrosion rate of stainless steel panles exposed to ozonated seawater for sixty days.

Corrosion Rate From Washers

The crevice corrosion that did occur usually took place between the PTFE and metal washers. Typical of trends seen thus far, attack has been more severe in ozonated seawater. However, chlorinated seawater was found to attack 316SS and F-255 slightly. AL6XN showed no attack and continues to have a extremely low corrosion rate. Figure 95 shows the corrosion rate of washers exposed chlorinated seawater for sixty days.

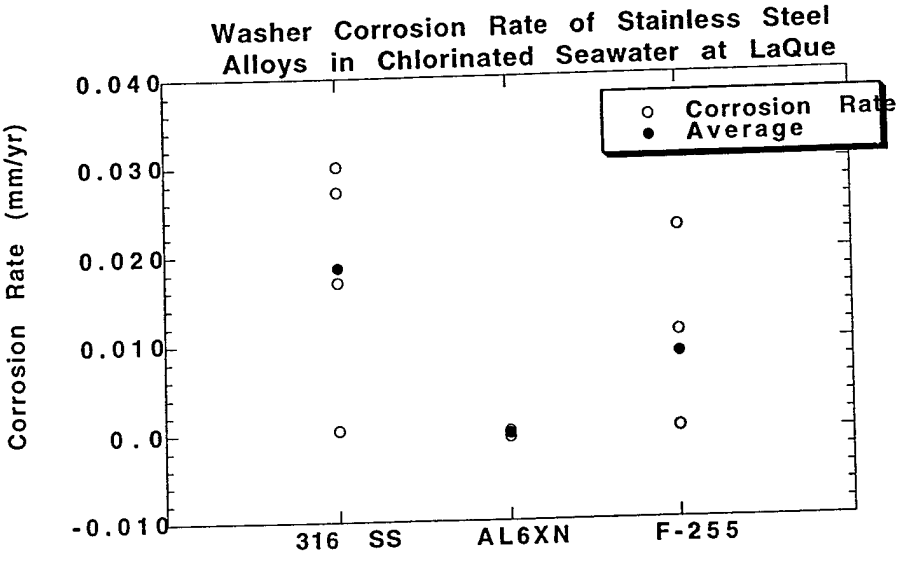

Figure 95. Corrosion rate of stainless steel washers exposed to chlorinated seawater at LaQue for sixty days.

In ozonated seawater corrosion rates are higher by at least an order of magnitude for 316SS and F-255. AL6XN continues to to show a nealry zero corrosion rate, with no visible signs of corrosion. The loss of mass for 316SS and F-255 is largely due to localized corrosion as evidenced by the loss of materials within the PTFE-metal crevice. The 316SS alloy actually saw corrosion penetrate the thickness of the washer (0.32cm) and attack the plate beneath. Figure 96 shows corrosion rate data from weight loss measurements for the stainless steel washers exposed to ozonated seawater.

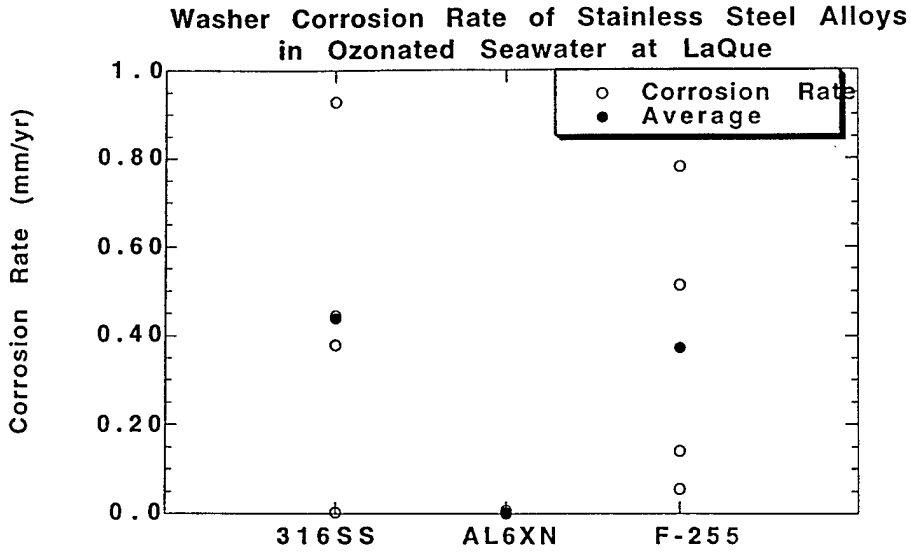

Figure 96. Corrosion rate for stainless steel washers exposed to ozonated seawater at LaQue for sixty days.

316SS Results

Upon removal from the seawater environments 316SS showed brown corrosion product primarily at the metal-PTFE crevice. The volume of corrosion product was greater in ozonated seawater than in chlorinated seawater . In ozonated seawater the corrosion product was observed at the metal-metal crevice in addition to the metal-PTFE crevice.

Cleaning of these samples revealed metal loss under the PTFE washer in both chlorinated and ozonated seawater. The attack was more severe in ozonated seawater. In ozonated seawater attack was also observed under the metal washer (on the metal plate). In one case it seemed that the corrosive solution under the PTFE washer was able to penetrate through the thickness of the metal washer and attack the plate beneath in sixty days. Figure 97 and 98 show 316SS after exposure for sixty days,to ozonated seawater, disassembly, and cleaning.

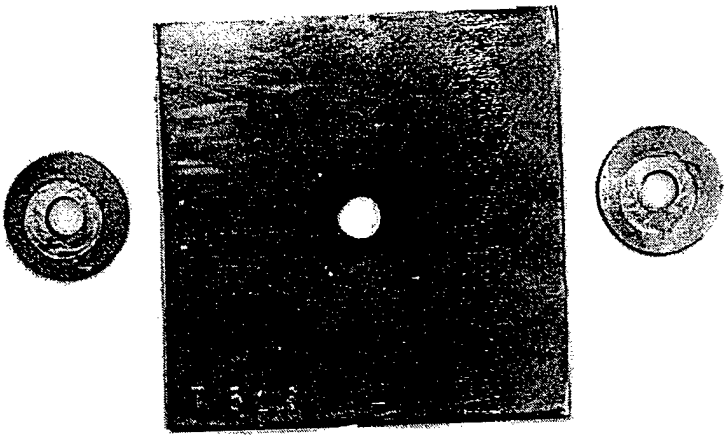

Figure 97. 316SS exposed to ozonated seawater for sixty days. Shown after disassembly and cleaning.

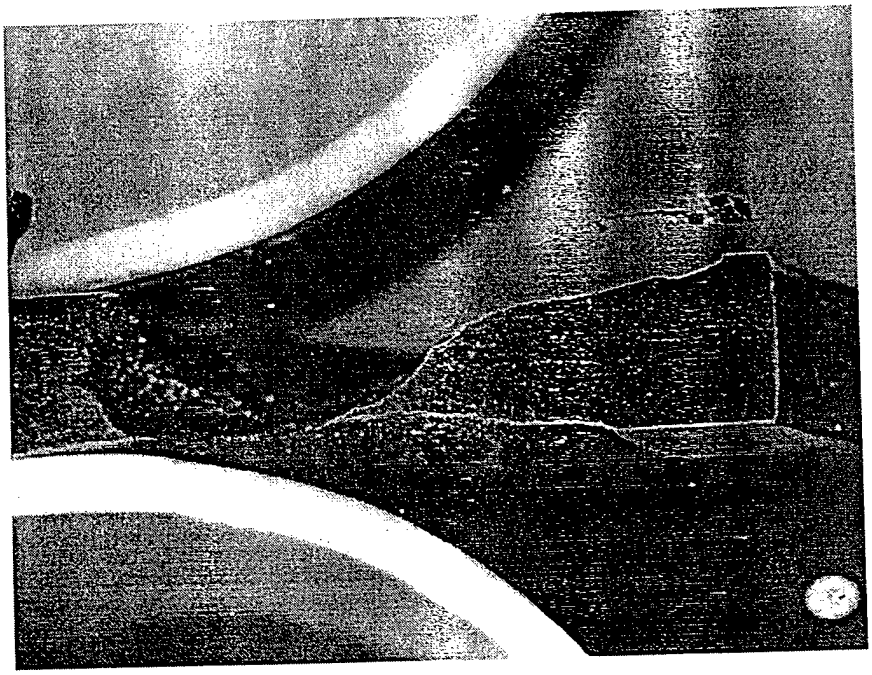

Figure 98. 316SS washer exposed to ooznated seawater for sixty days. The top side faced the PTFE washer, the bottom faced the metal plate.

AL6XN Results

In both chloriated and ozonated seawater Alloy AL6XN exhibited very little attack. No corrosion was observed in chlorinated seawater and in ozonated seawater AL6XN fared the best of the stainless steels, with little to no attack on the plate and minor attack underneath the PTFE washer. Figure 99 and 100 show attack for AL6XN in ozonated seawater.

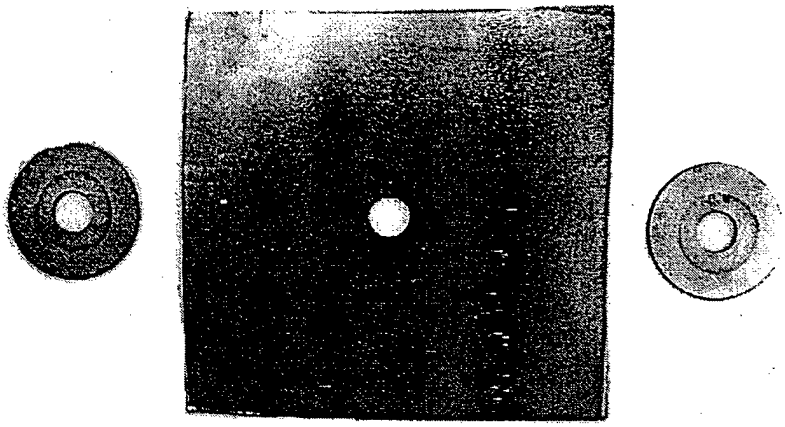

Figure 99. AL6XN after sixty days of exposure to ozonated seawater, disassembly, and cleaning.

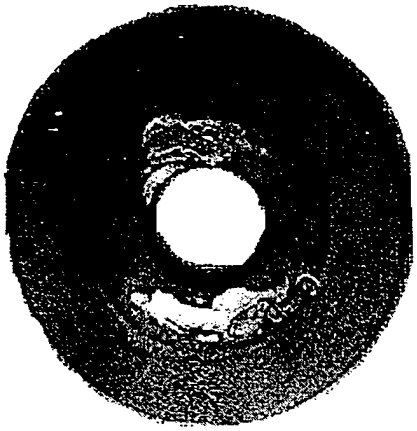

Figure 100. AL6XN washer after sixty days of exposure to ozonated seawater, disassembly, and cleaning, Attack is typical of the type seen of stainless steels in ozonated seawater.

Ferralium 255 Results

Ferralium 255 landed between the 316SS and AL6XN as far as corrosion attack is concerned. As with AL6XN, no attack was seen after exposure to chlorinated seawater.

Ferralium 255 also exhibited greater attack than 316SS but less attack than seen in AL6XN during exposure to ozonated seawater. A brown corrosion product was observed underneath both the metal-metal crevice and metal-PTFE crevice. More predominant corrosion was observed under the metal-PTFE crevice, as has been observed with all the stainless steel alloys. Metal dissolution occured under the PTFE washer and to a lesser extent under the metal washer. Attack within the crevice was not uniform, but more random and near the edge of the washer. The figures below show F-255 after exposure to ozonated seawater, disassembly, and cleaning.

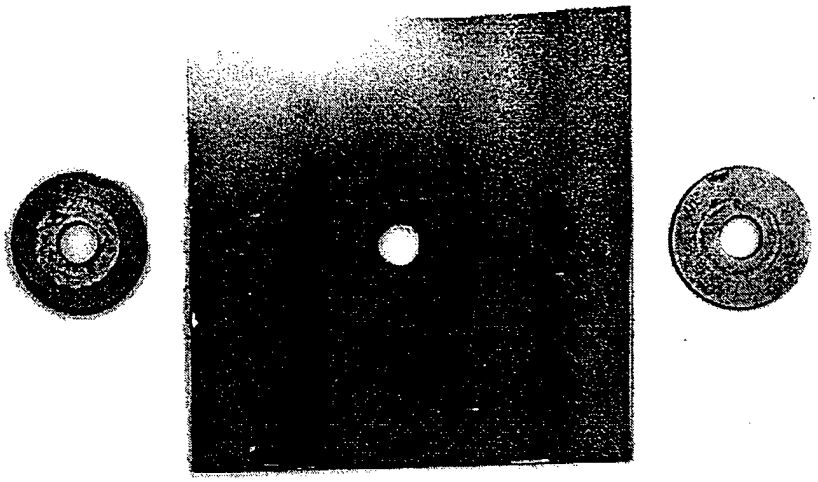

Figure 101. Ferralium 255 exposed for sixty days to ozonated seawater, disassembled, and cleaned.

It can be seen in figure 101 that crevice corrosion beneath the PTFE washers is significant but very little corrosion is present on the plate. Microscopic investigation revealed that one phase of this duplex alloy is being corroded preferentially as shown in figure 102 and 103.

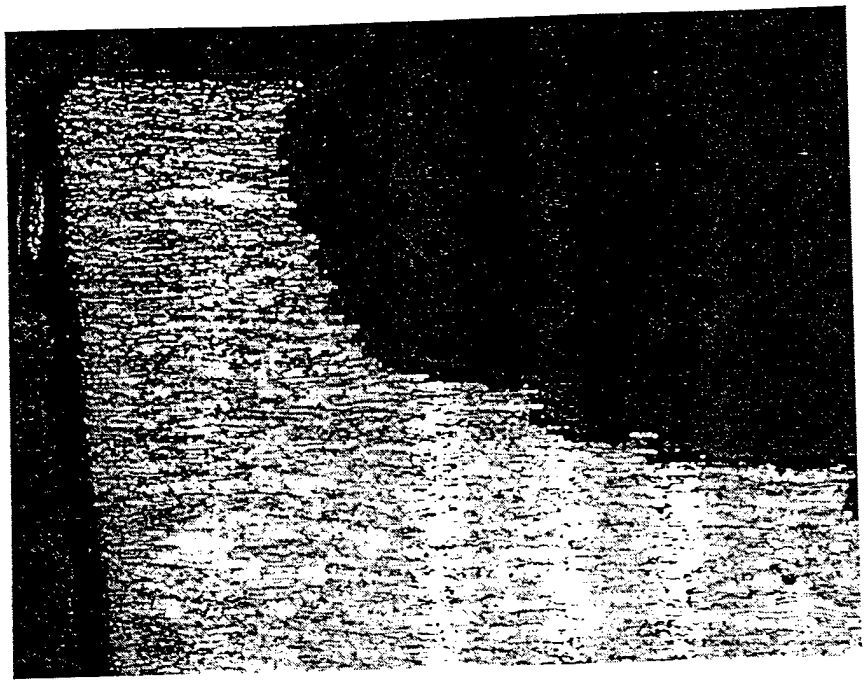

Figure 102. Cross section of F-255 washer after exposure for sixty days to ozonated seawater. Side shown was facing the PTFE washer. Electrolytic etch in oxalic acid at 2.3 V, 126X

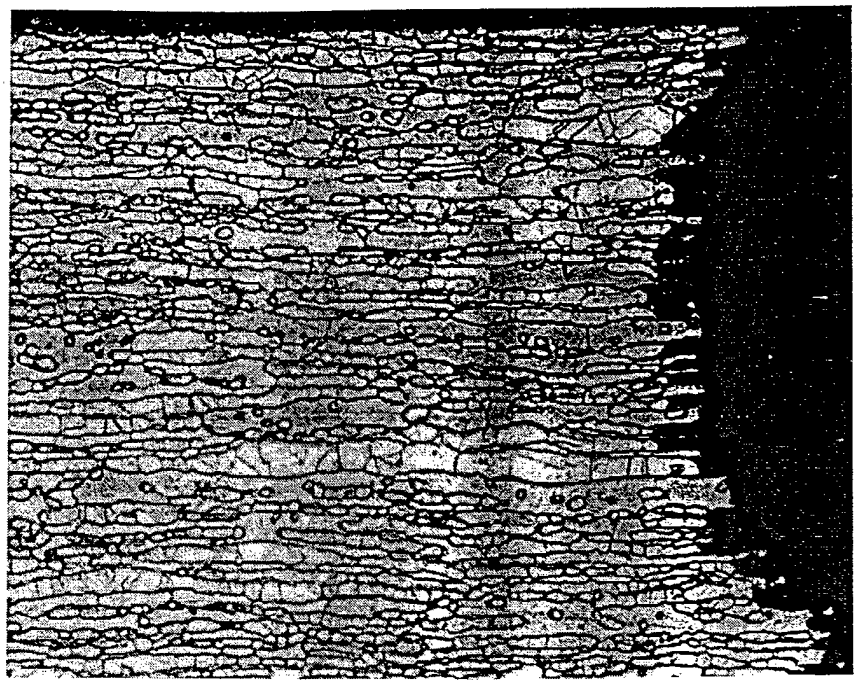

Figure 103. Cross-section of F-255 washer, close-up of previous picture. Notice the preferential corrosion of the lighter colored phase in this duplex alloy. Electrolytic etch in oxalic acid at 2.3V, 500X

Discussion

The stainless steel alloys studied here show resistance to general corrosion and crevice corrosion in aerated and chlorinated seawater. However, this is not the case in ozonated seawater. Both in lab studies and tests performed in natural seawater show that the presence of ozone increases crevice corrosion of these stainless steel alloys.

The more highly alloyed stainless steels (F-255, AL6XN) show better resistance to corrosion in this environment than 316SS. After sixty days of exposure to ozonated seawater 316SS exhibited extensive corrosion within the crevice. The highly alloyed stainless steels contain greater amounts of Mo and Cr both of which contribute to corroson resistance by the formation of a passive oxide film in oxidizing environments. Greater concentrations of these elements allow the formation of a more stable passive oxide film.

As has been observed throughout this series of tests and in tests performed earlier by Brown, Wyllie, and Duquette crevice corrosion was most severe under PTFE washers. The increased corrosion under this type of washer is due to breakdown of the washer forming a hydroflouric acid (HF).[36] The acid produced is highly corrosive inside the crevice.

The Ferralium 255 alloy was particularily interesting because of its duplex architecture. As was observedin the micrographs one phase exhibited more extensive corroson than the other during crevce corrosion. In a reducing atmmosphere is present in the crevice , as all the oxygen is consumed and limited transport is available to replenish the supply of oxygen. Without oxygen chromium is not allowed to play its role in the protection of these alloys and may actually be deterimental. As was seen in the nickel and copper based alloys, additions of chormium and molybdenum can accelerate corroion in certian instances because these elements are so active. Because of the similar crystal structure between chromium and ferrite it is assumed the ferrite phase of this duplex alloy will contain a greater amount of chromium. Because of the reducing atmosphere and the larger amount of chormium, a active element. It is believed that the phase being preferentially corroded is the ferrite phase in the duplex Ferralium 255 alloy.

The AL6XN alloy exhibited little to no corrosion even in the ozonated seawater environment, of all the alloys studied in these tests this stainless steel performed the best.

References

[1] Herbert H. Uhlig, The Corrosion Handbook, John Wiley & Sons, New York, 1948

[2] Herbert H. Uhlig, The Corrosion Handbook, John Wiley & Sons, New York, 1948 (Original Reference: H.U. Sverdrup, M.W. Johnson, and R.H. Fleming, *The Oceans*, Prentice-Hall, Inc. New York, 1942. J.Lyman and R.H. Fleming, *J. Marine Research*, Vol. 3, 134-146, 1940.

[3] F.W. Fink and W.K. Boyd, The Corrosion of Metals in Marine Environments, Bayer & Company, Columbus, 1970.

[4] Ozone in Water Treatment Application and Engineering, Editors: Bruno Langlais. David A. Reckhow, Deborah R. Brink, Lewis Publishers, Chelsea, Michigan, 1991 ,pp.2-3

[5] W.E. Wyllie II, B.E. Brown, and D.J. Duquette, "Interim Results on the Corrosion Behavior of Engineering Alloys in Ozonated Artificial Seawater." Office of Naval Research , Report 2, Contract No. N00014-94-1-0093, March 1996

[6] Denny A. Jones, Principles and Prevention of Corrosion 2nd ed., Prentice Hall, NJ. 1996

[7] Herbert H. Uhlig and R. Winston Revie, Corrosion and Corrosion Control, An Introduction To Corrosion Science and Engineering 3rd ed., John Wiley & Sons, New York, 1985

[8] Barbara E. Brown, The Effects of Dissolved Ozone on the Corrosion Behavior Of Nickel-Based Chromium-Molybdenum Alloys in Artificial Seawater, Ph.D. Thesis, Rensselaer Polytechnic Institute, Troy, NY, 1998

[9] R.J.McKay and R. Worthington, 2nd ed. edited by F.L. LaQue and H.R. Copson, Corrosion Resistance of Metals and Alloys 2nd ed., Reinhold Publishing Corporation, New York, 1963

[10] Barbara E. Brown, The Effects of Ozone on the Corrosion Behavior of 304 Stainless Steel, Monel 400, and Naval Brass in Artificial Sea Water, M.S. Thesis, Renesselaer Polytechnic Institute, Troy, NY, 1993

[11] ASM Committee on Corrosion of Copper, "Corrosion of Copper and Copper Alloys" in Metals Handbook 9th ed. Vol. 13, Corrosion, ASM International, Ohio, 1987, pp. 610-611

[12] Mars G. Fontana, Corrosion Engineering 3rd ed., McGraw-Hill Book Company, New York, 1986, pp.240

[13] B.Yang, D.A. Johnson, and S.H. Shim, "Effect of Ozone on Corrosion of Metals in Cooling Towers", *Corrosion*, Vol. 49, No. 6, June 1993, pp. 499-513

[14] H.H. Lu, The effect of Dissolved Chlorine And Ozone On The Corrosion Behavior Of Cu-30Ni and 304L Stainless Steel in 0.5N NaCl Solutions, M.S. Thesis, Rensselaer Polytechnic Institute, Troy, NY, 1990.

[15] H. Bader and J.Hoigne', Determination of Ozone in Water by the Indigo Method, *Water Research* ,15 (1981) p. 449-456

[16] H. Bader and J. Hoigne', Colorimetric Method for the Measurement of aqueous ozone based on the Decolorization of indigo Derivitives,"Ozonation Manual for Water and Wastewater Treatment, W.J. Masschelein (chichester: John Wiley & Sons, 1982) p. 169-172

[17] R.M. Kain, Private communication, LaQue Center for Corrosion Technology, April 2, 1997

[18] Standard Practice G 46-76, Annual Book of ASTM Standards, Vol. 3.02, ASTM, Philadelphia, p.197, 1988

[19] Susan Y. Leveillee, The Corrosion Effect of Ozonated Seawater Solution On Titanium In Polymer Generated Crevice Environments, Rensselaer Polytechnic Institute, Troy, NY, November 1997

[20]D.E.Dobb, J.P.Storvick, G.K. Pagenkopf, Pretreatment Procedures for Corrosion Studies of Cupro-Nickel Alloys in Seawater, *Corrosion Science*, Vol. 26, No. 7, 1986, 525-536

[21] M. Pourbaix, Atlas of Electrochemical Equilibria in Aqueous Solutions, (Houston, TX: National association of Corrosion Engineers, 1974).

[22] Robert C. Weast, editor, CRC Handbook of Chemistry and Physics 60th edition, CRC Press, Boca Raton, FL, 1980

[23] H. Kaesche, Metallic Corrosion, Principles of Physical Chemistry and Current Problems, Trans. R.A. Rapp, NACE, Houston, TX, 1985

[24] H.P.Dhar, R.E. White, R. Darby, L.R. Cornwell, R.B. Griffen, G.Burnell, Corroison Behavior of 70Cu-30Ni Alloy in 0.5NaCl and Synthetic Seawater, *Corrosion*, Vol. 41, No. 4, April 1995, 193-196

[25] R.J.K.Wood, S.P.Hutton, D.J.Schiffern, Mass Transfer Effects On Non-Cavitating Seawater On The Corrosion of Cu and 70Cu-30Ni, *Corrosion Science*, Vol. 30, No. 12, 1990, 1177-1201

[26] John Stevens, unpublished research, Rensselaer Polytechnic Institute, 1997

[27] R. Zanoni, G. Gusmano, G. Montesperelli, E. Traversa, X-Ray Photoelectron Spectroscopy Investigation Of Corrosion Behavior of ASTM C71640 Copper-Nickel Alloy In Seawater, *Corrosion*, Vol. 48, No. 5, May 1993, 404-410

[28] J.N.Al-Hajji, M.R. Reda, The Corrosion Of Copper-Nickel Alloys In Sulfide-Polluted Seawater: The Effect of Sulfide Concentration, *Corrosion Science*, Vol.34, No. 1, 1993, 163-177

[29] M.R. Reda, J.N.Al-Hajji, The Effect of Trace organic Compounds on the Corrosion of Cu/Ni Alloys in Sulfide Polluted Seawater, *Ind. Eng. Chem. Res.* Vol. 32, No. 5, 1993, 960-965

[30] John Stevens, Unpublished Research, Rensselaer Polytechnic Institute, April 1998

[31] Metals Handbook, ninth edition, Vol. 13 Corrosion, ASM International, Metals Park, OH, 1987

[32] Corrosion Resistant HASTELLOY ALLOY at a Glance, Haynes International Preliminary Data Sheet, H-2105, Haynes International, Inc., Kokomo, IN, Nov. 1995

[33] Barbara Brown, The Effects Of Dissolved Ozone On The Corrosion Behavior Of Nickel-Based Chromium-Molybdenum Alloys In Artificial Seawater, Ph.D. Thesis. Rensselaer Polytechnic Institute, May 1998

[34] A.J.Sedricks, Corrosion of Stainless Steels, Second Edition (New York, NY: John Wiley&Sons, Inc. 1996)p. 113

[35] A.J.Sedriks, "Crevice Corrosion of Cr Containing Alloys, "Paper No. (Houston: NACE, 1996).

[36] W.E. Wyllie II, B.E. Brown, and D.J.Duquette, "Interim, Results On The Corrosion Behavior Of Engineering Alloys In Ozonated Artifical Seawater" Report no. 2 to the Office of Naval Research, N00014-94-1-0093, March 1996